SURGICAL CAVITY CONTOUR AND SKIN MARKING VARIABILITY IN ACCELERATED PARTIAL BREAST IRRADIATION

by

Robert Kosztyla

B.Sc., The University of Waterloo, 2007
B.Ed., Queen's University, 2007

A THESIS SUBMITTED IN PARTIAL FULFILLMENT OF THE REQUIREMENTS FOR THE DEGREE OF

MASTER OF SCIENCE

in

The Faculty of Graduate Studies
(Physics)

THE UNIVERSITY OF BRITISH COLUMBIA
(Vancouver)

April 2009

ABSTRACT

Accelerated partial breast irradiation (APBI) has emerged as an attractive alternative to whole-breast radiotherapy (WBRT) in adjuvant radiotherapy of early stage breast cancers. Localization of the target, the surgical cavity (SC), is of the utmost important since a large dose per fraction is delivered during treatment. Differences in the shape and position of the SC between planning and treatment can result in a geographic miss of the target. Skin markings (SM) placed around the surgical scar potentially can be used to improve localization of the SC during treatment. However, analysis of such movements is complicated by interobserver and intraobserver variations in defining the SC. Thus, this thesis aims to (1) develop a method to construct a representative surgical cavity (RSC), a contour that combines contributions from multiple SC contours; (2) investigate contouring uncertainties and dosimetric coverage of the SC as contoured by multiple oncologists; and (3) use the RSC to quantify differences between the positions of the SMs and SC.

Twelve patients underwent four CT scans: one at the time of planning and three during treatment. Three radiation oncologists contoured the SC on each CT scan. Oncologists delineated two additional repeat contours for three patients. Interobserver and intraobserver contour variability was assessed by comparing the SC contours with a RSC. Volume-based and distance-based measurements were performed to assess contour variability. Clinical consequences of variability were assessed using the equivalent uniform dose (EUD) formalism. Correlations between the change in position of the SM centre-of-mass (COM) and RSC COM were quantified.

Interobserver volume, COM, and spatial variations of the SC contours were observed to be larger than intraobserver variations. However, dosimetric coverage of the SC was adequate despite these variations. The SM COM was found to be strongly correlated with the RSC COM in the lateral, anterior-posterior, and superior-inferior directions. The average change in the distance between the SM COM and RSC COM during treatment was more than 4 mm in less than 5% of cases, suggesting that planning margins for the SC can potentially be decreased if the SMs are used for patient setup.

TABLE OF CONTENTS

LIST OF TABLES

LIST OF FIGURES

LIST OF ABBREVIATIONS

3DCRT	Three-dimensional Conformal Radiotherapy
AP	Anterior-posterior
APBI	Accelerated Partial Breast Irradiation
BCT	Breast Conservation Therapy
CBCT	Cone beam CT
COM	Centre-of-mass
CT	Computed Tomography
CTV	Clinical Target Volume
CVS	Cavity Visualization Score
DEV	Dose Evaluation Volume
DVH	Dose Volume Histogram
EUD	Equivalent Uniform Dose
GTV	Gross Tumour Volume
IMRT	Intensity-modulated Radiotherapy
kV	Kilovoltage
LQ	Linear Quadratic
MU	Monitor Unit
MV	Megavoltage
NSABP	National Surgical Adjuvant Breast and Bowel Project
PTV	Planning Target Volume
RAPID	Randomized Trial in Accelerated Partial Irradiation

REB	Research Ethics Board
RMS	Root-mean-square
RSC	Representative Surgical Cavity
RTOG	Radiation Therapy Oncology Group
SC	Surgical Cavity
SD	Standard deviation
SI	Superior-inferior
SM	Skin Marking
WBRT	Whole-breast Radiotherapy

ACKNOWLEDGEMENTS

First of all, I would like to thank my research supervisor Dr. Vitali Moiseenko for his support and assistance throughout the completion of my studies and my research.

I would also like to extend my appreciation to members of the DIVA project at the BC Cancer Agency Fraser Valley Center (Surrey, BC) for their help in this work. In particular, I would like to thank Drs. Winkle Kwan, Hannah Carolan, and Susan Balkwill for their hard work in delineated the surgical cavities for this project. I also must extend my gratitude to the radiation therapists at the Fraser Valley Centre, particularly Sarah Kristensen, Craig Elith, and Jennifer Hayes for expertise with Eclipse™. In addition, I would like to thank Dr. Robert Olson for his support throughout the project.

I would like to express my thanks to my parents, sister, and my entire extended family for their continued support of my education and research. It is greatly appreciated. Additionally, I would like to thank Lex Teschke for her continued friendship.

DEDICATION

To mom and dad

1. INTRODUCTION

1.1. Breast Cancer

As is the case for all of Canada, breast cancer is the most prevalently diagnosed cancer in women in British Columbia (1-3). Statistics Canada reports that breast cancer was the most common cancer in women in Canada between 2001 and 2005, accounting for 27% to 29% of newly diagnosed cancers (1). The three-year averaged age-standardized rate of breast cancer incidence in women was 92.0 and 97.8 per 100,000 population in 2003 for British Columbia and all of Canada, respectively; the rate of incidence for all cancers was 324.0 and 349.0 (2). In 2006, breast cancer accounted for 29.4% of all new cancers in women in British Columbia (4). Furthermore, the BC Cancer Agency reports that between 1997 and 2005 breast cancer was the most common new cancer in women, with lung cancer the second-most diagnosed (3). Most women diagnosed with breast cancer are between the ages of 40 and 80. For example, 3.9%, 42.3%, 41.0%, and 12.8% of new breast cancer patients at the BC Cancer Agency in 2005 were between the ages of 20 and 39, 40 and 59, 60 and 79, and 80 and higher (5).

Despite the common occurrence of breast cancer in women, statistics suggest a high rate of survival, especially when compared with other cancers. The annual five-year survival estimate for breast cancer cases in 1999 in Canada was 87% (6). The one, three, and five-year relative survival rates of breast cancer for patients referred to the BC Cancer Agency in 2004, 2002, and 2000 respectively were 99%, 94% and 90%; for all cancers the relative survival rates were 78%, 67%, and 62% (7). Survival rates do not vary widely geographically within British Columbia. The five-year age-adjusted breast cancer survival rate between 2000 and 2005 was 90%, 89%, 92%, 89%, and

86% for the Interior, Fraser, Vancouver Coastal, Vancouver Island, and Northern Health Authority Regions (7).

Mastectomy, the surgical removal of breast tissue, is a common treatment option for breast cancer patients. However, Breast Conservation Therapy (BCT) can be used as an alternative to mastectomy for early stage breast cancers (8). BCT involves removal of the primary lesion (breast-conserving surgery or lumpectomy) followed by whole-breast radiotherapy (WBRT) (8). WBRT is typically delivered using two tangent megavoltage (MV) photon fields covering the entire breast. A typical field arrangement and dose distribution for WBRT is shown in Figure 1.1. The patient is treated with WBRT daily, five days per week for three-and-one-half to five weeks. BCT gives good to excellent cosmetic results with control rates of more than 90% (8). Experts recommend that the standard of care should be that all women carry through with WBRT after breast-conserving surgery to optimize local control of the cancer (8).

However, it has been well documented that many women opt not to receive WBRT following breast-conserving surgery. It has been reported that only 10% to 70% of women who are potential candidates for WBRT after lumpectomy actually receive the treatment (9). Since many breast cancer patients are older women and may reside far from the place of treatment, they may rather elect for mastectomy or lumpectomy without WBRT (8). In fact, it has been documented that there is a trend towards treatments with lumpectomy alone (8). The danger for women choosing not to receive WBRT after lumpectomy is that they may have a higher chance of in-breast recurrences following treatment. Prospective randomized trials investigating BCT have indicated that in-breast recurrences are more common in women who do not received WBRT

following lumpectomy (10). Studies by Veronesi *et al.* (11), Clark *et al.* (12), and the Uppsala-Orebro Breast Cancer Study Group (13) report that the occurrence of in-breast failures in women who did not receive WBRT following lumpectomy were 20.5%, 25.7%, and 5.7%, whereas for those who received WBRT following lumpectomy were 5.4%, 5.5%, and 2.2%. For these studies, the median follow-up time was 109, 43, and 33 months and included women with tumours not greater than 2.5 cm, 4 cm, and 2 cm, respectively.

1.2. Accelerated Partial Breast Irradiation (APBI)

Clinical evidence has shown that the majority of recurrences after lumpectomy are located around the surgical cavity (9). As noted by Arthur (10), prospective randomized studies have shown that between 4% and 22% of patients have recurrences at the site of lumpectomy and between 1% and 4% had recurrences elsewhere in the breast for lumpectomy treatments without WBRT (11-13). This data suggests that the entire breast does not need to be treated; the target requiring radiotherapy following lumpectomy is located in the 1 to 2 cm boundary region around the surgical cavity (8). If the volume of breast tissue treated is decreased, it may be possible to decrease the treatment time. In fact, a five day treatment is feasible if the target is reduced to less than 50% of the entire breast (8). Therefore, accelerated partial breast irradiation (APBI) has emerged as an alternative to WBRT.

APBI can be delivered using both brachytherapy and external beam techniques. Historically, the first was multicatheter-based interstitial APBI, which was originally developed to boost WBRT (8). For this treatment modality, 14 to more than 20 after-

loading catheters are placed around the surgical cavity (8). They are generally placed in intervals of 1 to 1.5 cm; the exact number of catheters is chosen to ensure proper dose coverage (10). Despite the invasive nature of the procedure, the majority of patients tolerate the treatment very well, with a minimal need of pain medication (8). A balloon-catheter APBI treatment has also been developed. The MammoSite® Radiation Therapy System, originally developed by Proxima Therapeutics Inc. (Alpharetta, GA, USA), is a balloon catheter system designed to simplify the procedure and improve reproducibility (8, 10). The system consists of a balloon with a centrally-located 15-cm double lumen catheter; the catheter is 6 mm in diameter and the diameter of the balloon can range from 4 to 5 cm or 5 to 6 cm (8). The balloon is inserted into the surgical cavity during or after excision and the treatment is delivered with a single, high-dose rate source to a distance 1 cm from the surface of the balloon (8).

APBI has also been administered in Europe using intraoperative radiotherapy. These treatments consist of one large fraction delivered at the time of surgery. The University College of London delivered this type of treatment using 50 kV x-rays, with prescription doses of 5 Gy and 25 Gy at depths of 1 cm and 0.2 cm (8). An alternate approach was used by the European Institute of Oncology in Milan where 21 Gy was delivered using 3 to 9 MeV electrons to patients following partial mastectomy (8).

As a result of technical innovations in external beam radiotherapy, APBI can also be delivered using three-dimensional conformal external beam radiotherapy (3DCRT). Unlike brachytherapy techniques, 3DCRT is attractive since it is non-invasive and it delivers a homogeneous dose distribution with decreased trauma to breast tissue (8). In 3DCRT APBI, four or five non-coplanar MV photon beams from a linear accelerator

are used to treat the surgical cavity. Unlike WBRT, the fields are non-opposing and require couch rotations. In order to plan the treatment, a radiation oncologist will contour the surgical cavity on a planning CT scan. The surgical cavity can be difficult to contour and may not be visible three to four months following excision (14). Treatment volumes as defined by ICRU Report No. 50 are used for planning. The clinical target volume (CTV) is the demonstrable tumour tissue and/or microscopic extent of the disease that needs to be treated; the CTV is the volume that must be treated in order to adequately treat the disease (15). The planning target volume (PTV) is the volume used to select appropriate beam arrangements to ensure that the CTV is adequately treated taking into account any setup uncertainties, patient motion (e.g., respiration), and other geometric uncertainties (15). The PTV is used to shape the treatment fields. For APBI, the CTV is defined as the surgical cavity plus a 1-cm symmetric margin, except for those portions that lie within 5 mm of the skin surface or within the chest wall or pectoralis major muscle. The PTV is defined as the CTV plus a 1-cm symmetric margin. In many cases, the PTV can extend outside the body or inside the chest wall and lung; hence, a dose evaluation volume (DEV) is defined as the portion of the PTV that lies within 5 mm from the skin surface and does not extend into the chest wall or pectoralis major muscle. The DEV is used for plan optimization. Typically, 38.5 Gy are prescribed to the surgical cavity and treatment is delivered in 10 fractions given twice daily (i.e., five day treatment time). Each dose delivery must be separated by six to eight hours to allow recovery of normal tissues (14). Figure 1.2 shows a typical field arrangement and dose distribution for 3DCRT APBI.

Since only a portion of breast tissue is treated, there may be a potential reduction to normal breast toxicity when using 3DCRT (8). However, this technique can significantly increase integral dose received by surrounding normal tissues and its consequences are largely unknown (8). Normal tissues of particular interest are the ipsilateral lung, heart, contralateral breast, and thyroid. Hence, conservative dose constraints are used for planning and this limits the patients who can be treated with 3DCRT (8). Table 1.1 shows typical dose-volume constraints used for APBI planning. The dose constraints that are hardest to meet during planning are those on the contralateral breast and heart. For example, high doses can be delivered to portions of the heart for left-breast patients treated with four fields, as is shown in Figure 1.2(b). A fifth treatment field is often used to help meet the heart's dose constraint for left-breast treatments. Intensity-modulated radiotherapy (IMRT) may also be used for APBI. In fact, it has been recently reported that IMRT improves normal tissue sparing in the ipsilateral breast when compared to 3DCRT (16). Another treatment planning study has also shown that 3DCRT, IMRT, and tomotherapy provided treatment plans that are more conformal than WBRT without significantly increasing the dose to normal structures, while maintaining dose homogeneity in the surgical cavity (17).

Several phase I and II clinical trials have been completed to investigate the clinical equivalence of WBRT and APBI in local control, such as freedom from in-breast failure and recurrence-free survival. Vicini *et al.* (18, 19) treated 199 patients with interstitial brachytherapy following lumpectomy. Each patient was matched with one from a database of 1,388 patients who had previously received WBRT. It was found that there were no statistically significant differences in breast failures between APBI and

WBRT, as well as no statistically significant differences in the rates of distant metastasis and disease-free survival (18, 19). Several other studies have shown similar results for in-breast failures and have reported that the proportion of patients with good to excellent cosmesis following APBI is greater than 75% (10, 20-25). Phase III clinical trials are ongoing to validate these results. Currently, the National Surgical Adjuvant Breast and Bowel Project (NSABP) and the Radiation Therapy Oncology Group (RTOG) in the United States are completing a phase III randomized trial in APBI (NSABP B-39; RTOG-0413). In particular, the study is examining multicatheter, MammoSite®, and 3DCRT APBI modalities (26). The Randomized Trial in Accelerated Partial Breast Irradiation (RAPID) is the phase III randomized trial currently ongoing in Canada to compare 3DCRT APBI and WBRT (14).

Localization of the surgical cavity in APBI is of the utmost importance because of the large dose per fraction delivered during treatment. Any differences in the shape and position of the surgical cavity between planning and treatment, or during treatment, can result in a geographic miss of the target. Contouring of the surgical cavity is critical in its localization and difficulty in visualizing the cavity may result in large contour variability amongst radiation oncologists. A study by Landis *et al.* (27) showed that surgical cavities that appeared more heterogeneous on CT scans and had more distinct borders had lower shifts in centre-of-mass and significantly more overlap of volumes contoured by multiple observers. In addition, it has been reported that proper guidelines and training improve consistency in surgical cavity contouring (28). Several studies have also endeavoured to improve localization of the surgical cavity during treatment. For example, MV computed tomography (CT) images obtained using a

tomotherapy unit resulted with improved alignment to the surgical cavity to 2 mm (29). It also has been reported that the use of cone beam CT (CBCT) may minimize large random setup errors which can have a great impact on APBI and its use may allow reduction in the PTV margins (30). Surgical clips can also be placed in the cavity at the time of excision. A study by Hasan *et al.* (31) has shown that the use of the breast surface or surgical clips as surrogates for the surgical cavity results in improved localization as compared to bony registration. Moreover, CBCT localization of the surgical cavity using surgical clips is feasible and possibly may allow reduction of the PTV margins (32).

Ongoing at the BC Cancer Agency Fraser Valley Center is the DIVA Project: development of an improved target volume localization technique for APBI utilizing new image guidance technology. The project is a two-phase feasibility study whose ultimate goal is to develop improved surgical cavity localization in APBI through the use of image-guided technologies such as CBCT, MV cine acquisition, and kilovoltage (kV) x-ray (33). The first stage (Stage I) is investigating whether skin markings placed around the surgical scar (as required by the RAPID trial) are representative of the location of the surgical cavity by quantifying any changes in the position of the surgical cavity and skin markings; dosimetric consequences of changes in the surgical cavity's position and size will also be examined (33). Figure 1.3 shows the location of the skin markings placed on the patient. The second stage (Stage II) aims to investigate the use of the aforementioned imaging techniques to improve localization of the surgical cavity (33). Continued research into these on-board imaging techniques may allow the decrease of the surgical cavity planning margins.

1.3. Purpose of this Thesis

Any studies that endeavour to investigate changes in size or position of the surgical cavity must include an analysis of interobserver and intraobserver contouring variability. This is important since any perceived changes in the surgical cavity's size or position cannot be further understood unless any potential interobserver and intraobserver variability in the contours are accounted for properly. The goal of the work presented in this thesis is to establish any interobserver and intraobserver surgical cavity contour variability that may be important in Stage I of the DIVA project. In addition, a preliminary analysis for Stage I of the relationship between the skin markings and the centre-of-mass of the surgical cavity is completed.

Hence, the purpose of this thesis is threefold. Firstly, a method is developed to calculate a representative surgical cavity (RSC) using surgical cavity contours delineated by several radiation oncologists or repeat contours from a single radiation oncologist. Secondly, the RSC is used to assess interobserver and intraobserver surgical cavity contour variability. It is important to investigate whether the resultant planning volume, created from the CTV and PTV margins applied to the planning surgical cavity, will be sufficient to contain the surgical cavities as contoured by other radiation oncologists. Primarily, this is done by ensuring adequate dosimetric coverage of the surgical cavity as contoured by multiple oncologists. Dosimetric coverage during treatment is assessed by reapplying planning fields to CT scans obtained during treatment. Lastly, correlations between changes in the position of the RSC centre-of-mass (COM) and skin markings during treatment are quantified in order to determine if patient setup using the skin markings is feasible.

Table 1.1 Dose-volume constraints used for APBI planning in the RAPID trail

Dose-volume constraints used for planning 3DCRT APBI in the RAPID trial are shown.

Structure	Dose-volume Constraint[1,2,3]
DEV	$V_{95} = 100\%$, maximum dose of 41.20 Gy (107%) to an area of 2 cm^2
Ipsilateral Lung	$V_{30} \leq 10\%$
Ipsilateral Breast	$V_{95} < 25\%$ (up to 35%), $V_{50} < 50\%$ (up to 60%)
Contralateral Breast	$D_{max} = 11.55$ Gy (3%)
Thyroid	$D_{max} = 11.55$ Gy (3%)
Heart:	
right breast	$D_5 \leq 1.93$ Gy (5%)
left breast, except LIQ[4]	$D_5 \leq 3.85$ Gy (10%)
left breast, LIQ	$D_5 \leq 5.78$ Gy (15%)

1. V_x is the volume of a structure that receives a dose of at least x% of the prescribed dose.
2. D_x is the maximum dose received by x% of the total volume of the structure. Doses as a percent of the prescription dose are shown in parentheses.
3. D_{max} is the maximum dose.
4. LIQ: lower inner quadrant.

Figure 1.1 Whole-breast radiotherapy field arrangement and dose distribution

(a) A typical field arrangement for whole breast radiotherapy. The surgical cavity is shown in blue. Orientation of wedges is shown in orange. (b) The dose distribution for the field arrangement show in (a). Green and yellow lines show the 95% and 103% isodose lines. Orientation of wedges is shown in orange.

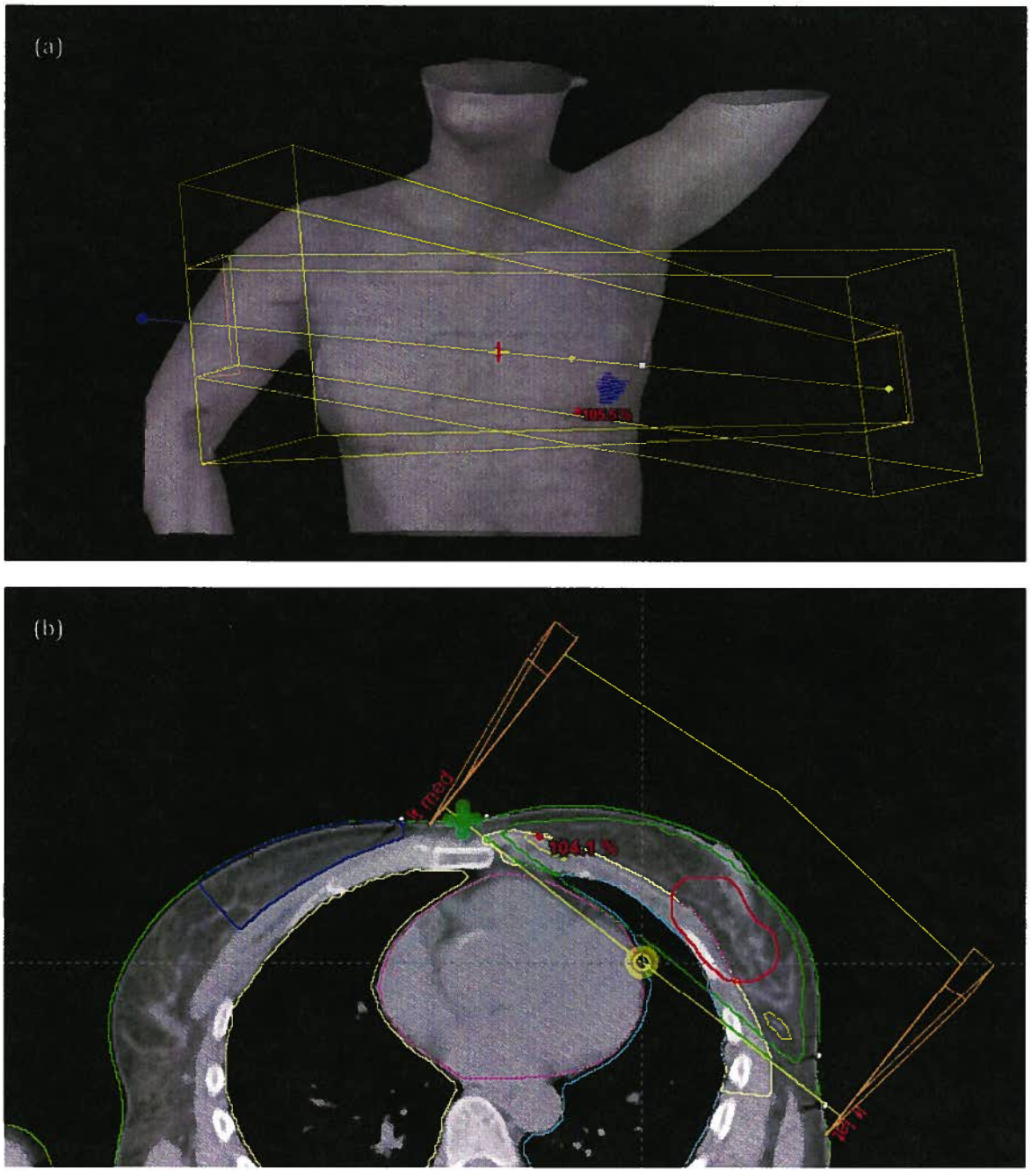

Figure 1.2 APBI 3DCRT field arrangement and dose distribution

(a) A typical field arrangement for APBI. (b) The dose distribution for the field arrangement shown in (a). The CTV, PTV, and DEV are shown in orange, red, and magenta. The 95% and 90% isodose lines are shown in green and blue.

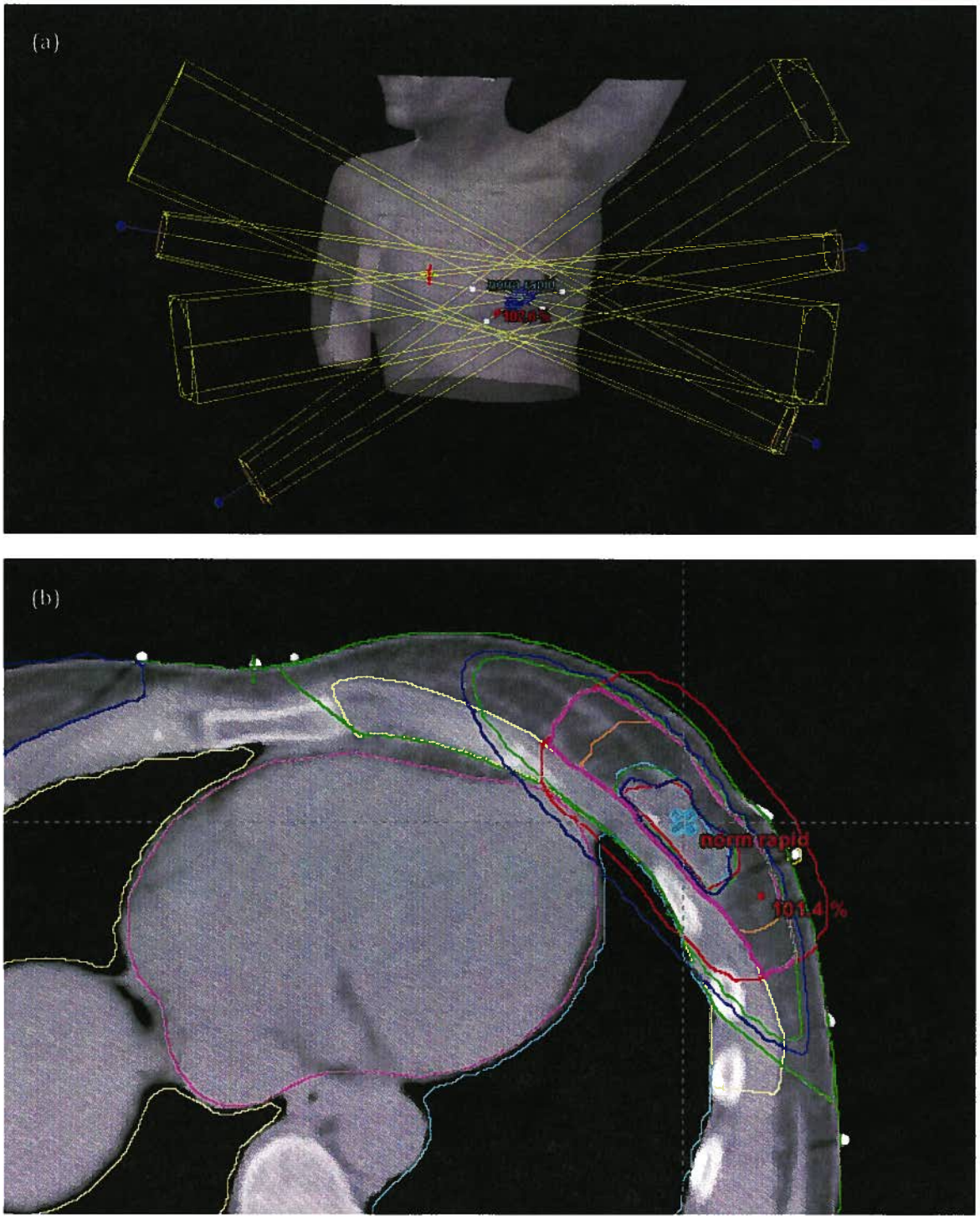

Figure 1.3 Skin markings placed around the surgical scar in the RAPID trial

Skin markings placed on the patient as required by the RAPID trial are shown in yellow. Four markings are placed around the surgical scar and one is placed lateral and posterior to the scar. The surgical cavity contours are shown in blue.

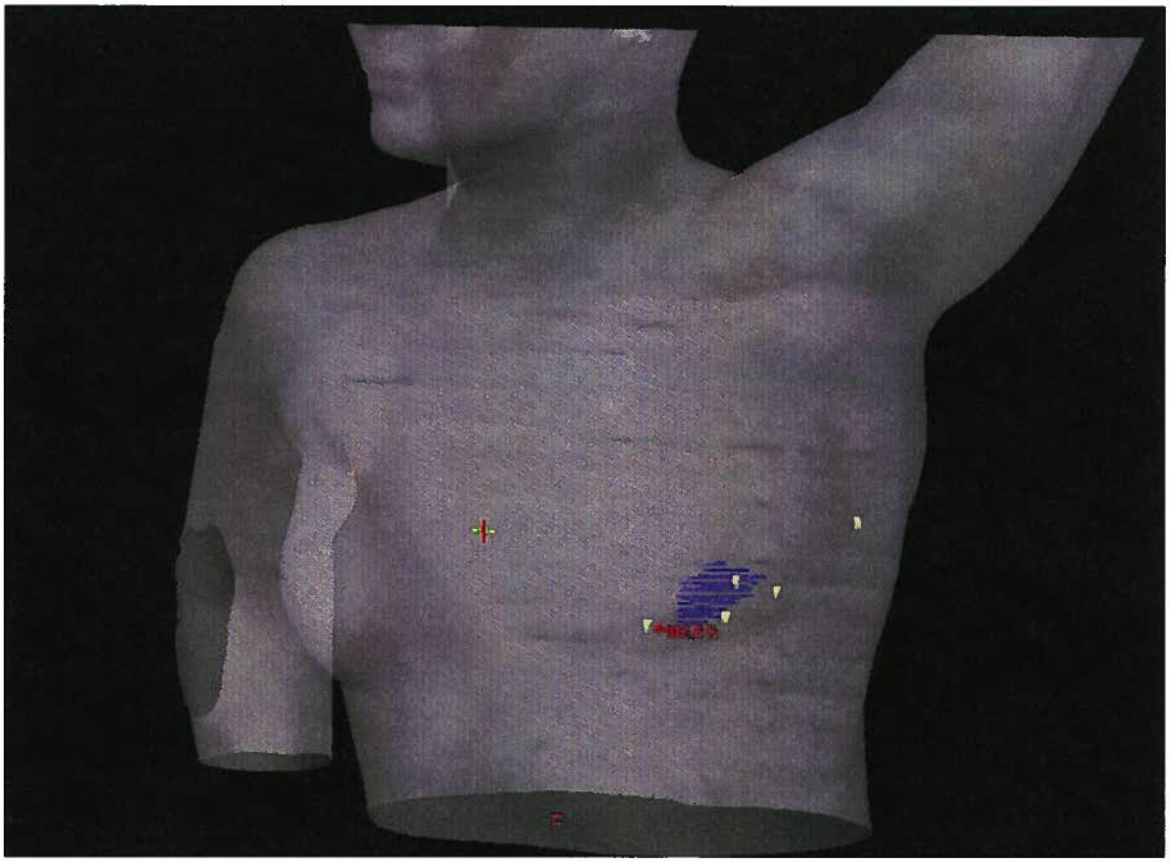

2. DATA ACQUISITION AND THE REPRESENTATIVE SURGICAL CAVITY

2.1. Delineation of the Surgical Cavity

Data from twelve patients enrolled in the RAPID and DIVA studies were analyzed for assessment of surgical cavity contour variability and changes in the positions of the skin markings. Patients received four CT scans: one CT scan at the time of planning and three repeat CT scans on days one, three, and five of treatment. Research ethics board (REB) approval was obtained for repeat CT scans. Patients were setup during CT scans to the treatment position required by the RAPID trial and radio-opaque markers were placed on the anterior and medial setup tattoos and skin markings on the patient.

Three experienced radiation oncologists contoured the surgical cavity on each CT scan in Eclipse™ (Varian Medical Systems, Palo Alto, CA, USA) for all patients. Sample contours are shown in Figure 2.1. The radiation oncologists also recorded the cavity visualization score (CVS) for the surgical cavity at the time of contouring. The CVS ranges from 1 to 5, where CVS 1 indicates the cavity cannot be visualized and CVS 5 indicates the presence of a heterogeneous cavity with well defined margins (27). In addition, two repeat contours were delineated by the radiation oncologists on all CT scans for three patients in order to assess intraobserver contour variability. The positions of the skin markings were recorded in Eclipse™ by locating each skin marking on the CT scans and placing a reference point at its position. The reference frame for all measurements was a Cartesian coordinate system centred at each patient's anterior tattoo with the positive x, y, and z directions defined to be in the left, posterior, and superior directions. An example of the coordinate system for a sample patient is shown in Figure 2.2.

The coordinates of the contour points and the skin markings were exported from Eclipse™ to in-house software created using MATLAB® (The MathWorks, Natick, MA, USA). The in-house software was used to construct a representative surgical cavity (RSC) for each CT scan using the contours on the given CT scan. The contour coordinates of the RSC were then imported to Eclipse™, where all dose calculations were completed.

2.2. Calculation of the Representative Surgical Cavity

In order to take into account variations in the surgical cavity, a contour that combines contributions from multiple contours has to be constructed. In the studies described here, this contour is called the RSC and it can be considered to be an average of the multiple contours. In the most ideal case, the RSC would coincide with the actual surgical cavity.

Previous studies examining interobserver and intraobserver prostate contour variability have also used the concept of a representative or mean contour. In a study by Deurloo *et al.* (34), a mean gross tumour volume (GTV) was used to assess changes in the volume and shape of the prostate and seminal vesicles. Using multiple GTV contours, a coverage probability matrix was constructed. This was accomplished by scoring how many times each volume element, or voxel, in a 1-mm grid was inside each GTV contour. The 50% isosurface of the coverage probability matrix was then used to define the mean GTV. A disadvantage of this method is that a large number of contours are required in order to create an adequate coverage probability matrix. In this study, 9

to 13 (12 on average) were used to construct the mean GTV (34). Since only three contours are available in this study, this method for RSC construction is not ideal.

In another contour variability study, Song *et al.* (35) constructed a mean prostate surface using the structures delineated by several radiation oncologists. First, the two-dimensional contours were used to create a three-dimensional tessellated prostate surface using a symmetric-correspondence algorithm (35, 36). The mean prostate surface is then calculated by finding the mean radial distance along a ray from the centre-of-mass (COM) of the prostate contours for multiple azimuthal and polar angles. In this study, the contours of seven observers were used to construct the mean prostate surface (35). This method is most easily used for surfaces that have regular shapes, such as the prostate. Surfaces that have concavities would be more difficult to approach using this method since the rays used to construct the mean surface may intersect a single surface multiple times. Surgical cavity contours can have such irregular shapes and hence a more detailed approach must be taken to calculate a mean contour.

A hybrid of these mean contour calculation methods was used to construct the RSC using the contours that had been delineated. In this study, the RSC was defined as the mean surgical cavity contour on each CT slice where at least 50% of the structures have been contoured. For example, if four separate surgical cavity contours were delineated on a CT scan, then the RSC would only be calculated on CT slices where two or more of the contours were present. In order to calculate the RSC on a given CT slice, a reference point was chosen to calculate the mean surgical cavity contour. The reference point was chosen to ensure that it is central to all surgical cavity contours. The COM of the contours on a CT slice could be used for the reference point, similar to the approach

by Song *et al.* (35), as long as the reference point does not lie outside one or more of the surgical cavity contours. However, the variation in the shapes of the surgical cavity contours was observed to be large enough for the COM to lie outside a contour. Hence, it was not an appropriate choice for the reference point. However, the COM of the area common to all contours will lie within all surgical cavity contours, as is shown in Figure 2.3. Hence, the reference point was calculated by finding the COM of the area common to all contours on a given CT slice. This was done by affixing a 1-mm square grid to the CT slice and scoring how many times each voxel was inside the grid. The voxels which were within all contours were then used to calculate the reference point.

The reference point on a CT slice was used to define the origin of a polar coordinate system. The mean surgical cavity contour was then calculated by finding the mean radial distance from the reference point for several polar angles. Hence, it was necessary to interpolate the surgical cavity contours on each CT slice to a common set of 200 equally spaced angles θ ($-180° < \theta \leq 180°$, $\Delta\theta = 1.8°$). This was accomplished by defining a Cartesian axis (x', y') at the reference point with θ defined as the angle from the positive x'-axis. Each surgical cavity contour was rotated around the reference point and the radial distance $r_i(\theta, z)$ for contour i at angle θ on slice z was calculated from the intersection of positive y'-axis and the line that connects the two points closest and on either side of the positive y'-axis. This process is illustrated in Figure 2.4. First, the contour was rotated by 270° so that the first point that is interpolated is near $\theta = -180°$ (Figure 2.4). The contour is then rotated clockwise by $\Delta\theta$ and the next radial distance is interpolated (Figure 2.5). If there are multiple intersections of the positive y'-axis and the contour, the contour can be rotated in the opposite direction to ensure

that all radial distances are properly interpolated. An example of this situation is shown in Figure 2.6. This process continues until all radial distances $r_i(\theta, z)$ have been calculated, as is shown in Figure 2.7.

Once all interpolated surgical cavity contours were obtained, the RSC was calculated by finding the mean radial distance of the interpolated radial distances of each contour. Example of RSC contours are shown in Figure 2.8. The calculation of the RSC is straightforward if there is only a single radial distance interpolated for each contour. This situation is illustrated in Figure 2.8(a). In this situation, the radial distance $r_{\text{RSC}}(\theta, z)$ for the RSC is

$$r_{\text{RSC}}(\theta, z) = \frac{1}{N}\sum_{i=1}^{N} r_i(\theta, z)\,. \tag{2.1}$$

However, more care must be taken in calculating the RSC radial distances if there are multiple interpolated distances for any of the contours (i.e., interpolation of a contour involved multiple intersections). In these situations, the multiple radial distances can be grouped to calculate multiple RSC radial distances for one angle. For example, if contours have two radial distances each for a given angle, the innermost radial distances can be used to calculate one contour point for the RSC and the outermost radial distances can be used to calculate another RSC contour point. This situation is illustrated in Figure 2.8(b). In some cases, the interpolated distances could not be grouped and thus the RSC radial distance could not be calculated; the RSC calculations for these angles were omitted. This situation is also illustrated in Figure 2.8(b). Although omission of angles is not ideal, in practice this was sufficient to create the RSC since a large number of angles were used in the calculation.

Once the RSC radial distances were calculated, the contour points needed to be reordered to ensure that points will be connected properly by the treatment planning software. This was only necessary when multiple radial distances for an angle were calculated for the RSC contour. This reordering was accomplished by finding the nearest neighbour for each point. Once the points were properly reordered, the RSC calculation on a given CT slice was complete. This process was repeated on all CT slices where at least 50% of the contours were present.

Figure 2.1 Surgical cavity contours from several radiation oncologists

The surgical cavity contours of three radiation oncologists are shown in blue, purple, and yellow. Other contours visible are the heart (magenta), chest wall (yellow), ipsilateral breast (green), and surface (brown).

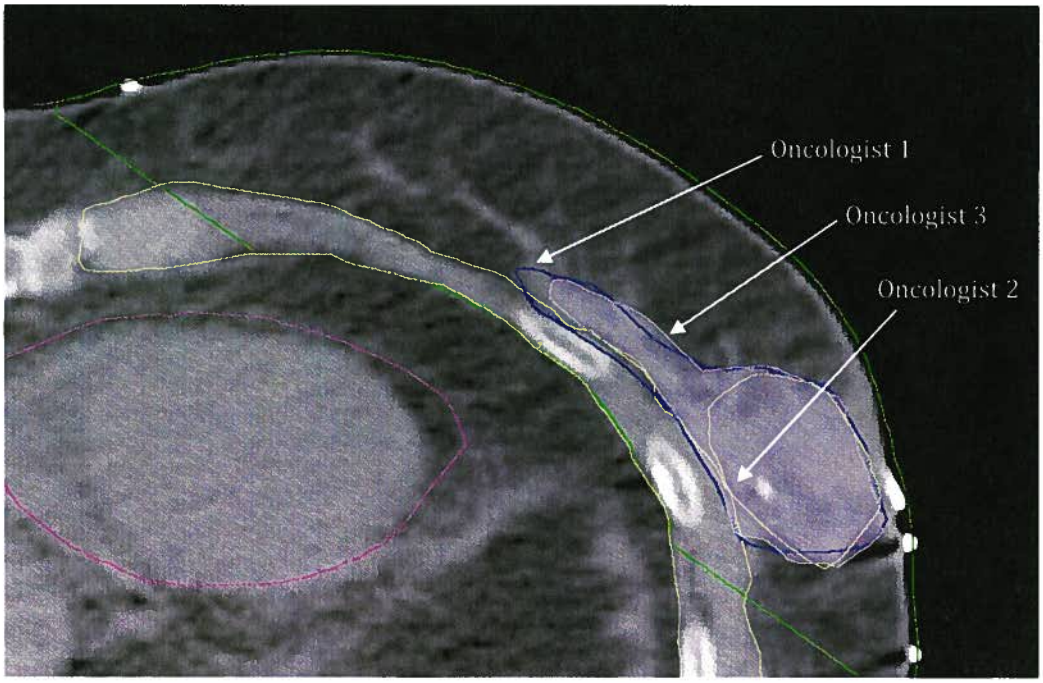

Figure 2.2 Coordinate system used for measurements

The Cartesian coordinate system used for all measurements is shown. The positive x, y, and z directions are in the left, posterior, and superior directions. The origin is located at the patient's anterior tattoo (as shown here for a patient treated for a left-sided lesion).

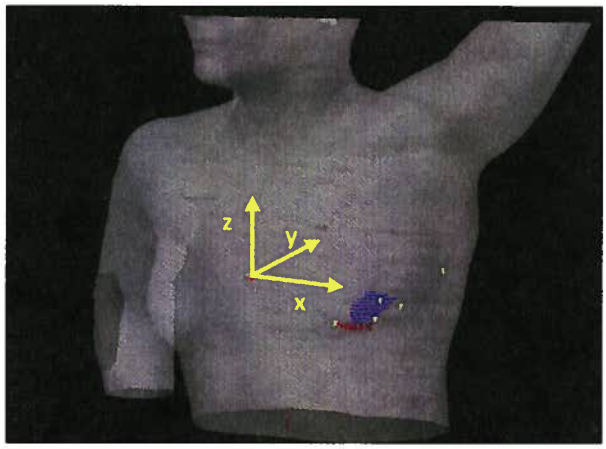

Figure 2.3 Reference point location used for interpolation and RSC calculations

The reference point used for interpolation of contours and RSC calculations was calculated by finding the centre-of-mass of the area that is common to all contours.

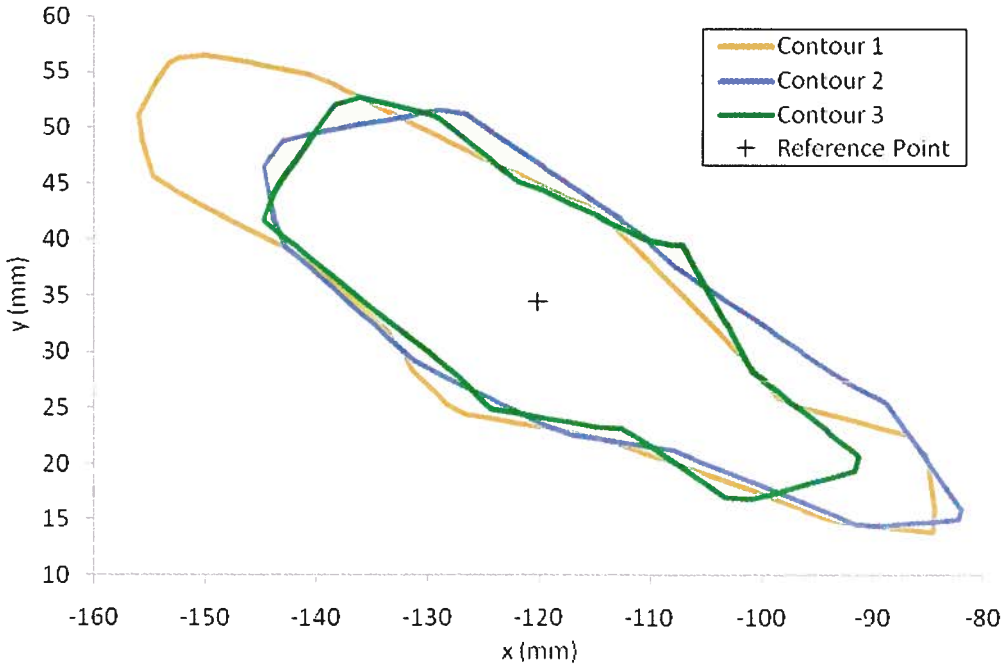

Figure 2.4 First step of the interpolation process used for surgical cavity contours

An example of interpolation of a surgical cavity contour with the reference point located at the origin. (a) The original contour provided by a radiation oncologist is shown in blue. (b) The contour is rotated to the first interpolation point (near −180°). A point (red) is interpolated by finding the intersection of the original contour with the y'-axis.

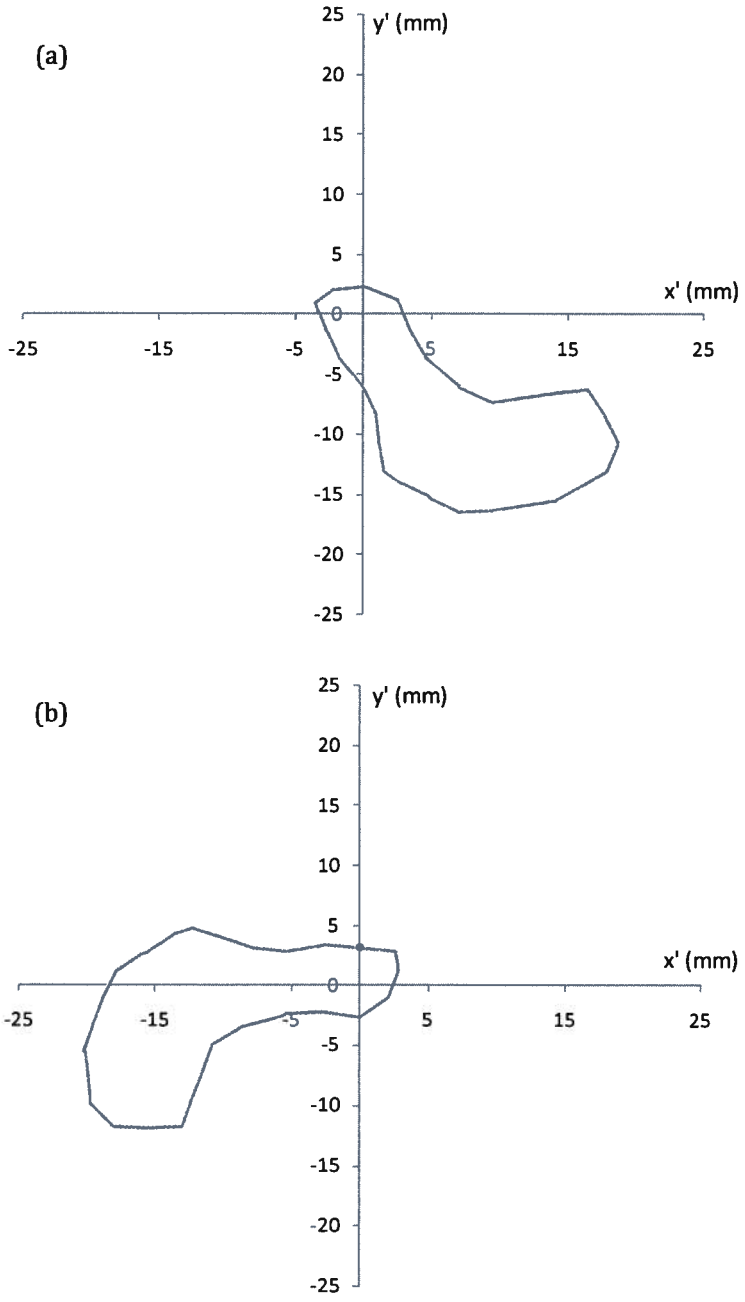

Figure 2.5 Continuation of the interpolation process

A continuation of the interpolation process from Figure 2.4. The original contour is shown in blue. The interpolated points are shown in red. (a) The contour is continued to be interpolated by rotating it clockwise. (b) The contour is further interpolated. Gaps in the interpolation can occur in instances when the contour lines are in the radial direction.

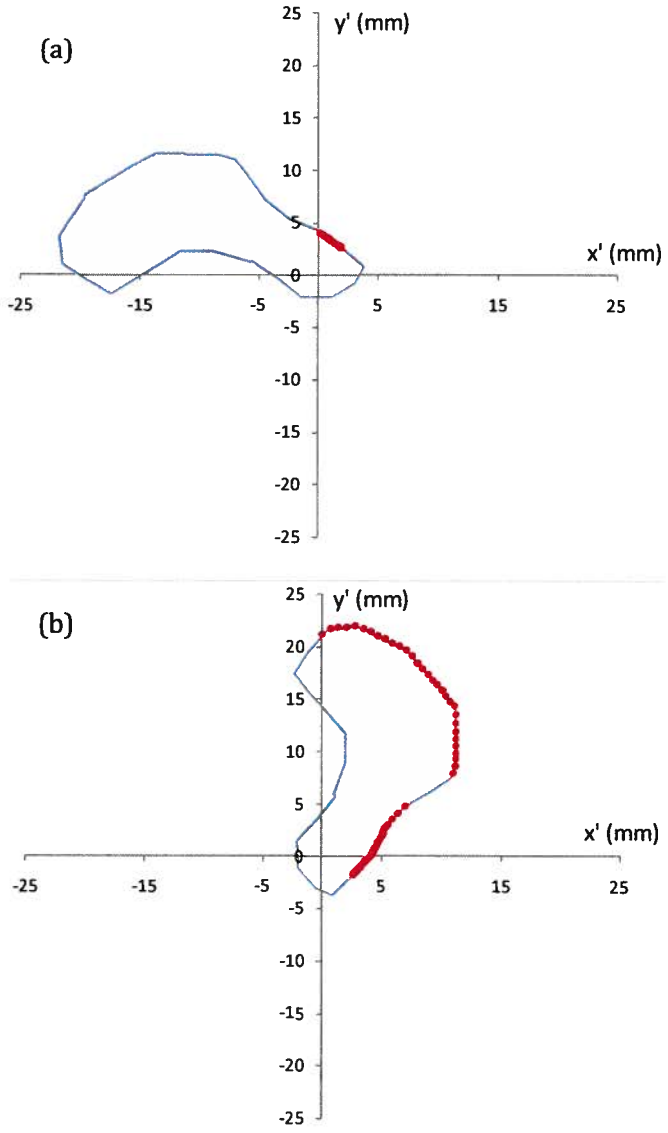

Figure 2.6 Dealing with multiple intersections during interpolation

A continuation of the interpolation process from Figure 2.5. The original contour is shown in blue. The interpolated points are shown in red. (a) At this point, the contour must be rotated counter-clockwise in order to continue interpolating points. (b) The contour continues to be rotated counter-clockwise in order to interpolate points.

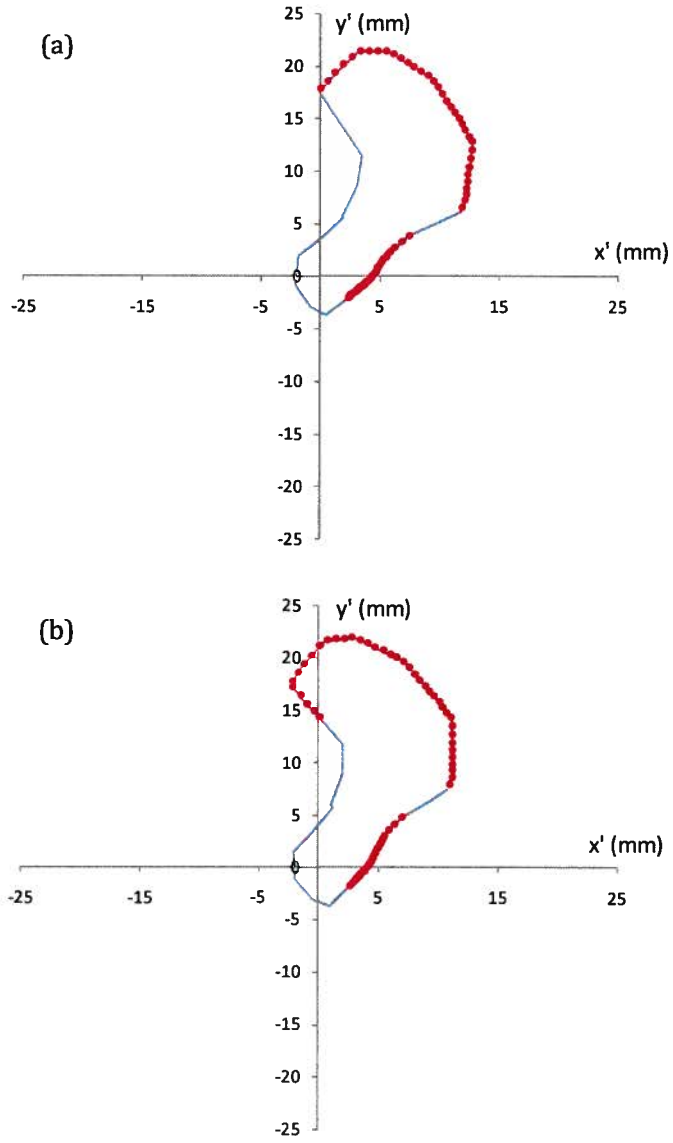

Figure 2.7 Example of an interpolated surgical cavity

The interpolation process continues until points have been interpolated for all 200 angles. This is the final interpolated contour from Figure 2.6. The original contour is shown in blue. The interpolated points are shown in red.

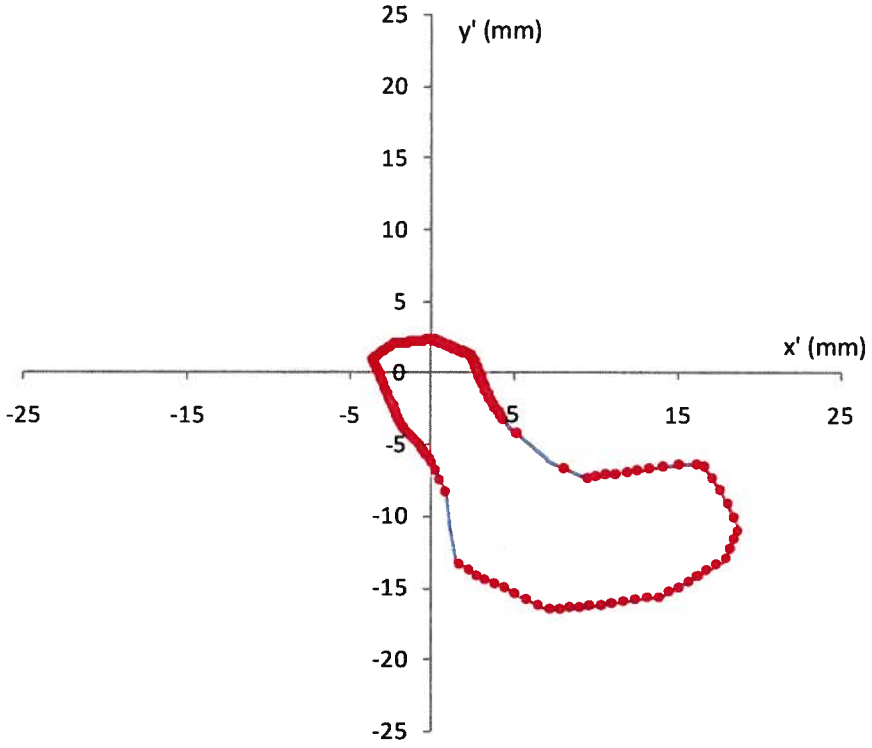

Figure 2.8 Examples of the representative surgical cavity (RSC)

(a) An example of the RSC (red) calculated on a slice with three contours (orange, blue, and green). (b) Despite the complex shape of the contours in this example, the RSC can still be calculated by grouping of radial distance when there are multiple radial distances. In some cases the RSC cannot be calculated for angles where grouping is not possible, as is shown.

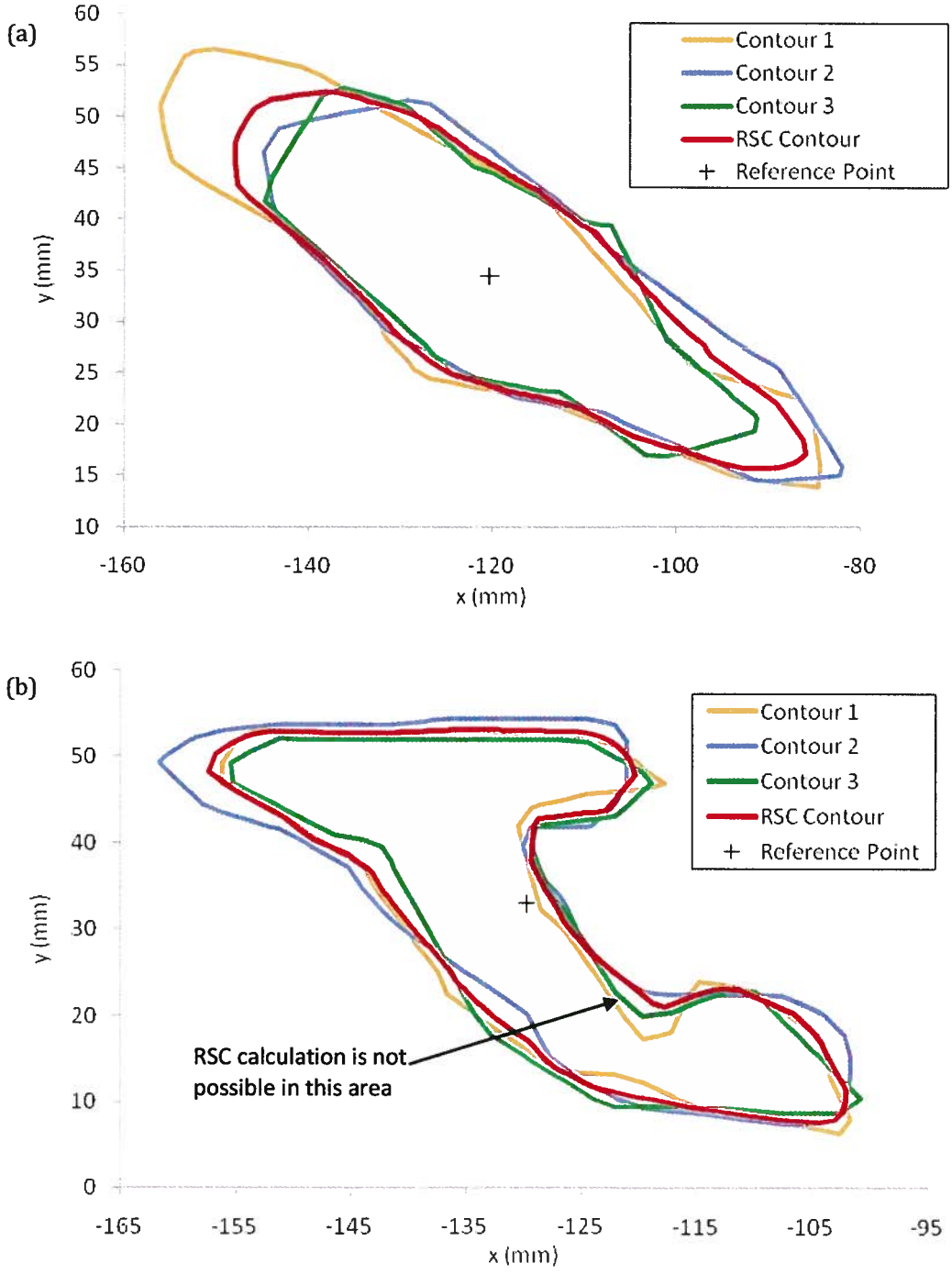

3. VARIABILITY OF THE SURGICAL CAVITY CONTOUR AND SKIN MARKINGS

3.1. Introduction

Localization of the surgical cavity is of the utmost importance in APBI during planning and throughout treatment. Thus, a preliminary study was completed to assess the degree of interobserver and intraobserver variability in the surgical cavity volume and COM. Then, more thorough interobserver and intraobserver contour variability studies were completed by comparing the surgical cavity contours from the radiation oncologists with a RSC. Previous prostate and breast multi-observer studies quantified differences between contours through volume-based (27, 28, 35, 37-40) and distance-based measurements (27, 34, 35, 39). In addition, the dosimetric consequences of contour variations have also been assessed (38). The interobserver and intraobserver surgical cavity contour variability studies described below use similar methods to quantify differences.

The RSC by definition is the structure that is expected to be contoured on average. In other words, the RSC is similar to a mean surgical cavity contour. Therefore, the differences between the surgical cavity contours and RSC can be used to quantify interobserver and intraobserver contour variability. Differences between the RSC and surgical cavity contours will quantify interobserver variability if the RSC is constructed using the contours of different radiation oncologists. On the other hand, intraobserver contour variability can be quantified by constructing the RSC using the repeat contours of a single radiation oncologist.

The RSC COM can also be used to denote the expected position of the surgical cavity in each CT scan. Hence, changes in the RSC COM between planning and treatment

were compared to changes in the position of each patient's skin markings to determine if the skin markings are representative of the position of the surgical cavity.

3.2. Preliminary Study

A preliminary study into interobserver and intraobserver contour variability was first undertaken in order to become familiar with the degree of variations in delineations of the surgical cavity. The preliminary study did not include an analysis of the RSC. The goal of the preliminary study was to quantify the maximum interobserver and intraobserver volume and COM variations for three patients. The volumes and COM of each contour (including repeat contours) were calculated by superimposing a 1-mm × 1-mm × 3-mm grid on each contour. For each CT scan, the maximum change in volume and COM position was computed using all contours to assess interobserver differences. This was repeated using the contours of a single radiation oncologist for all oncologists to assess intraobserver differences.

3.3. Interobserver Contour Study

3.3.1. RSC Construction and Volume-based Measurements

Interobserver variations were assessed by quantifying the differences between the delineated surgical cavity contours and RSCs. In the interobserver study, the RSC was constructed using the contours of all three radiation oncologists on each CT scan for all twelve patients. Contour variability was assessed using volume-based, distance-based, and dose measurements.

The volume of each surgical cavity contour and RSC was calculated by superimposing a 1-mm × 1-mm × 3-mm grid on each contour and counting the number of voxels that were inside each contour. The grid thickness in the superior-inferior direction was chosen to be 3 mm to match the CT slice thickness. Interobserver volume differences from the RSC were calculated by finding the root-mean-square (RMS) of the difference in volume from the RSC on each CT scan for every patient. The RMS difference in volume from the RSC (δV) is given by

$$\delta V = \sqrt{\frac{1}{N}\sum_{i=1}^{N}(V_i - V_{\mathrm{RSC}})^2}\ , \tag{3.1}$$

where V_i are the volumes of the surgical cavities delineated by the radiation oncologists, V_{RSC} is the volume of the RSC, and N is the number of contours used to construct the RSC ($N = 3$).

Volume variability was also quantified by comparing the volume that is common to all surgical cavity contours with the volume that is encompassed by all surgical cavity contours. The use of common and encompassing volumes was used by Rasch *et al.* (40) and has been used in several studies of interobserver and intraobserver volume variations (27, 35, 41). The common volume V_{common} is defined as the largest volume that is common to all contours and the encompassing volume $V_{\mathrm{encompassing}}$ is defined as the smallest volume that contains all contours (35, 40). Figure 3.1 illustrates the differences between the common and encompassing volumes. Variability can be assessed by calculating the ratio of V_{common} and $V_{\mathrm{encompassing}}$ (27, 41) or by calculating the percent difference Δvol in V_{common} and $V_{\mathrm{encompassing}}$ (35), where

$$\Delta\text{vol} = \frac{V_{\text{encompassing}} - V_{\text{common}}}{V_{\text{encompassing}}} \times 100\% . \quad (3.2)$$

The percent difference ranges from 0% to 100%, where 0% indicates that all contours are identical ($V_{\text{encompassing}} = V_{\text{common}}$) and 100% indicates that contours do not overlap ($V_{\text{common}} = 0$) (35).

In the interobserver study, Δvol was calculated to quantify volume variability. The common and encompassing volumes were calculated on each CT scan for all patients by superimposing a 1-mm × 1-mm × 3-mm grid on the surgical cavity contours and scoring the number of times each voxel in the grid was inside a contour. The percent difference in volumes was then calculated on every CT scan for each patient using Equation 3.2.

3.3.2. Distance-based Measurements

Changes in the COM and spatial dimensions of the surgical cavities and the RSC were used to quantify spatial interobserver contour variability. The COM of each surgical cavity and RSC on each CT scan was calculated by superimposing a 1-mm × 1-mm × 3-mm grid on each contour. The COM was calculated relative to the position of the anterior tattoo on each patient. The spatial dimensions of each contour were calculated in the superior-inferior (SI), anterior-posterior (AP), and lateral directions by finding the range in SI, AP, and lateral contour coordinates for each surgical cavity contour and the RSC on each CT scan.

To compare the COM of the surgical cavity contours and the RSC, the RMS difference in COM from the RSC was calculated in the lateral (δx_{COM}), AP (δy_{COM}), and SI (δz_{COM}) directions on each CT scan. The RMS differences in COM are given by

$$\delta x_{\mathrm{COM}} = \sqrt{\frac{1}{N}\sum_{i=1}^{N}\left(x_{\mathrm{COM},i} - x_{\mathrm{COM,RSC}}\right)^2}, \tag{3.3}$$

$$\delta y_{\mathrm{COM}} = \sqrt{\frac{1}{N}\sum_{i=1}^{N}\left(y_{\mathrm{COM},i} - y_{\mathrm{COM,RSC}}\right)^2}, \tag{3.4}$$

$$\delta z_{\mathrm{COM}} = \sqrt{\frac{1}{N}\sum_{i=1}^{N}\left(z_{\mathrm{COM},i} - z_{\mathrm{COM,RSC}}\right)^2}, \tag{3.5}$$

where $(x_{\mathrm{COM},i}, y_{\mathrm{COM},i}, z_{\mathrm{COM},i})$ is the COM coordinates of the surgical cavity contoured by radiation oncologist i, $(x_{\mathrm{COM,RSC}}, y_{\mathrm{COM,RSC}}, z_{\mathrm{COM,RSC}})$ is the COM coordinates of the RSC, and N is the number of contours used to construct the RSC.

Similarly, the RMS difference in the spatial dimensions from the RSC was calculated on every CT scan in the lateral (δx), AP (δy), and SI (δz) directions. The RMS differences in spatial dimensions are given by

$$\delta x = \sqrt{\frac{1}{N}\sum_{i=1}^{N}(x_i - x_{\mathrm{RSC}})^2}, \tag{3.6}$$

$$\delta y = \sqrt{\frac{1}{N}\sum_{i=1}^{N}(y_i - y_{\mathrm{RSC}})^2}, \tag{3.7}$$

$$\delta z = \sqrt{\frac{1}{N}\sum_{i=1}^{N}(z_i - z_{\mathrm{RSC}})^2}\,, \tag{3.8}$$

where x_i, y_i, and z_i are the lateral, AP, and SI dimensions of the surgical cavity contoured by radiation oncologist i, x_{RSC}, y_{RSC}, and z_{RSC} are the lateral, AP, and SI dimensions of the RSC, and N is the number of contours used to construct the RSC.

In addition, spatial interobserver contour variability was quantified by calculating the standard deviation (SD) at each point where the RSC was calculated on each CT scan. This is similar to the approach used by other authors who have calculated mean contours (34, 35). The RSC SD gives a measure of the spatial variability in the axial plane. The RSC SD $\sigma(\theta, z)$ at angle θ on slice z is given by

$$\sigma(\theta,z) = \sqrt{\frac{1}{N-1}\sum_{i=1}^{N}\left(r_i(\theta,z) - r_{\mathrm{RSC}}(\theta,z)\right)^2}\,, \tag{3.9}$$

where $r_i(\theta,z)$ is the radial distance to the surgical cavity contoured by radiation oncologist i, $r_{\mathrm{RSC}}(\theta,z)$ is the radial distance to the RSC calculated using Equation 2.1, and N is the number of contours used to calculate the RSC. The spatial distribution of RSC SDs was assessed by mapping each SD onto the RSC for each CT scan on every patient. In addition, cumulative histograms of the distribution of the RSC SDs were calculated.

3.3.3. Dose Measurements

Dosimetric consequences of interobserver surgical cavity contour variations were assessed for three patients. The original treatment fields from the planning CT

scan were applied to the repeat CT scans for these patients. An example is shown in Figure 3.2. The isocentre for all plans was placed with the same shifts from the anterior tattoo on each CT scan. The isocentre shifts are those used for the original plan. Dose calculations were performed using Eclipse™ using the same number of monitor units (MUs) as the original treatment plan. Dose volume histograms (DVHs) were calculated in Eclipse™ for the surgical cavity and RSC on each CT scan. For each DVH, the volume contained by the 95% isodose line (V_{95}) was calculated. A typical cumulative DVH for the surgical cavity illustrating V_{95} is shown in Figure 3.3.

The original planning objective for the DEV is $V_{95} = 100\%$. Differences in V_{95} between the surgical cavity contours and the RSC were assessed by calculating the RMS difference in V_{95} on each CT scan. The RMS difference in V_{95} (δV_{95}) is given by

$$\delta V_{95} = \sqrt{\frac{1}{N}\sum_{i=1}^{N}\left(V_{95,i} - V_{95,\mathrm{RSC}}\right)^2}, \tag{3.10}$$

where $V_{95,i}$ is V_{95} for the surgical cavity contoured by radiation oncologist i, $V_{95,\mathrm{RSC}}$ is V_{95} for the RSC, and N is the number of contours used to construct the RSC.

In addition, the equivalent uniform dose (EUD) formalism was used to assess the dosimetric consequences of interobserver contour variations. Previous studies have used the EUD formalism to give strong evidence for the continued use of 3.85 Gy per fraction as the prescription dose for 3DCRT APBI (42) and to compare different APBI techniques (43). For the interobserver study, the EUD was calculated using the linear quadratic (LQ) formalism presented by Bovi *et al.* (43). From the LQ formalism, the survival fraction S of cells irradiated is given by

$$S = \exp[-(\alpha D + \beta G D^2 - \gamma T)] \tag{3.11}$$

where D is the total dose of the irradiated cells, $G = 1/n$ for fractionated treatments, T is the treatment time ($T = 5$ days for APBI), α and β characterize the intrinsic radiosensitivity of the cells, and γ characterizes the proliferation of the cells (43). If T_d is the tumour-cell doubling time, then $\gamma = \ln 2 / T_d$. Most authors suggest the use of $\alpha = 0.3\ \text{Gy}^{-1}$, $\alpha/\beta = 10$ Gy, and $T_d = 15$ days for breast tissue (42, 43). If d is the dose per fraction, then Equation 3.11 can be rewritten as

$$S = \exp[-(\alpha n d + \beta d D - \gamma T)]\,, \tag{3.12}$$

where n is the number of fractions and $D = nd$.

Equation 3.11 assumes that that all cells receive the same dose. For a heterogeneous dose distribution, the survival fraction is given by

$$S = \sum_i \frac{V_i}{V_0} S(D_i)\,, \tag{3.13}$$

where $S(D_i)$ is the survival fraction for a dose of D_i as calculated by Equation 3.11, V_i is the volume of the structure that receives a dose of D_i, and V_0 is the total volume of the structure (43). D_i and V_i are obtained using a differential DVH. A typical differential DVH for a surgical cavity is shown in Figure 3.4. The EUD is the dose that if given uniformly to a structure will give the same biological effect as the actual heterogeneous dose distribution, assuming that the same dose per fraction is maintained during treatment. Then $D = \text{EUD}$ in Equation 3.12 gives

$$S = \exp\left(-\alpha \cdot \text{EUD} - \beta d \cdot \text{EUD} + 0.5\gamma \frac{\text{EUD}}{d}\right). \tag{3.14}$$

In Equation 3.14, the treatment time T for APBI is

$$T = \frac{n}{2} = 0.5 \cdot \frac{\text{EUD}}{d}. \tag{3.15}$$

Thus, the EUD is given by

$$\text{EUD} = \frac{-\ln S}{\alpha + \beta d - 0.5\gamma/d}. \tag{3.16}$$

For APBI treatments, d = 3.85 Gy.

To assess dosimetric consequences using the EUD formalism, differential DVHs were obtained for the surgical cavities and the RSC on the CT scans. Using Equations 3.11 and 3.13, the survival fraction for each surgical cavity and RSC was calculated. The EUD was then calculated using Equation 3.16. Differences in the EUD between the RSC and surgical cavity contours were quantified by calculating the RMS difference in EUD (δEUD) on each CT scan. The RMS difference in EUD is given by

$$\delta\text{EUD} = \sqrt{\frac{1}{N}\sum_{i=1}^{N}(\text{EUD}_i - \text{EUD}_{\text{RSC}})^2}, \tag{3.17}$$

where EUD_i is the EUD for the surgical cavity contoured by radiation oncologist i, EUD_{RSC} is the EUD for the RSC, and N is the number of contours used to calculate the RSC.

3.4. Intraobserver Contour Study

For the intraobserver study, the RSC was constructed using the repeat contours of the radiation oncologists for three patients. Thus, there will be three RSCs on each CT scan, one corresponding to the surgical cavity contours of each radiation oncologist.

Using these RSCs, contour variations were assessed separately for each radiation oncologist using the same methods as for the interobserver study.

3.5. Skin Markings and Surgical Cavity Localization

In order to investigate a possible correlation between the positions of the surgical cavity and skin markings, it must be shown that the position of the surgical cavity does not depend on its contouring uncertainty. This can be investigated by finding the intraobserver surgical cavity COM variability. Hence, contouring uncertainty in the COM was investigated as described in Sections 3.2, 3.3.2, and 3.4. If contouring uncertainty in the surgical cavity is small, the RSC COM can be used to denote the position of the surgical cavity in each CT scan. Thus, changes in the position of the skin markings can be compared with changes in position of the RSC COM to investigate any correlations between the positions of the surgical cavity and skin markings.

To investigate the positions of the skin markings, their position was identified on each CT scan for every patient (see Section 2.1). The skin markings' COM (SM COM) was calculated by finding the COM of the five skin markings. The change in position of the SM COM was calculated on each treatment CT scan by finding the change in position of the SM COM from its position on the planning CT scan. Similarly, the RSC COM was obtained from the interobserver study and the change in position of the RSC COM was calculated on each treatment CT scan by finding the change in position of the RSC COM from its position on the planning CT scan. Changes in the RSC and SM COMs in the SI, AP, and lateral directions were assessed using Pearson's correlation coefficient.

Figure 3.1 Definition of common and encompassing volumes

The definition of the (a) common and (b) encompassing volume is illustrated using two contours.

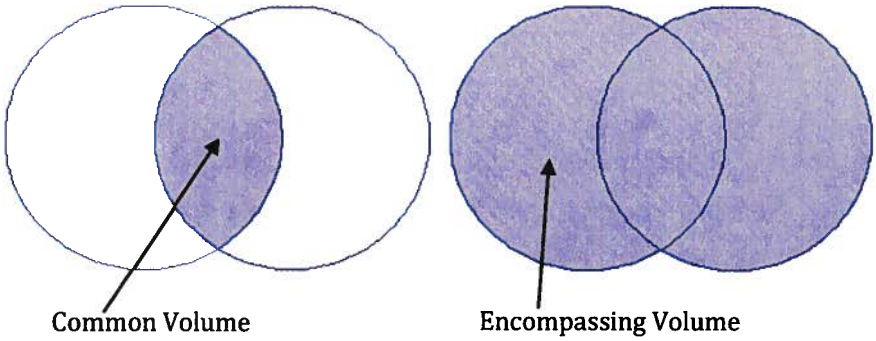

Figure 3.2 Treatment fields applied to planning and treatment CT scans

(a) The original treatment fields are shown on the planning CT scan. The RSC contour is shown in cyan. The isocentre of the fields is indicated by the yellow ring. (b) The original treatment field has been applied to a CT scan obtained during treatment. The isocentre is positioned by using the same shifts from the anterior tattoo as for the planning CT scan. Note the change in the patient's anatomy and RSC.

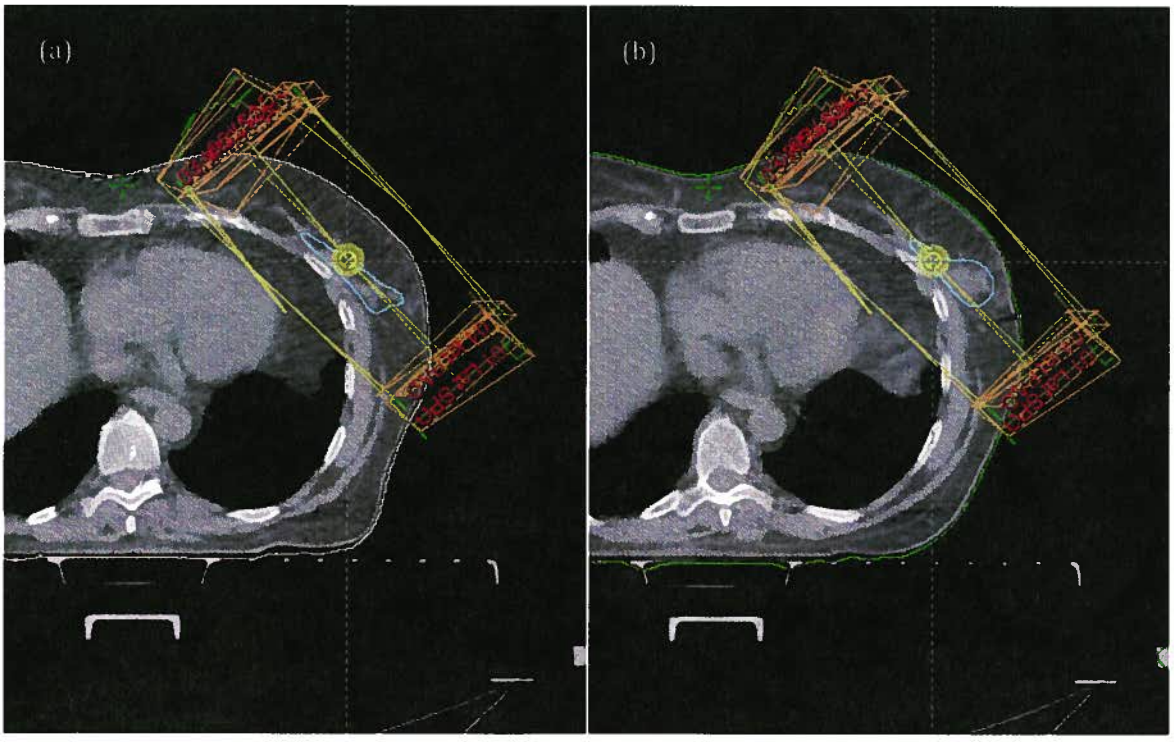

Figure 3.3 Example of a cumulate DVH for the surgical cavity

The cumulate DVH for a surgical cavity with $V_{95} = 99.5\%$.

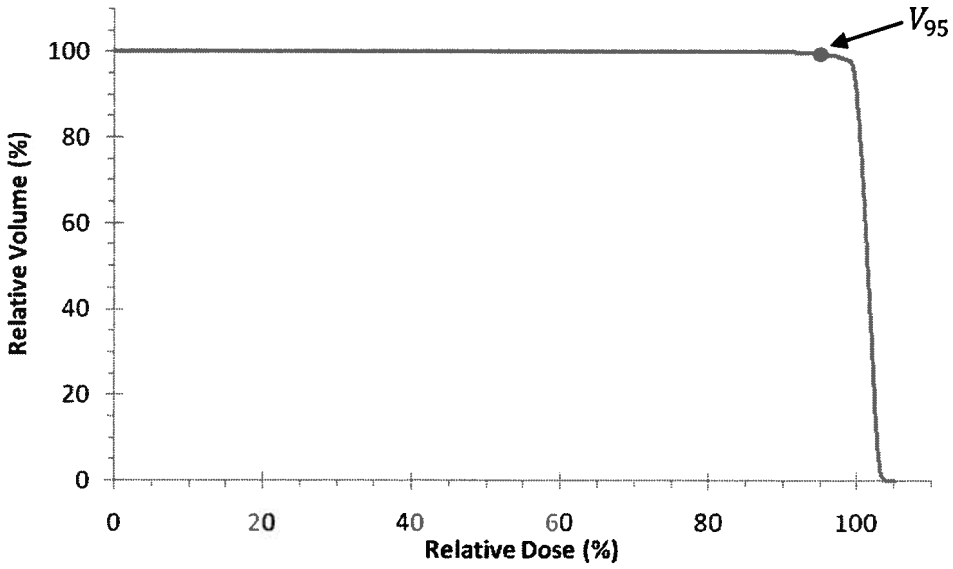

Figure 3.4 Example of a differential DVH for the surgical cavity

The differential DVH for the same surgical cavity as in Figure 3.3.

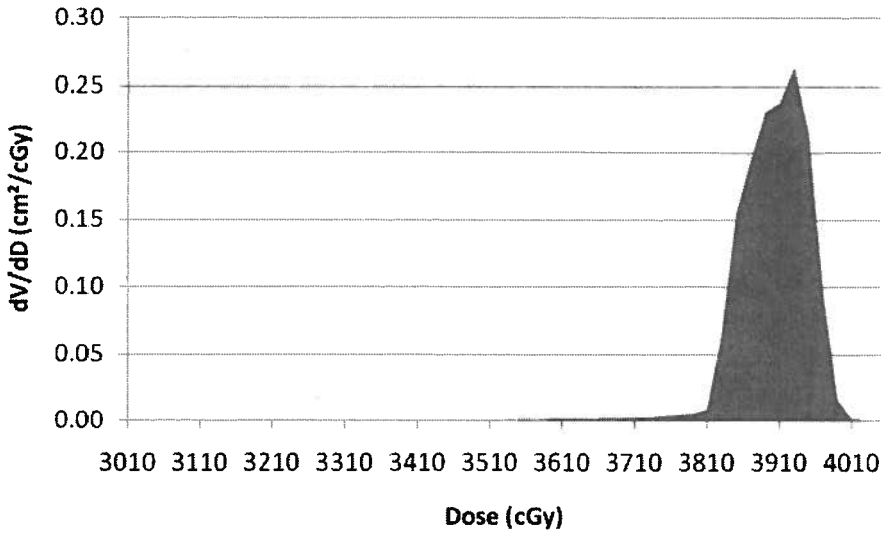

4. RESULTS AND DISCUSSION

4.1. Patient Characteristics

Data was collected from the planning and repeat CT scans of twelve patients enrolled in the RAPID clinical trial and DIVA project. Characteristics of the patients are shown in Table 4.1. Repeat contours were performed on Patients 1, 2, and 3. The preliminary study of contour variability and intraobserver contour variability study were completed using data from Patients 1, 2, and 3. The interobserver contour variability study and assessment of changes in the positions of the skin markings were done using the CT scans from all twelve patients. Dose calculations to assess the clinical impact of interobserver and intraobserver contour variability were performed on Patients 1, 2, and 3.

4.2. Preliminary Study

For three patients, the maximum interobserver and intraobserver volume and COM differences were calculated. Results from this preliminary study are shown in Table 4.2. On average, the maximum interobserver volume difference was 12.02 cm^3, which was larger than the maximum intraobserver difference of 2.76 cm^3. Similarly, the maximum interobserver COM difference in the lateral, AP, and SI directions was 0.79 cm, 0.55 cm, and 0.52 cm, respectively. This was smaller than the maximum intraobserver COM differences of 0.23 cm, 0.16 cm, and 0.16 cm. This suggests that surgical cavity contour differences are largely a function of interobserver variations,

rather than intraobserver variations. For this reason, repeat contours were only performed on the first three patients (Patients 1, 2, and 3).

4.3. Interobserver and Intraobserver Contour Studies

4.3.1. Volume-based Measurements

In general, interobserver volume differences were larger than intraobserver differences. Average interobserver volume variations are summarized in Table 4.3. There was a large range of surgical cavity volumes in the interobserver study. RSC volumes ranged from 6.00 cm^3 to 69.76 cm^3. The interobserver RMS-volume difference when averaged over CT scans ranged from 0.88 cm^3 to 5.96 cm^3; the overall patient average was 2.62 cm^3. Average intraobserver volume variations are shown in Table 4.4. There was a smaller range in RSC volumes in the intraobserver study (5.30 cm^3 to 28.04 cm^3) since only three patients were included in this study. Intraobserver RMS-volume differences when averaged over CT scans ranged from 0.30 cm^3 to 1.50 cm^3 for all radiation oncologists. The patient-averaged differences were 0.82 cm^3, 1.03 cm^3, 0.74 cm^3 for Oncologists 1, 2, and 3, respectively. The RMS-volume difference when averaged over all radiation oncologists was 0.86 cm^3.

Similar results were observed for the percent difference in common and encompassing volumes (Δvol). The patient-averaged percent difference in common and encompassing volumes for interobserver differences was 49.1%. The percent difference was largest for Patient 10 (71.8%) and smallest for Patient 12 (24.3%). In general, intraobserver percent differences were smaller than interobserver differences. The patient-averaged percent-difference in common and encompassing volumes in the

intraobserver study was 36.0%, 37.9%, and 31.2% for Oncologists 1, 2, and 3, and 35.0% when averaged over all radiation oncologists. Hence, there was a better agreement in the SC volumes delineated by a single radiation oncologist than in volumes delineated by multiple radiation oncologists.

There was evidence of a tentative correlation between the RSC volume and the RMS-difference in the interobserver study ($r = 0.36, p = 0.012$). In the intraobserver study, there was a strong correlation between the RSC volume and RMS-volume difference for the contours of Oncologist 1 ($r = 0.82, p < 0.001$); the correlations for Oncologist 2 ($r = 0.40, p = 0.20$) and Oncologist 3 ($r = 0.43, p = 0.17$) were not statistically significant. In addition, there was a strong negative correlation between the RSC volume and Δvol in the interobserver study ($r = -0.60, p < 0.001$) and the intraobserver study for Oncologist 1 ($r = -0.81, p = 0.001$). Correlations between RSC volume and Δvol were not statistically significant in the intraobserver study for Oncologist 2 ($r = -0.07, p = 0.83$) and Oncologist 3 ($r = -0.39, p = 0.22$).

4.3.2. Distance-based Measurements

Interobserver variations in the surgical cavity COM are summarized in Table 4.5. Differences in the surgical cavity COM in the interobserver study were on average less than 2 mm in all directions. The average RMS-difference of the surgical cavity COM in the lateral, AP, and SI directions was 0.16 cm (range: 0.02 cm – 0.44 cm), 0.10 cm (0.03 cm – 0.33 cm), and 0.14 cm (0.03 cm – 0.32 cm), respectively. Intraobserver variations of the SC COM are summarized in Table 4.6. In general, intraobserver surgical cavity COM differences were approximately 1 mm smaller than interobserver differences. For

Oncologist 1, the average RMS difference of the COM was 0.06 cm, 0.04 cm, and 0.04 cm in the lateral, AP, and SI directions. Similarly, the average RMS-differences were 0.06 cm, 0.03 cm, and 0.05 cm for Oncologist 2, and 0.05 cm, 0.05 cm, and 0.03 cm for Oncologist 3.

Similar results were obtained for the maximum spatial dimensions of the surgical cavity. Interobserver variations of the dimensions of the surgical cavity are summarized in Table 4.7. Intraobserver variations of the surgical cavity dimensions are shown in Table 4.8. The dimensions of the surgical cavity for all patients ranged from 2.87 cm to 7.40 cm in the lateral direction, 2.44 cm to 5.94 cm in the AP direction, and 1.65 cm to 5.85 cm in the SI direction. In general, interobserver differences of the surgical cavity dimensions were larger than intraobserver differences. The average interobserver RMS-difference in the lateral, AP, and SI directions was 0.55 cm, 0.36 cm, and 0.31 cm, whereas the average intraobserver difference was 0.28 cm, 0.23 cm, and 0.11 cm. Intraobserver differences were 0.37 cm, 0.30 cm, and 0.18 cm for Oncologist 1, 0.25 cm, 0.21 cm, and 0.14 cm for Oncologist 2, and 0.22 cm, 0.20 cm, and 0.01 cm for Oncologist 3. Results in the SI dimensions are consistent with the CT slice thickness of 3 mm. Interobserver SI differences was one CT slice on average, whereas there was very little change in the number of slices in the intraobserver study.

RSC SDs were calculated for all RSCs constructed in the interobserver and intraobserver studies. Figure 4.1 shows a sample interobserver RSC with the SD mapped to each RSC contour point. Figure 4.2 shows a sample intraobserver RSC SD map. Representative RSC SD maps for each patient in the interobserver and intraobserver studies are included in Appendix A. In general, SDs tended to be largest in

the most superior and inferior slices of the RSC for both the interobserver and intraobserver studies. A typical example is shown in Figure 4.1. In addition, it was observed that SDs were larger in places where there was a significant change in the shape of the RSC. A typical example of this situation is shown in Figure A.3.

The distribution of RSC SDs was also assessed using cumulative histograms. Sample cumulative histograms for the interobserver and intraobserver studies are shown in Figure 4.3. Representative cumulative histograms for each patient in the intraobserver and intraobserver studies are included in Appendix B. The mean, maximum, and standard deviation of the RSC SDs was calculated for each cumulative histogram. These statistics for interobserver RSC SDs are shown in Table 4.9. On average, the mean RSC SD for all patients was 0.19 cm. The maximum RSC SD was observed for Patient 3 (3.07 cm); the maximum RSC SD was 1.50 cm when averaged over all patients. The maximum and mean RSC SD was smaller in the intraobserver study. The statistics for intraobserver RSC SDs are summarized in Table 4.10. On average, the maximum and mean RSD SDs were 0.92 cm and 0.13 cm for Oncologist 1, 0.86 cm and 0.15 cm for Oncologist 2, 0.93 cm and 0.12 cm for Oncologist 3. The largest intraobserver RSC SD was observed for the RSCs from Oncologist 3 for Patient 3 (1.55 cm). In addition, cumulative histograms for both interobserver and intraobserver studies were compared for patients for whom radiation oncologists completed repeat surgical cavity contours, as is shown in Figure 4.3. It was observed that interobserver RSC SDs were larger than intraobserver RSC SDs for all CT scans, except the planning CT scan for Patient 2 where interobserver and intraobserver RSC SDs were similar.

4.3.3. Dose Measurements

Dosimetric consequences of surgical cavity contour variability were assessed for three patients. Table 4.11 summarizes interobserver variability in V_{95} and EUD. Intraobserver variations are shown in Table 4.12. On average, RMS differences in V_{95} and EUD were slightly larger in the interobserver study than in the intraobserver study. The patient-averaged RMS difference in V_{95} and EUD was 0.76% and 0.20 Gy in the interobserver study. The average RMS differences in V_{95} were 0.45%, 0.67%, and 0.16% for Oncologists 1, 2, and 3 in the intraobserver study; RMS differences in EUD were 0.07 Gy, 0.13 Gy, and 0.04 Gy.

Despite interobserver variations, there were not significant variations in V_{95} and EUD. V_{95} for the RSC was on average 99.5% and 98.8% in the interobserver and intraobserver studies; these values varied by 0.5% and 1.1%. These values are consistent with the planning objective that the DEV is covered by the 95% isodose line. It should be noted that V_{95} for the RSC is slightly lower than 100% since the RSC may extend outside the DEV. Similarly, there is little variation in the EUD. On average, the EUD was 38.9 Gy and 38.2 Gy in the interobserver and intraobserver studies. Average variations in the EUD were 0.3 Gy and 0.1 Gy, respectively. This suggests that dose coverage in the surgical cavity was similar for all CT scans for a given patient.

The values of V_{95} and EUD for each surgical cavity also suggests that dosimetric coverage is similar in each structure. Figures 4.4, 4.5, and 4.6 show V_{95} and EUD for all contoured surgical cavities for Patients 1, 2, and 3, respectively. V_{95} was higher than 90% in all CT studies. Only 14.8% and 7.4% of the CT studies had V_{95} less than 98% and 95%, respectively. Values of V_{95} were smallest for Patient 1 (Figure 4.4(a)). For this

patient, V_{95} was more than 99.1%, 91.7%, and 97.3% for surgical cavities contoured by Oncologist 1, 2, and 3. Values of V_{95} were more consistent for Patient 2 (Figure 4.5(a)). V_{95} was more than 99.4%, 97.9%, and 98.3% for the surgical cavities contoured by Oncologists 1, 2, and 3 for Patient 2. Values of V_{95} for Patient 3 were remarkably similar (Figure 4.6(a)). In fact, V_{95} was greater than 99.8% for all surgical cavity contours for Patient 3. These results suggest that V_{95} is clinically acceptable for all surgical cavities.

Similar results were obtained for the EUD for each surgical cavity. The EUD was less than 38.5 Gy, 38.0 Gy, and 37.2 Gy in 33.3%, 9.3%, and 0.0% for all CT studies. The EUD was smallest for Patient 1 (Figure 4.4(b)). In addition, the EUD was more than 37.9 Gy, 37.2 Gy, and 38.1 Gy for the surgical cavity contours of Oncologist 1, 2, and 3 for this patient. EUD values were largest for Patient 2 (Figure 4.5(b)); the maximum EUD was 40.1 Gy. The EUD was more than 38.9 Gy, 38.5 Gy, and 38.5 Gy for the surgical cavity contours of Oncologist 1, 2, and 3 for this patient. EUD values for Patient 3 were largest for the surgical cavity contours of Oncologist 2 (Figure 4.6(b)). The EUD was larger than 38.6 Gy, 39.0 Gy, and 38.7 Gy for the SC contours of Oncologist 1, 2, and 3 for this patient. Overall, there is not a significant range of EUD values, which suggests that the dose received by each surgical cavity is similar. Hence, the planning margins used were sufficient to provide adequate dose coverage despite interobserver and intraobserver variations. It should be noted that this may not be the case if the planning margins are decreased.

4.4. Skin Markings and Surgical Cavity Localization

As was discussed in Section 4.3.2, interobserver COM variations were less than 2 mm on average, and intraobserver COM variations were approximately 1 mm smaller than interobserver variations. Contouring variability did not cause significant variations in the RSC COM. Therefore, changes in the position of the skin markings and surgical cavity could be assessed by using the RSC contour to define the surgical cavity COM for all patients. Changes in the position of the skin marking (SM) COM and RSC COM during treatment were calculated. Correlations in the change of position of the SM and RSC COMs were calculated in the lateral, AP, and SI direction using Pearson's correlation coefficient. Correlations are shown in Figures 4.7, 4.8, and 4.9. There was a strong correlation between the SM COM and RSC COM in the lateral ($r = 0.79, p < 0.001$), AP ($r = 0.74, p < 0.001$), and SI ($r = 0.85, p < 0.001$) directions.

Moreover, the relative change in position between the SM and RSC COMs was calculated on each repeat CT scan in each direction. Table 4.13 summarizes the correlations and changes in relative position between the SM and RSC COMs. The mean change in relative position of the SM and RSC COM was 1.24 mm, 1.80 mm, and 1.23 mm in the lateral, AP, and SI direction. In addition, the change in relative position between the SM and RSC COM was more than 4 mm in only 4.8% of repeat CT scans. This suggests that it is feasible to decrease planning setup margins if patients are setup for treatment using the SMs rather than using the anterior and lateral tattoos placed on the patient.

Table 4.1 Patient characteristics

A summary of the characteristics for all twelve patients is shown. Repeat contours were only performed on the first three patients.

Patient	Left/Right Breast	APBI/WBRT Arm	Mean (Range) of CVS[1]	Days between Planning and Treatment	Repeat Contours
1	Right	WBRT[2]	2.4 (2–3)	12	Yes
2	Right	APBI	3.6 (3–4)	18	Yes
3	Left	APBI	3.0 (2–4)	33	Yes
4	Left	WBRT	3.8 (3–4)	21	No
5	Left	WBRT	4.6 (4–5)	32	No
6	Left	WBRT	3.7 (3–4)	21	No
7	Right	APBI	2.7 (2–3)	26	No
8	Right	APBI	2.3 (2–3)	18	No
9	Right	WBRT	3.3 (2–4)	21	No
10	Right	WBRT	2.3 (2–3)	11	No
11	Left	APBI	3.6 (3–4)	21	No
12	Right	WBRT	4.1 (4–5)	24	No

1. The CVS is an integer between 1 and 5. The mean value is the CVS averaged over radiation oncologists and CT scans.
2. Although Patient 1 was treated with WBRT, an APBI treatment plan was also completed for this patient.

Table 4.2 Results of preliminary contour variability study

The maximum differences in RSC volume and position of the surgical cavity COM in the lateral, AP, and SI directions are shown for intraobserver and interobserver differences in the preliminary study. Results have been averaged over all three patients.

Study	Difference in RSC Volume (cm^3)	Difference in COM coordinate (cm)		
		Lateral	AP	SI
Oncologist 1	2.21	0.26	0.16	0.20
Oncologist 2	3.42	0.23	0.14	0.20
Oncologist 3	2.63	0.22	0.19	0.08
Average Intraobserver	2.76	0.23	0.16	0.16
Interobserver	12.02	0.79	0.55	0.52

Table 4.3 Interobserver variability of the surgical cavity volumes

The interobserver variability of the surgical cavity volume for all twelve patients is shown. In addition, the common volume, encompassing volume, and Δvol have been calculated. For each patient, results have been averaged over CT scans. Standard deviations are shown in parentheses. The root-mean-square (rms) has been calculated where appropriate.

Patient	V_{RSC} (cm³)	δV (cm³)	V_{common} (cm³)	$V_{encompassing}$ (cm³)	Δvol (%)
1	6.00 (0.45)	1.05 (0.33)	4.07 (0.29)	9.15 (0.59)	55.34 (4.85)
2	23.45 (2.56)	3.51 (1.15)	18.01 (2.21)	33.79 (2.27)	46.83 (3.10)
3	20.61 (2.19)	5.96 (1.09)	10.88 (2.32)	33.64 (4.17)	67.77 (4.82)
4	37.84 (3.32)	3.12 (1.11)	31.46 (3.01)	45.89 (2.84)	31.54 (3.14)
5	31.85 (6.82)	3.35 (0.55)	25.94 (7.30)	39.11 (6.38)	34.45 (7.45)
6	7.36 (0.43)	1.13 (0.11)	5.58 (0.23)	9.58 (0.58)	41.68 (2.91)
7	10.85 (1.07)	0.88 (0.23)	7.22 (0.98)	15.54 (1.20)	53.66 (3.64)
8	37.48 (1.83)	4.38 (1.59)	26.71 (1.97)	56.11 (3.47)	52.39 (2.13)
9	16.37 (2.57)	1.30 (0.38)	9.17 (1.18)	22.35 (3.81)	58.77 (2.49)
10	12.64 (0.94)	3.29 (0.68)	6.01 (0.90)	21.45 (1.02)	71.80 (5.41)
11	7.03 (1.46)	1.16 (0.48)	5.13 (1.22)	9.68 (2.07)	46.96 (4.80)
12	69.76 (22.47)	2.54 (1.19)	60.92 (20.33)	80.22 (25.52)	24.30 (1.46)
Average	23.26 (7.00_{rms})	2.62 (0.87_{rms})	17.41 (6.42_{rms})	31.21 (7.94_{rms})	49.10 (4.17_{rms})

Table 4.4 Intraobserver variability of the surgical cavity volumes

The intraobserver variability of the surgical cavity volume for three patients is shown. In addition, the common volume, encompassing volume, and Δvol have been calculated. For each patient, results have been averaged over CT scans. Averages for each radiation oncologist and the overall oncologist average (Onc. Avg.) have also been calculated. Standard deviations are shown in parentheses. The root-mean-square (rms) has been calculated where appropriate.

Patient	V_{RSC} (cm³)	δV (cm³)	V_{common} (cm³)	$V_{encompassing}$ (cm³)	Δvol (%)
Oncologist 1					
1	5.63 (0.49)	0.30 (0.03)	4.65 (0.33)	7.96 (0.62)	41.52 (0.83)
2	28.04 (2.79)	1.29 (0.28)	23.86 (2.23)	35.54 (3.76)	32.78 (0.91)
3	23.20 (1.66)	0.87 (0.40)	19.63 (2.37)	29.57 (1.00)	33.75 (5.90)
Average	18.96 (1.90_{rms})	0.82 (0.28_{rms})	16.05 (1.89_{rms})	24.36 (2.27_{rms})	36.02 (3.48_{rms})
Oncologist 2					
1	8.07 (0.43)	0.89 (0.35)	6.71 (0.63)	10.71 (0.43)	37.40 (4.77)
2	21.99 (2.14)	1.50 (0.87)	18.40 (1.94)	29.50 (3.12)	37.54 (4.02)
3	12.35 (2.95)	0.70 (0.22)	10.05 (2.26)	16.37 (3.38)	38.62 (4.33)
Average	14.14 (2.12_{rms})	1.03 (0.55_{rms})	11.72 (1.76_{rms})	18.86 (2.67_{rms})	37.85 (4.38_{rms})
Oncologist 3					
1	5.30 (0.85)	0.32 (0.24)	4.51 (0.43)	7.04 (1.36)	34.88 (7.59)
2	20.93 (2.81)	1.14 (0.45)	18.39 (2.51)	25.51 (2.77)	28.01 (3.27)
3	26.16 (4.02)	0.75 (0.40)	22.94 (3.94)	33.11 (4.53)	30.70 (7.00)
Average	17.46 (2.87_{rms})	0.74 (0.38_{rms})	15.28 (2.71_{rms})	21.88 (3.17_{rms})	31.20 (6.25_{rms})
Onc. Avg.	16.85 (2.47_{rms})	0.86 (0.45_{rms})	14.35 (2.29_{rms})	21.70 (2.88_{rms})	35.02 (5.13_{rms})

Table 4.5 Interobserver variability of the surgical cavity COM

The interobserver variability of the surgical cavity COM for all twelve patients is shown in the lateral (x), AP (y), and SI (z) directions. For each patient, results have been averaged over CT scans. Standard deviations are shown in parentheses. The root-mean-square (rms) has been calculated where appropriate.

Patient	$x_{COM,RSC}$ (cm)	δx_{COM} (cm)	$y_{COM,RSC}$ (cm)	δy_{COM} (cm)	$z_{COM,RSC}$ (cm)	δz_{COM} (cm)
1	-14.06 (0.20)	0.14 (0.04)	5.78 (0.09)	0.04 (0.01)	-0.39 (0.12)	0.11 (0.03)
2	-11.80 (0.08)	0.17 (0.05)	3.19 (0.48)	0.08 (0.03)	3.98 (0.36)	0.12 (0.06)
3	13.56 (0.17)	0.44 (0.06)	5.00 (0.29)	0.33 (0.06)	-3.53 (0.11)	0.24 (0.07)
4	16.73 (0.31)	0.07 (0.02)	6.70 (0.08)	0.04 (0.01)	-0.64 (0.15)	0.04 (0.02)
5	15.07 (0.12)	0.06 (0.02)	5.93 (0.25)	0.03 (0.03)	0.30 (0.16)	0.05 (0.03)
6	10.69 (0.09)	0.06 (0.02)	3.53 (0.15)	0.04 (0.02)	-2.50 (0.27)	0.04 (0.01)
7	-12.77 (0.20)	0.12 (0.04)	4.13 (0.33)	0.06 (0.04)	3.74 (0.15)	0.16 (0.01)
8	-13.09 (0.29)	0.12 (0.04)	3.41 (0.18)	0.13 (0.03)	4.05 (0.28)	0.21 (0.09)
9	-10.49 (0.22)	0.18 (0.02)	3.93 (0.27)	0.09 (0.02)	2.42 (0.26)	0.32 (0.04)
10	-8.36 (0.18)	0.38 (0.05)	2.61 (0.13)	0.30 (0.06)	1.97 (0.06)	0.24 (0.06)
11	11.10 (0.10)	0.12 (0.02)	1.69 (0.17)	0.07 (0.04)	0.88 (0.14)	0.05 (0.01)
12	-11.02 (0.04)	0.02 (0.01)	4.22 (0.08)	0.03 (0.01)	1.89 (0.21)	0.03 (0.02)
Average	—	0.16 (0.04_{rms})	—	0.10 (0.03_{rms})	—	0.14 (0.05_{rms})

Table 4.6 Intraobserver variability of the surgical cavity COM

The intraobserver variability of the surgical cavity COM for three patients is shown in the lateral (x), AP (y), and SI (z) directions. For each patient, results have been averaged over CT scans. Averages for each radiation oncologist and the overall oncologist average (Onc. Avg.) have also been calculated. Standard deviations are shown in parentheses. The root-mean-square (rms) has been calculated where appropriate.

Patient	$x_{COM,RSC}$ (cm)	δx_{COM} (cm)	$y_{COM,RSC}$ (cm)	δy_{COM} (cm)	$z_{COM,RSC}$ (cm)	δz_{COM} (cm)
Oncologist 1						
1	-13.86 (0.23)	0.06 (0.01)	5.80 (0.06)	0.03 (0.01)	-0.26 (0.14)	0.08 (0.01)
2	-12.10 (0.11)	0.07 (0.07)	3.34 (0.51)	0.04 (0.02)	3.80 (0.42)	0.05 (0.01)
3	13.24 (0.21)	0.06 (0.02)	4.82 (0.22)	0.04 (0.01)	-3.70 (0.14)	0.03 (0.02)
Average	-4.24 (0.19_{rms})	0.06 (0.04_{rms})	4.66 (0.32_{rms})	0.04 (0.02_{rms})	-0.05 (0.27_{rms})	0.05 (0.02_{rms})
Oncologist 2						
1	-14.18 (0.23)	0.05 (0.01)	5.83 (0.10)	0.02 (0.01)	-0.45 (0.14)	0.05 (0.03)
2	-11.76 (0.08)	0.07 (0.05)	3.19 (0.49)	0.03 (0.01)	4.02 (0.41)	0.05 (0.02)
3	14.11 (0.12)	0.05 (0.02)	5.37 (0.33)	0.05 (0.03)	-3.87 (0.21)	0.04 (0.02)
Average	-3.94 (0.15_{rms})	0.06 (0.03_{rms})	4.80 (0.35_{rms})	0.03 (0.02_{rms})	-0.10 (0.28_{rms})	0.05 (0.02_{rms})
Oncologist 3						
1	-14.11 (0.17)	0.02 (0.01)	5.72 (0.10)	0.03 (0.03)	-0.46 (0.16)	0.03 (0.02)
2	-11.80 (0.03)	0.06 (0.03)	3.16 (0.47)	0.04 (0.02)	3.99 (0.37)	0.03 (0.02)
3	13.21 (0.10)	0.06 (0.04)	4.60 (0.37)	0.07 (0.04)	-3.38 (0.10)	0.03 (0.02)
Average	-4.23 (0.11_{rms})	0.05 (0.03_{rms})	4.49 (0.35_{rms})	0.05 (0.03_{rms})	0.05 (0.24_{rms})	0.03 (0.02_{rms})
Onc. Avg.	—	0.06 (0.03_{rms})	—	0.04 (0.02_{rms})	—	0.04 (0.02_{rms})

Table 4.7 Interobserver variability the surgical cavity dimensions

The interobserver variability of the surgical cavity dimensions for all twelve patients is shown in the lateral (x), AP (y), and SI (z) directions. For each patient, results have been averaged over CT scans. Standard deviations are shown in parentheses. The root-mean-square (rms) has been calculated where appropriate.

Patient	x_{RSC} (cm)	δx (cm)	y_{RSC} (cm)	δy (cm)	z_{RSC} (cm)	δz (cm)
1	2.87 (0.10)	0.14 (0.08)	2.44 (0.21)	0.20 (0.17)	2.48 (0.15)	0.27 (0.22)
2	6.14 (0.37)	1.01 (0.31)	3.59 (0.29)	0.45 (0.16)	3.15 (0.17)	0.74 (0.16)
3	6.13 (0.63)	1.41 (0.15)	5.43 (0.46)	0.87 (0.24)	2.80 (0.28)	0.44 (0.16)
4	7.40 (0.37)	0.29 (0.09)	4.45 (0.25)	0.27 (0.21)	3.23 (0.15)	0.28 (0.07)
5	6.89 (0.08)	0.32 (0.05)	4.81 (0.22)	0.33 (0.20)	3.30 (0.00)	0.27 (0.11)
6	3.44 (0.17)	0.43 (0.08)	3.89 (0.08)	0.23 (0.06)	2.28 (0.15)	0.12 (0.08)
7	3.62 (0.23)	0.25 (0.08)	4.76 (0.13)	0.21 (0.12)	2.93 (0.29)	0.21 (0.04)
8	5.92 (0.32)	0.55 (0.21)	5.94 (0.27)	0.09 (0.02)	5.93 (0.15)	0.09 (0.10)
9	5.17 (0.21)	0.34 (0.15)	3.42 (0.07)	0.13 (0.04)	4.25 (0.48)	0.47 (0.20)
10	6.65 (0.21)	0.98 (0.09)	4.64 (0.21)	0.62 (0.11)	3.15 (0.17)	0.49 (0.08)
11	4.02 (0.20)	0.47 (0.18)	2.90 (0.38)	0.65 (0.12)	1.65 (0.17)	0.17 (0.00)
12	7.03 (0.85)	0.33 (0.09)	5.67 (0.50)	0.24 (0.13)	5.85 (0.71)	0.19 (0.04)
Average	5.41 (0.37_{rms})	0.55 (0.15_{rms})	4.32 (0.29_{rms})	0.36 (0.15_{rms})	3.42 (0.30_{rms})	0.31 (0.12_{rms})

Table 4.8 Intraobserver variability the surgical cavity dimensions

The intraobserver variability of the surgical cavity dimensions for three patients is shown in the lateral (x), AP (y), and SI (z) directions. For each patient, results have been averaged over CT scans. Averages for each radiation oncologist and the overall oncologist average (Onc. Avg.) have also been calculated. Standard deviations are shown in parentheses. The root-mean-square (rms) has been calculated where appropriate.

Patient	x_{RSC} (cm)	δx (cm)	y_{RSC} (cm)	δy (cm)	z_{RSC} (cm)	δz (cm)
Oncologist 1						
1	3.10 (0.05)	0.25 (0.04)	2.38 (0.04)	0.23 (0.08)	2.40 (0.00)	0.21 (0.04)
2	7.50 (0.32)	0.62 (0.22)	3.97 (0.23)	0.28 (0.08)	4.20 (0.24)	0.18 (0.16)
3	6.68 (0.21)	0.23 (0.01)	5.60 (0.31)	0.39 (0.16)	3.03 (0.21)	0.13 (0.10)
Average	5.76 (0.22_{rms})	0.37 (0.13_{rms})	3.98 (0.23_{rms})	0.30 (0.12_{rms})	3.21 (0.18_{rms})	0.18 (0.11_{rms})
Oncologist 2						
1	2.99 (0.09)	0.18 (0.07)	2.54 (0.17)	0.14 (0.02)	2.70 (0.00)	0.10 (0.12)
2	6.01 (0.25)	0.37 (0.13)	3.72 (0.24)	0.25 (0.05)	2.70 (0.24)	0.15 (0.18)
3	4.17 (0.22)	0.21 (0.10)	4.83 (0.18)	0.24 (0.11)	2.15 (0.50)	0.16 (0.11)
Average	4.39 (0.20_{rms})	0.25 (0.10_{rms})	3.70 (0.2_{rms} 0)	0.21 (0.07_{rms})	2.52 (0.32_{rms})	0.14 (0.14_{rms})
Oncologist 3						
1	2.65 (0.14)	0.12 (0.03)	2.35 (0.23)	0.17 (0.09)	2.10 (0.42)	0.00 (0.00)
2	5.53 (0.40)	0.31 (0.14)	3.58 (0.30)	0.13 (0.08)	2.93 (0.29)	0.04 (0.09)
3	7.01 (0.15)	0.22 (0.14)	6.27 (0.28)	0.29 (0.18)	2.80 (0.28)	0.00 (0.00)
Average	5.06 (0.26_{rms})	0.22 (0.12_{rms})	4.07 (0.27_{rms})	0.20 (0.12_{rms})	2.61 (0.34_{rms})	0.01 (0.05_{rms})
Onc. Avg.	5.07 (0.23_{rms})	0.28 (0.12_{rms})	3.92 (0.23_{rms})	0.23 (0.11_{rms})	2.78 (0.29_{rms})	0.11 (0.11_{rms})

Table 4.9 Summary of interobserver RSC SDs

The maximum (Max.), mean, and standard deviation (SD) of the distribution of RSC SDs obtained in the interobserver study for all twelve patients is shown. For each patient, results have been averaged over CT scans.

Patient	Max. (cm)	Mean (cm)	SD (cm)
1	0.62	0.16	0.12
2	1.68	0.18	0.18
3	3.07	0.32	0.40
4	1.47	0.17	0.16
5	1.64	0.16	0.17
6	0.73	0.13	0.11
7	1.16	0.20	0.20
8	2.47	0.23	0.30
9	1.19	0.16	0.14
10	2.00	0.26	0.23
11	0.95	0.15	0.15
12	1.07	0.14	0.10
Average	1.50	0.19	0.19

Table 4.10 Summary of intraobserver RSC SDs

The maximum (Max.), mean, and standard deviation (SD) of the distribution of RSC SDs obtained in the intraobserver study is shown for three patients. For each patient, results have been averaged over CT scans.

Patient	Max. (cm)	Mean (cm)	SD (cm)
Oncologist 1			
1	0.48	0.10	0.08
2	1.17	0.14	0.12
3	1.13	0.15	0.14
Patient Average	0.92	0.13	0.11
Oncologist 2			
1	0.50	0.11	0.08
2	1.04	0.17	0.14
3	1.03	0.16	0.12
Patient Average	0.86	0.15	0.11
Oncologist 3			
1	0.44	0.10	0.08
2	0.80	0.12	0.10
3	1.55	0.15	0.15
Patient Average	0.93	0.12	0.11
Oncologist Average	0.90	0.13	0.11

Table 4.11 Interobserver dosimetric variability of the surgical cavity

The interobserver variability of V_{95} and EUD of the surgical cavity for three patients is shown. For each patient, results have been averaged over CT scans. Standard deviations are shown in parentheses. The root-mean-square (rms) has been calculated where appropriate.

Patient	$V_{95,RSC}$ (%)	δV_{95} (%)	EUD_{RSC} (Gy)	δEUD (Gy)
1	98.88 (0.77)	2.03 (1.51)	38.27 (0.10)	0.26 (0.21)
2	99.75 (0.47)	0.23 (0.29)	39.48 (0.58)	0.11 (0.10)
3	100.00 (0.00)	0.02 (0.03)	38.87 (0.06)	0.22 (0.11)
Average	99.54 (0.52_{rms})	0.76 (0.89_{rms})	38.88 (0.34_{rms})	0.20 (0.15_{rms})

Table 4.12 Intraobserver dosimetric variability of the surgical cavities

The intraobserver variability of V_{95} and EUD of the surgical cavity for three patients is shown. For each patient, results have been averaged over CT scans. Averages for each radiation oncologist and the overall oncologist average (Onc. Avg.) have also been calculated. Standard deviations are shown in parentheses. The root-mean-square (rms) has been calculated where appropriate.

Patient	$V_{95,RSC}$ (%)	δV_{95} (%)	EUD_{RSC} (Gy)	δEUD (Gy)
Oncologist 1				
1	98.78 (2.12)	1.26 (2.04)	38.21 (0.16)	0.14 (0.20)
2	99.93 (0.13)	0.06 (0.11)	39.48 (0.50)	0.02 (0.02)
3	100.00 (0.00)	0.02 (0.02)	38.73 (0.05)	0.04 (0.02)
Average	99.57 (1.23_{rms})	0.45 (1.18_{rms})	38.81 (0.30_{rms})	0.07 (0.12_{rms})
Oncologist 2				
1	96.45 (3.19)	1.74 (2.19)	37.95 (0.38)	0.26 (0.29)
2	99.66 (0.67)	0.26 (0.31)	39.44 (0.62)	0.07 (0.08)
3	100.00 (0.00)	0.02 (0.03)	39.22 (0.18)	0.06 (0.02)
Average	98.70 (1.88_{rms})	0.67 (1.28_{rms})	38.87 (0.43_{rms})	0.13 (0.17_{rms})
Oncologist 3				
1	98.76 (1.13)	0.37 (0.22)	38.28 (0.10)	0.05 (0.03)
2	99.65 (0.69)	0.10 (0.17)	39.44 (0.63)	0.06 (0.06)
3	100.00 (0.00)	0.01 (0.01)	38.83 (0.05)	0.02 (0.01)
Average	99.47 (0.76_{rms})	0.16 (0.16_{rms})	38.85 (0.37_{rms})	0.04 (0.04_{rms})
Onc. Avg.	98.76 (1.13_{rms})	0.37 (0.22_{rms})	38.28 (0.10_{rms})	0.05 (0.03_{rms})

Table 4.13 Correlations between the skin markings and RSC

Pearson's correlation coefficient (r) for correlations between the skin markings COM and RSC COM are shown, as well as the mean change in relative distance between the skin markings COM and RSC COM (SM-RSC difference). The standard deviation and range are shown in parentheses.

Direction	r	SM-RSC difference (mm)
Lateral	0.785	1.24 (0.76; 0.08-3.38)
AP	0.741	1.80 (1.58; 0.03-6.51)
SI	0.853	1.23 (1.12; 0.05-4.91)

Figure 4.1 Sample interobserver RSC SD map

The RSC SD map obtained using the contours of all radiation oncologists (interobserver) on the day three treatment CT scan for Patient 11 is shown.

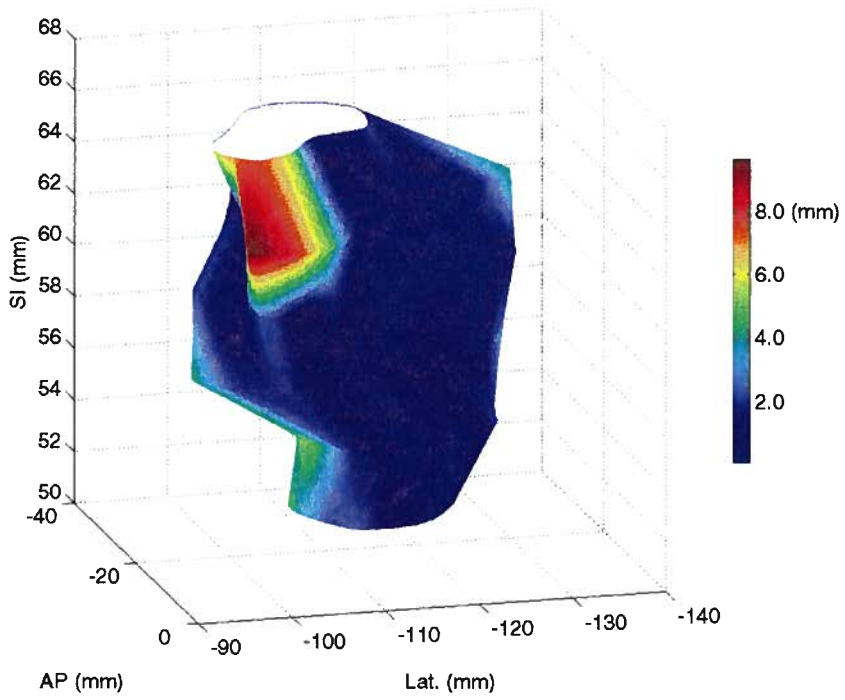

Figure 4.2 Sample intraobserver RSC SD map

The RSC SD map obtained using the contours of Oncologist 2 (intraobserver) on the planning CT scan for Patient 2 is shown.

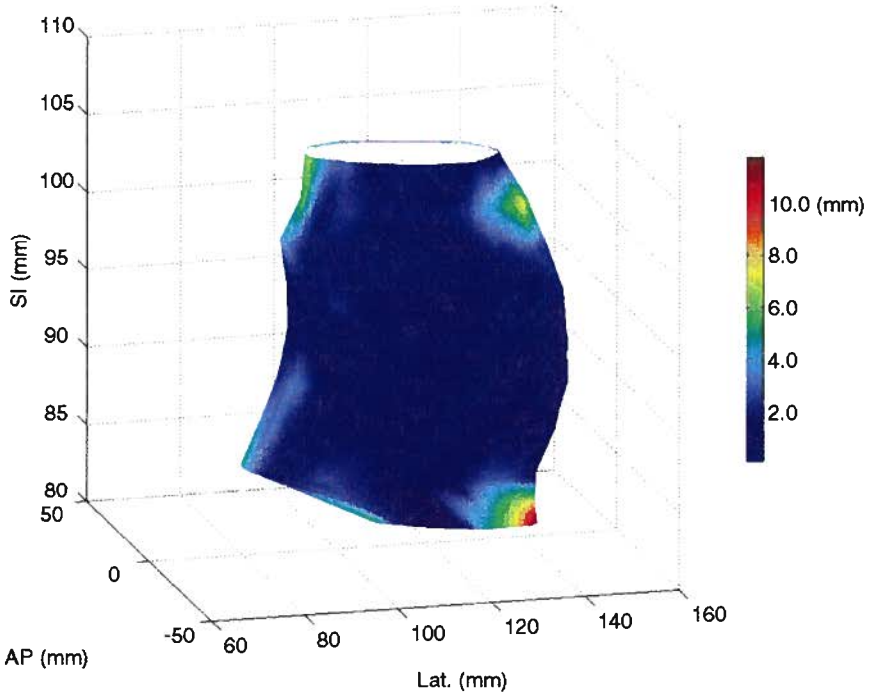

Figure 4.3 Sample RSC SD cumulative histograms

RSC SD cumulative histograms are shown for the RSCs obtained using the contours of Oncologist 1 (red), 2 (green), 3 (blue), and all oncologists (magenta) for the day one treatment CT scan for Patient 2.

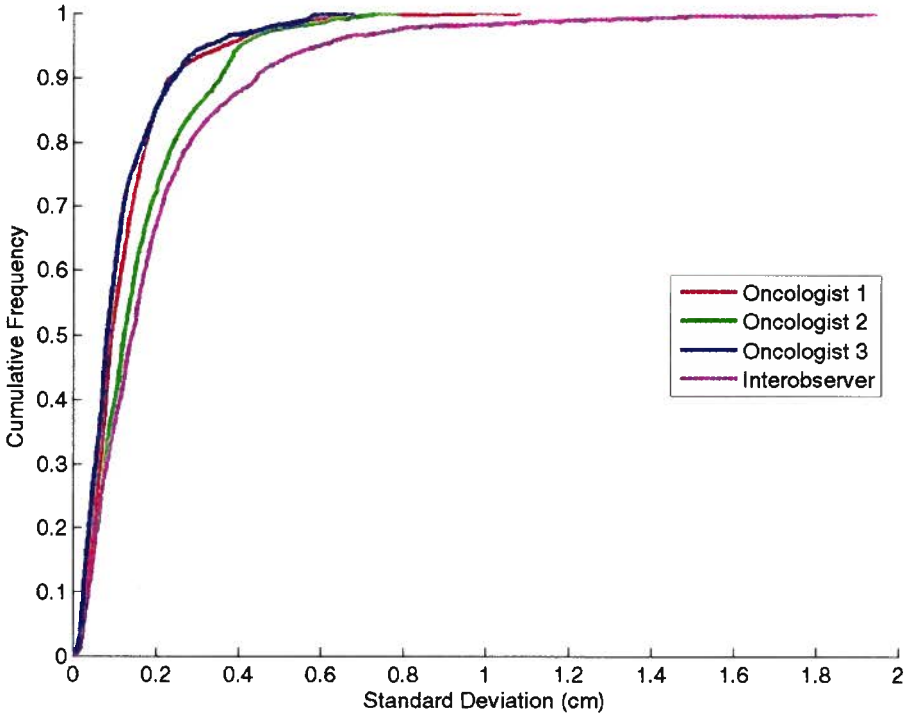

Figure 4.4 V_{95} and EUD for the surgical cavities of Patient 1

(a) V_{95} and (b) EUD for all surgical cavities contoured for Patient 1 is shown for each radiation oncologist.

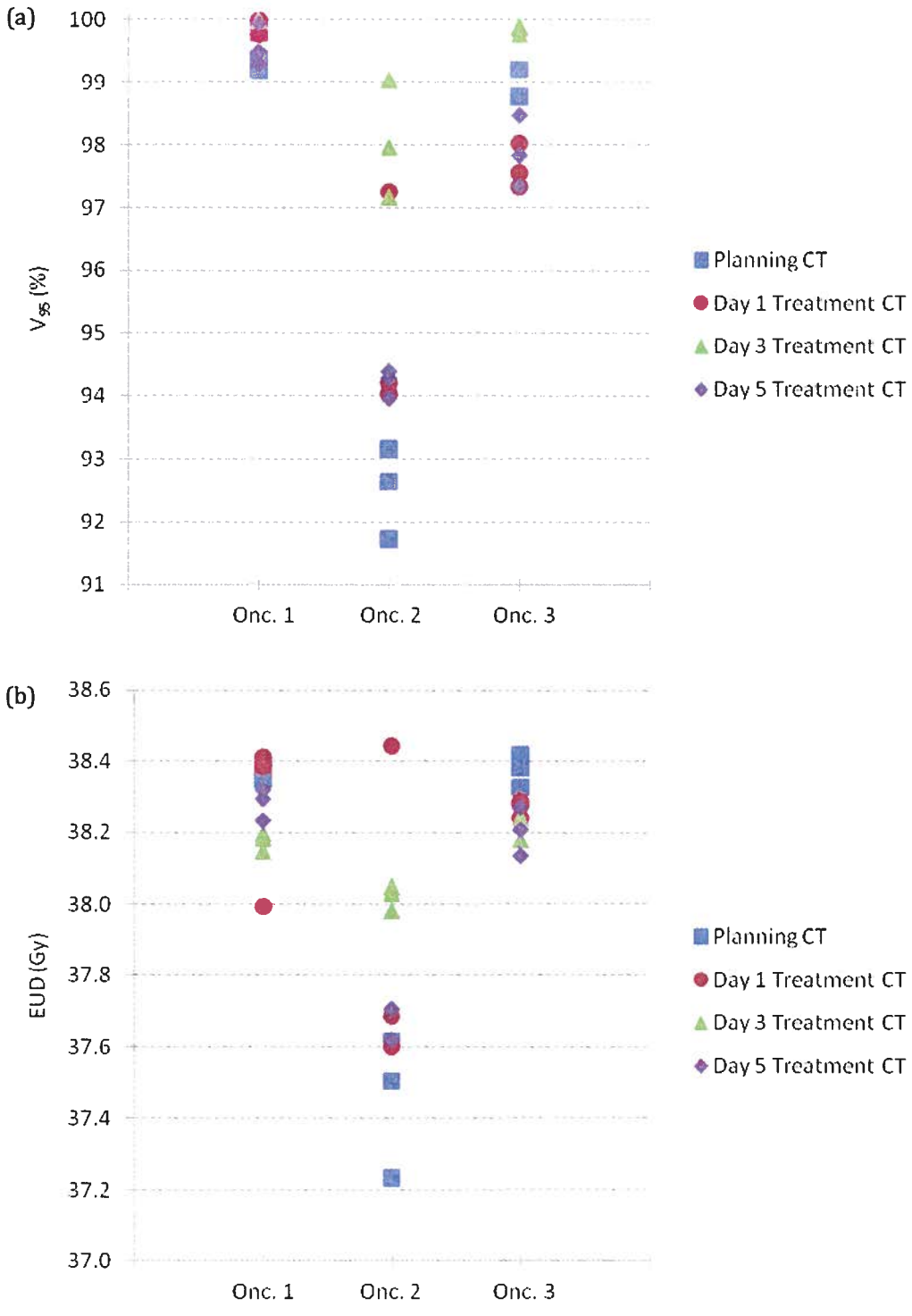

Figure 4.5 V_{95} and EUD for the surgical cavities of Patient 2

(a) V_{95} and (b) EUD for all surgical cavities contoured for Patient 2 is shown for each radiation oncologist.

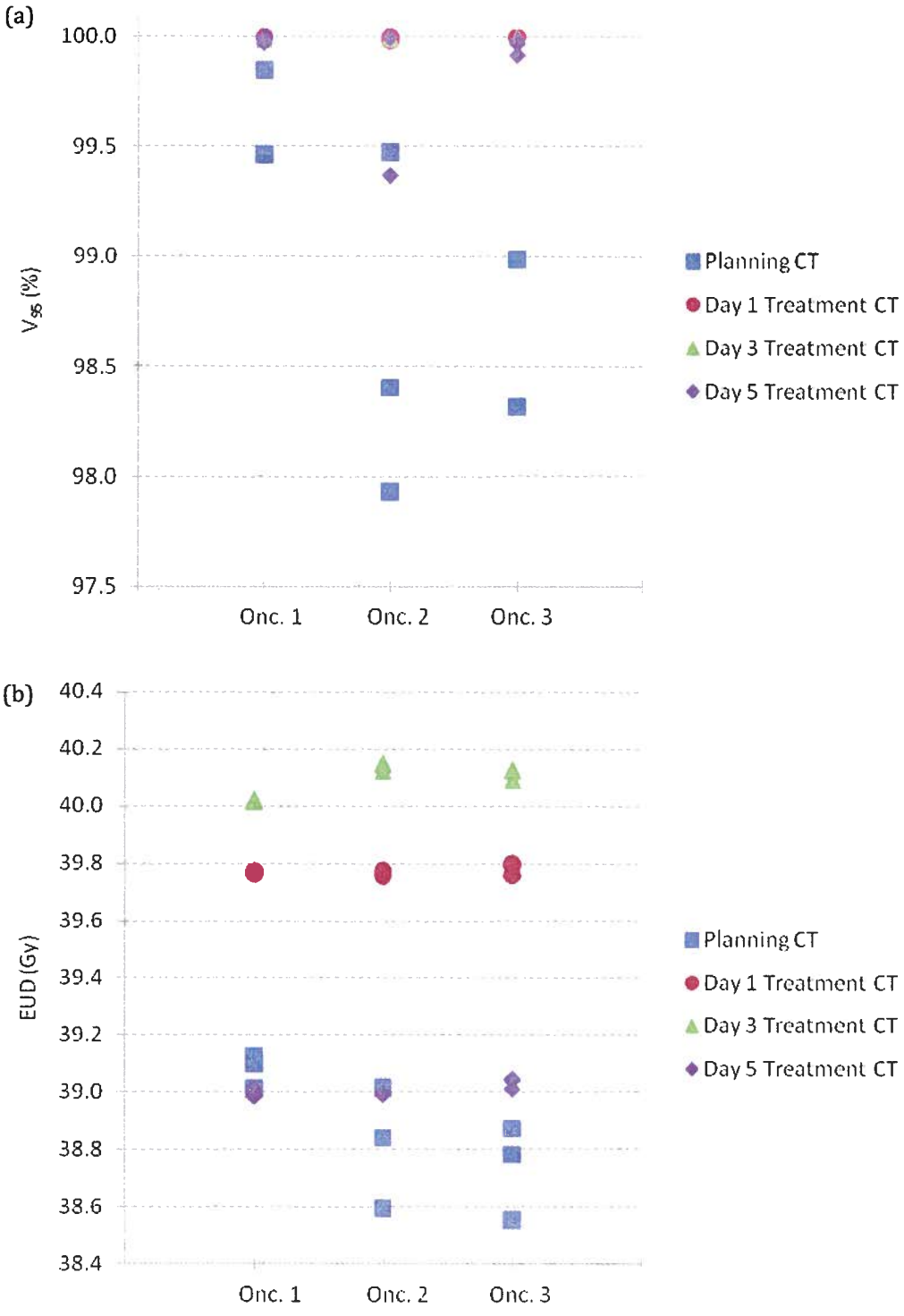

Figure 4.6 V_{95} and EUD for the surgical cavities of Patient 3

(a) V_{95} and (b) EUD for all surgical cavities contoured for Patient 3 is shown for each radiation oncologist.

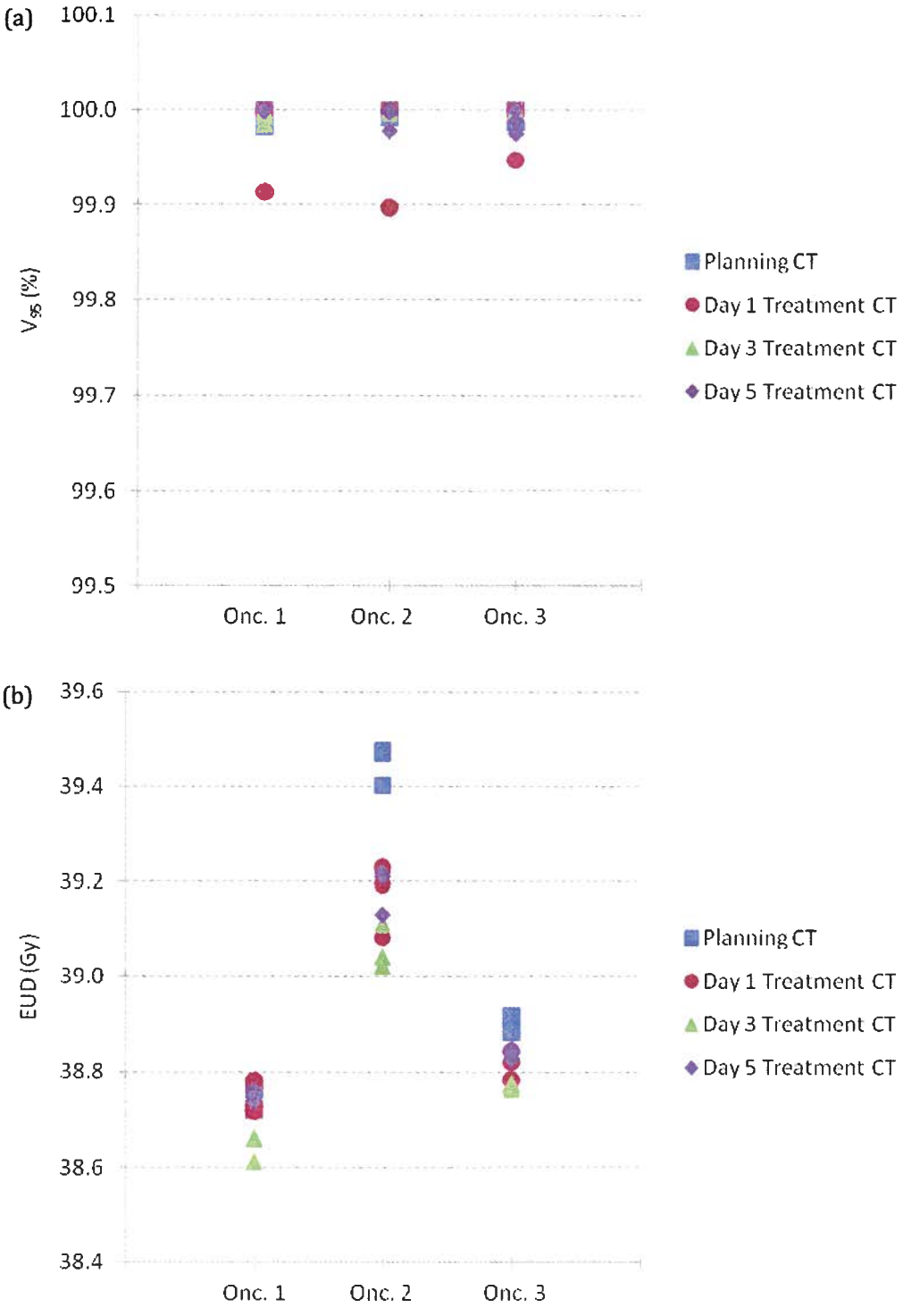

Figure 4.7 Correlations between the SM COM and RSC COM in the lateral direction

The correlation between the change in position of the skin markings COM and RSC COM on the repeat CT scans is shown in the lateral direction.

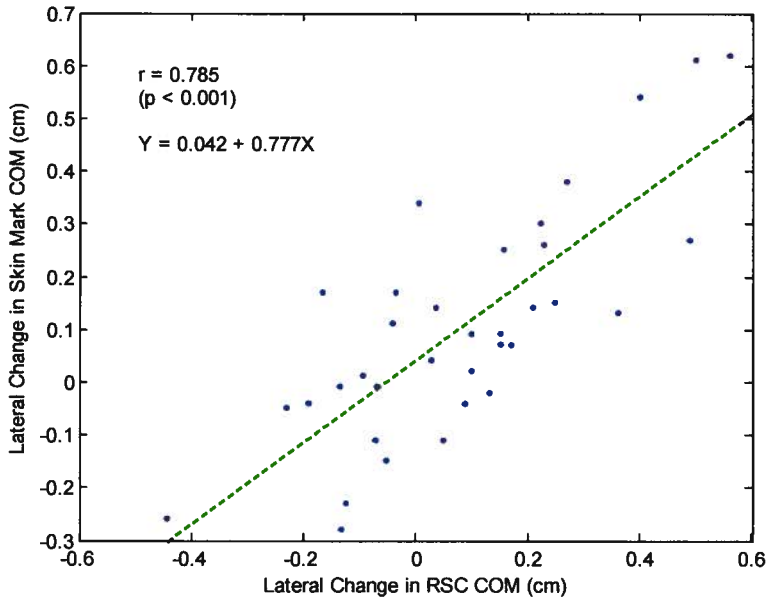

Figure 4.8 Correlations between the SM COM and RSC COMs in the AP direction

The correlation between the change in position of the skin markings COM and RSC COM on the repeat CT scans is shown in the AP direction.

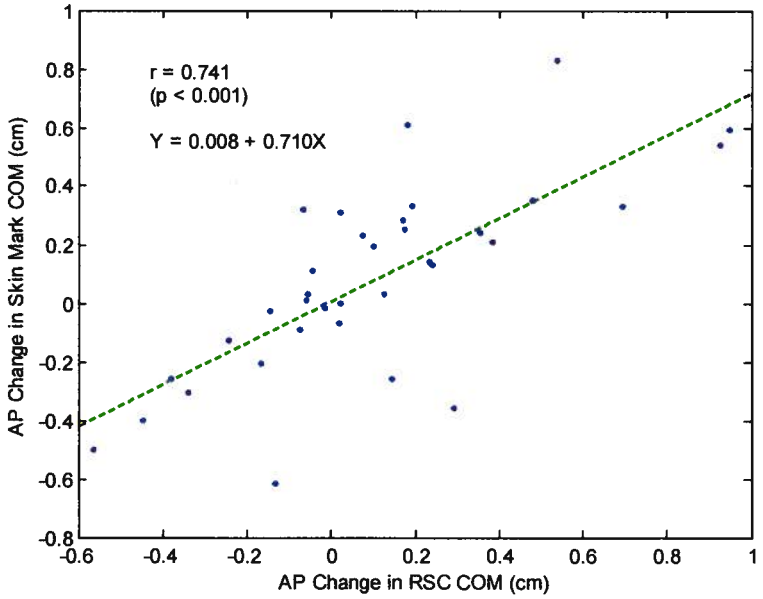

Figure 4.9 Correlations between the SM COM and RSC COM in the SI direction

The correlation between the change in position of the skin markings COM and RSC COM on the repeat CT scans is shown in the SI direction.

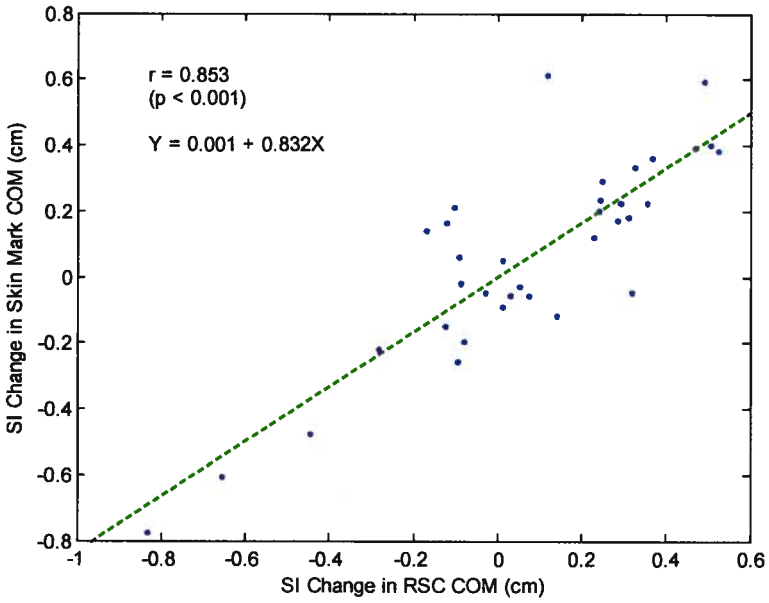

5. CONCLUSION AND FURTHER WORK

5.1. Conclusion

The method used to create the representative surgical cavity (RSC) proved useful in the analysis of interobserver and intraobserver surgical cavity contour variability as well as in assessment of the correlations between the positions of the skin markings and surgical cavity COM. This method used for RSC construction should continue to be used for interobserver and intraobserver contour variability studies. RSC SD maps are also a useful aid for visualization of interobserver and intraobserver contour variability. Hence, RSC SD maps should be used to assist radiation oncologists, radiation therapists, and other professionals in contour training.

Interobserver surgical cavity contour variations in volume, COM, spatial dimensions, and dose were observed to be larger than intraobserver variations. Moreover, surgical cavity COM variations were on average less than 2 mm in the lateral, AP, and SI directions. Variations in the axial plane of the surgical cavity contours were observed to be largest at the most superior and inferior extent of the contours in both interobserver and intraobserver studies; variations in the axial plane were on average 0.19 cm and 0.13 cm, respectively. Despite these interobserver and intraobserver differences, measurements of V_{95} and EUD suggest that current planning margins are sufficient to provide adequate dose coverage to the surgical cavity. Nevertheless, studies that endeavour to investigate changes in shape, size, and position of the surgical cavity should be careful to take into account these interobserver and intraobserver differences.

It was determined that the change in position of the SM COM during treatment was strongly correlated to changes in position of the RSC COM in the lateral, AP, and SI directions. Hence, patient setup using skin markings is plausible during treatment. In addition, it was observed that the average change in the distance between the SM COM and RSC COM during treatment was more than 4 mm in less than 5% of cases. The average change in distance was 1.24 mm, 1.80 mm, and 1.23 mm in the lateral, AP, and SI directions, respectively. Planning margins for the surgical cavity can potentially be reduced if skin markings are used for patient setup, but further study would be prudent to ensure that adequate dose coverage of the surgical cavity is achievable if planning margins are smaller. Nevertheless, skin marking setup can be readily done without the need for surgical clips or daily contouring. For example, the skin marking positions can be localized daily by infrared sensors or on-board imaging techniques and the patient can be realigned to ensure the SM COM is at always at the desired position for treatment. If further studies show that skin marking setup is dosimetrically equivalent to other possible localization methods under study, such as imaging of surgical clips with cone beam CT, skin marking setup should be sufficient to decrease planning margins.

5.2. Further Work

Ongoing work in Stage I of the DIVA project will continue to investigate the correlation between the positions of the SM COM and RSC COM until the patient recruitment goal is met for the study. Furthermore, the dosimetric consequences of changes in the position and size of the surgical cavity will be assessed using the repeat

CT scans for all patients in the study. In addition, an investigation of the dose received to normal tissues during treatment using the repeat CT scans is underway to verify if their dose-volume constraints are met during treatment. Following will be the commencement of DIVA Stage II, which hopes to make use of on-board imaging techniques, such as CBCT, to localize surgical clips around the surgical cavity during treatment. The ultimate goal is to develop a method that allows improved localization of the surgical cavity and a potential decrease in the planning margins used for 3DCRT APBI.

In addition, construction of the representative contours provides a novel method that can find a contour that takes into account contributions from many contours, even if the contour shapes are complex. Comparisons of contours with the representative contour should continue to be used as a method to assess interobserver and intraobserver contour variations. In addition, calculations of the standard deviation at points of calculation of the representative contour provide a spatial distribution of contour variations. Hence, mapping the standard deviations to the representative contour should continue to be used as a method to visualize changes in contour variations. Ideally, such studies should use volume-based, distance-based, and dose measurement for assessment of contour variability.

REFERENCES

1. Statistics Canada. Cancer, new cases, by selected primary site of cancer, by sex. Available from: http://www40.statcan.ca/l01/cst01/hlth61-eng.htm. Last Updated: 2009 Feb 02. Accessed: 2009 Mar 8.
2. Statistics Canada. Table 103-0403 - Cancer incidence, by selected sites of cancer and sex, three-year average, Canada, provinces, territories and health regions (June 2005 boundaries), occasional (age-standardized rate per 100,000 population). *CANSIM (database)*. Available from: http://cansim2.statcan.gc.ca/cgi-win/cnsmcgi.exe?Lang=E&CNSM-Fi=CII/CII_1-eng.htm. Last Updated: 2009 Feb 03. Accessed: 2009 Mar 8.
3. Reid S. Ten most frequent cancer types in BC by year of diagnosis 1997 to 2005. Available from: http://www.bccancer.bc.ca/NR/rdonlyres/2FB52EE7-FDAD-4684-A141-7194C1C6B7A/24858/TenMostFrequentCancerTypesinBC.pdf. Last Updated: 2007 Sep. Accessed: 2009 Mar 8.
4. Table 103-0550 - new cases for ICD-O-3 primary sites of cancer (based on the july 2008 CCR tabulation file), by age group and sex, Canada, provinces and territories, annual. *CANSIM (database)*. Available from: http://cansim2.statcan.gc.ca/cgi-win/cnsmcgi.exe?Lang=E&CNSM-Fi=CII/CII_1-eng.htm. Last Updated 2009 Feb 03. Accessed: 2009 Mar 8.
5. BC cancer agency statistics by cancer type: Breast (female). Available from: http://www.bccancer.bc.ca/NR/rdonlyres/AC6262BC-634F-4227-BF14-1631

82197EDF/27956/breastfemale.pdf. Last Updated: 2007 Nov 01. Accessed: 2009 Mar 8.

6. Statistics Canada. Table 103-1561 - Five-year survival estimates for breast cancer cases, ICD-O-3 (January 2008 CCR file), by age group and sex, population aged 15 to 99, 1 year of cases, Canada (excluding Quebec), annual (percent unless otherwise noted). *CANSIM (database)*. Available from: http://cansim2.statcan.gc.ca/cgi-win/cnsmcgi.exe?Lang=E&CNSM-Fi=CII/CII_1-eng.htm. Last Updated: 2008 Jun 03. Accessed: 2009 Mar 8.
7. Coldman A, Phillips N, Reid S. BC Cancer Agency survival statistics 2005. Available from: http://www.bccancer.bc.ca/NR/rdonlyres/D82 91ED8-FAEE-4692-A256-5320928187F2/29082/Survival_Statistics_2006.pdf. Last Updated: 2008 Mar 19. Accessed: 2009 Mar 8.
8. Arthur DW, Vicini FA. Accelerated partial breast irradiation as a part of breast conservation therapy. *J Clin Oncol.* 2005;23:1726–1735.
9. Baglan KL, Sharpe MB, Jaffray D, Frazier RC, Fayad J, Kestin LL, et al. Accelerated partial breast irradiation using 3D conformal radiation therapy (3DCRT). *Int J Radiat Oncol Biol Phys.* 2003;55:302–311.
10. Arthur D. Accelerated partial breast irradiation: A change in treatment paradigm for early stage breast cancer. *J Surg Oncol.* 2003;84:185–191.
11. Veronesi U, Marubini E, Mariani L, Galimberti V, Luini A, Veronesi P, et al. Radiotherapy after breast-conserving surgery in small breast carcinoma: Long-term results of a randomized trial. *Ann Oncol.* 2001;12:997–1003.

12. Clark RM, McCulloch PB, Levine MN, Lipa M, Wilkinson RH, Mahoney LJ, et al. Randomized clinical trial to assess the effectiveness of breast irradiation following lumpectomy and axillary dissection for node-negative breast cancer. *J Natl Cancer Inst.* 1992;84:683–689.

13. Sector resection with or without postoperative radiotherapy for stage I breast cancer: A randomized trial. Uppsala-Orebro Breast Cancer Study Group. *J Natl Cancer Inst.* 1990;82:277–282.

14. RAPID: Randomized trial of accelerated partial breast irradiation. *clinicaltrials.gov.* Available from: http://www.clinicaltrials.gov/ct2/show/NCT00282035. Last Updated: 2009 Jan 8. Accessed: 2009 Mar 16.

15. Podgorsak EB, ed. Radiation oncology physics : a handbook for teachers and students. Vienna: International Atomic Energy Agency, 2005.

16. Rusthoven KE, Carter DL, Howell K, Kercher JM, Henkenberns P, Hunter KL, et al. Accelerated partial-breast intensity-modulated radiotherapy results in improved dose distribution when compared with three-dimensional treatment-planning techniques. *Int J Radiat Oncol Biol Phys.* 2008;70:296–302.

17. Oliver M, Chen J, Wong E, Van Dyk J, Perera F. A treatment planning study comparing whole breast radiation therapy against conformal, IMRT and tomotherapy for accelerated partial breast irradiation. *Radiother Oncol.* 2007;82:317–323.

18. Vicini FA, Baglan KL, Kestin LL, Mitchell C, Chen PY, Frazier RC, et al. Accelerated treatment of breast cancer. *J Clin Oncol.* 2001;19:1993–2001.

19. Vicini FA, Kestin L, Chen P, Benitez P, Goldstein NS, Martinez A. Limited-field radiation therapy in the management of early-stage breast cancer. *J Natl Cancer Inst.* 2003;95:1205–1210.

20. King TA, Bolton JS, Kuske RR, Fuhrman GM, Scroggins TG, Jiang XZ. Long-term results of wide-field brachytherapy as the sole method of radiation therapy after segmental mastectomy for T(is,1,2) breast cancer. *Am J Surg.* 2000;180:299–304.

21. Polgar C, Sulyok Z, Fodor J, Orosz Z, Major T, Takacsi-Nagy Z, et al. Sole brachytherapy of the tumor bed after conservative surgery for T1 breast cancer: Five-year results of a phase I-II study and initial findings of a randomized phase III trial. *J Surg Oncol.* 2002;80:121–128.

22. Krishnan L, Jewell WR, Tawfik OW, Krishnan EC. Breast conservation therapy with tumor bed irradiation alone in a selected group of patients with stage I breast cancer. *Breast J.* 2001;7:91–96.

23. Arthur DW, Koo D, Zwicker RD, Tong S, Bear HD, Kaplan BJ, et al. Partial breast brachytherapy after lumpectomy: Low-dose-rate and high-dose-rate experience. *Int J Radiat Oncol Biol Phys.* 2003;56:681–689.

24. Wazer DE, Berle L, Graham R, Chung M, Rothschild J, Graves T, et al. Preliminary results of a phase I/II study of HDR brachytherapy alone for T1/T2 breast cancer. *Int J Radiat Oncol Biol Phys.* 2002;53:889–897.

25. Lawenda BD, Taghian AG, Kachnic LA, Hamdi H, Smith BL, Gadd MA, et al. Dose-volume analysis of radiotherapy for T1N0 invasive breast cancer treated by local excision and partial breast irradiation by low-dose-rate interstitial implant. *Int J Radiat Oncol Biol Phys.* 2003;56:671–680.

26. McCormick B. Partial-breast radiation for early staged breast cancers: Hypothesis, existing data, and a planned phase III trial. *J Natl Compr Canc Netw.* 2005;3:301–307.

27. Landis DM, Luo W, Song J, Bellon JR, Punglia RS, Wong JS, et al. Variability among breast radiation oncologists in delineation of the postsurgical lumpectomy cavity. *Int J Radiat Oncol Biol Phys.* 2007;67:1299–308.

28. Wong EK, Truong PT, Kader HA, Nichol AM, Salter L, Petersen R, et al. Consistency in seroma contouring for partial breast radiotherapy: Impact of guidelines. *Int J Radiat Oncol Biol Phys.* 2006;66:372–376.

29. Langen KM, Buchholz DJ, Burch DR, Burkavage R, Limaye AU, Meeks SL, et al. Investigation of accelerated partial breast patient alignment and treatment with helical tomotherapy unit. *Int J Radiat Oncol Biol Phys.* 2008;70:1272–1280.

30. White EA, Cho J, Vallis KA, Sharpe MB, Lee G, Blackburn H, et al. Cone beam computed tomography guidance for setup of patients receiving accelerated partial breast irradiation. *Int J Radiat Oncol Biol Phys.* 2007;68:547–554.

31. Hasan Y, Kim L, Martinez A, Vicini F, Yan D. Image guidance in external beam accelerated partial breast irradiation: Comparison of surrogates for the lumpectomy cavity. *Int J Radiat Oncol Biol Phys.* 2008;70:619–25.

32. Kim LH, Wong J, Yan D. On-line localization of the lumpectomy cavity using surgical clips. *Int J Radiat Oncol Biol Phys.* 2007;69:1305–1309.

33. Do skin markings reflect the location of the surgical cavity during daily radiotherapy treatment? *clinicaltrials.gov*. Available from: http://www.clinicaltrials.gov/ct2/show/NCT00578747. Last Updated: 2008 Nov 24. Accessed: 2009 Mar 8.

34. Deurloo KE, Steenbakkers RJ, Zijp LJ, de Bois JA, Nowak PJ, Rasch CR, et al. Quantification of shape variation of prostate and seminal vesicles during external beam radiotherapy. *Int J Radiat Oncol Biol Phys.* 2005;61:228–238.

35. Song WY, Chiu B, Bauman GS, Lock M, Rodrigues G, Ash R, et al. Prostate contouring uncertainty in megavoltage computed tomography images acquired with a helical tomotherapy unit during image-guided radiation therapy. *Int J Radiat Oncol Biol Phys.* 2006;65:595–607.

36. Papademetris X, Sinusas AJ, Dione DP, Constable RT, Duncan JS. Estimation of 3-D left ventricular deformation from medical images using biomechanical models. *IEEE Trans Med Imaging.* 2002;21:786–800.

37. Dubois DF, Prestidge BR, Hotchkiss LA, Prete JJ, Bice WS,Jr. Intraobserver and interobserver variability of MR imaging- and CT-derived prostate volumes after transperineal interstitial permanent prostate brachytherapy. *Radiology.* 1998;207:785–789.

38. Lee WR, Roach M, Michalski J, Moran B, Beyer D. Interobserver variability leads to significant differences in quantifiers of prostate implant adequacy. *Int J Radiat Oncol Biol Phys.* 2002;54:457–461.

39. Fiorino C, Reni M, Bolognesi A, Cattaneo GM, Calandrino R. Intra- and inter-observer variability in contouring prostate and seminal vesicles: Implications for conformal treatment planning. *Radiother Oncol.* 1998;47:285–292.

40. Rasch C, Barillot I, Remeijer P, Touw A, van Herk M, Lebesque JV. Definition of the prostate in CT and MRI: A multi-observer study. *Int J Radiat Oncol Biol Phys.* 1999;43:57–66.

41. Hurkmans CW, Borger JH, Pieters BR, Russell NS, Jansen EP, Mijnheer BJ. Variability in target volume delineation on CT scans of the breast. *Int J Radiat Oncol Biol Phys.* 2001;50:1366–1372.

42. Cuttino LW, Todor D, Pacyna L, Lin PS, Arthur DW. Three-dimensional conformal external beam radiotherapy (3DCRT) for accelerated partial breast irradiation (APBI): What is the correct prescription dose? *Am J Clin Oncol.* 2006;29:474–478.

43. Bovi J, Qi XS, White J, Li XA. Comparison of three accelerated partial breast irradiation techniques: Treatment effectiveness based upon biological models. *Radiother Oncol.* 2007;84:226–232.

APPENDICES

A. Interobserver RSC Standard Deviation Maps

Figure A.1 Interobserver RSC SD map for Patient 1, Planning CT

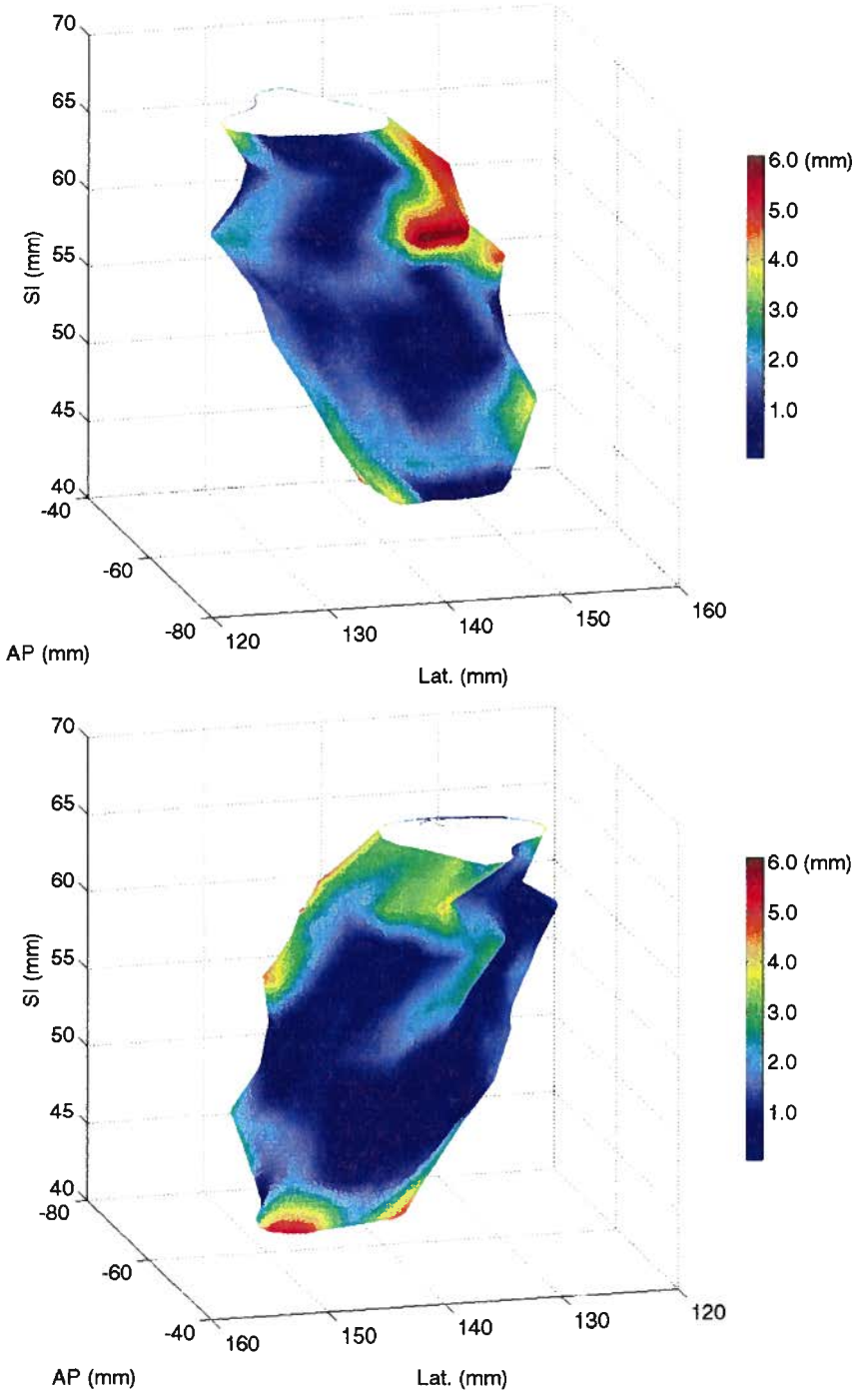

Figure A.2 Interobserver RSC SD map for Patient 2, Day 1 Treatment CT

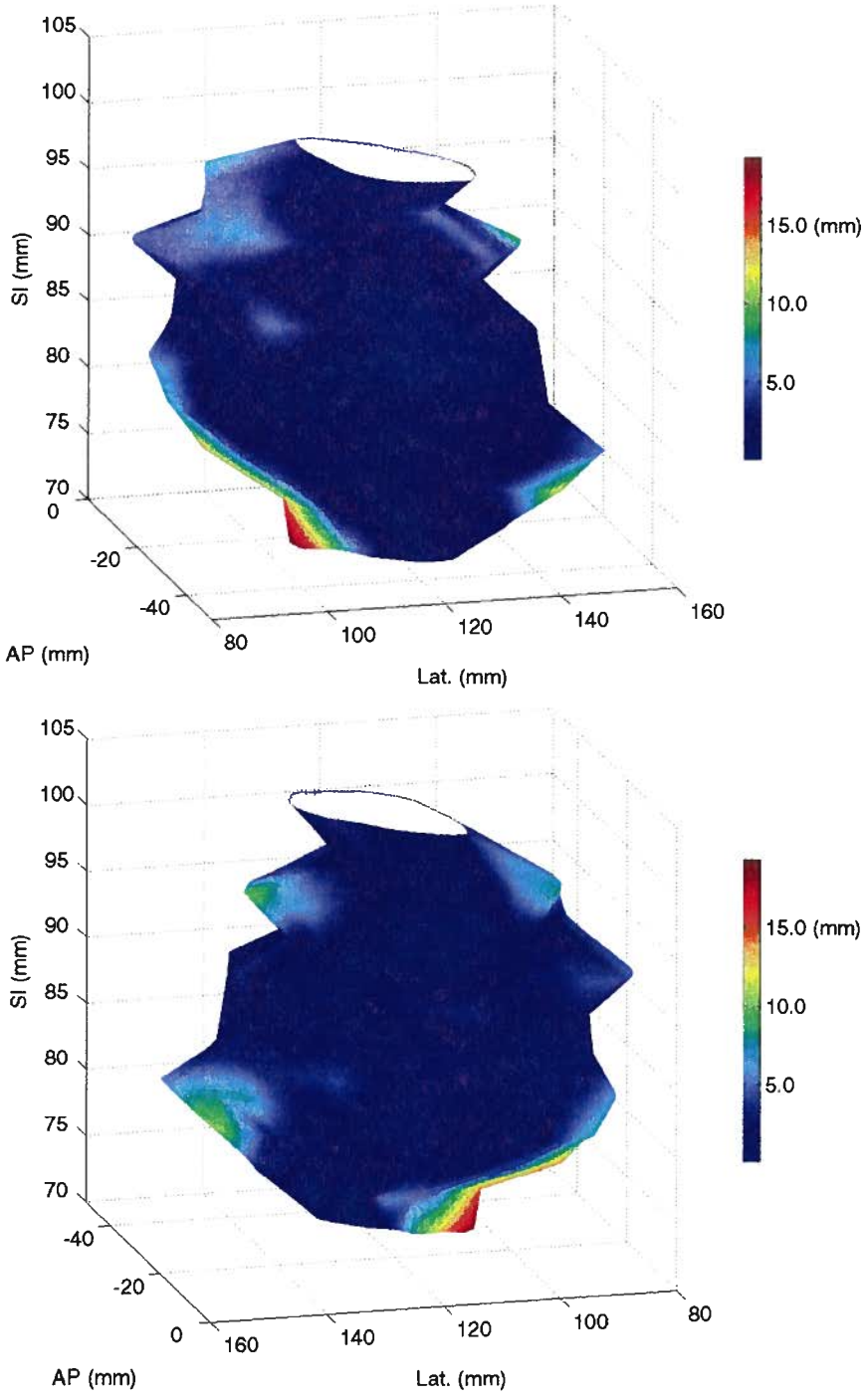

Figure A.3 Interobserver RSC SD map for Patient 3, Day 3 Treatment CT

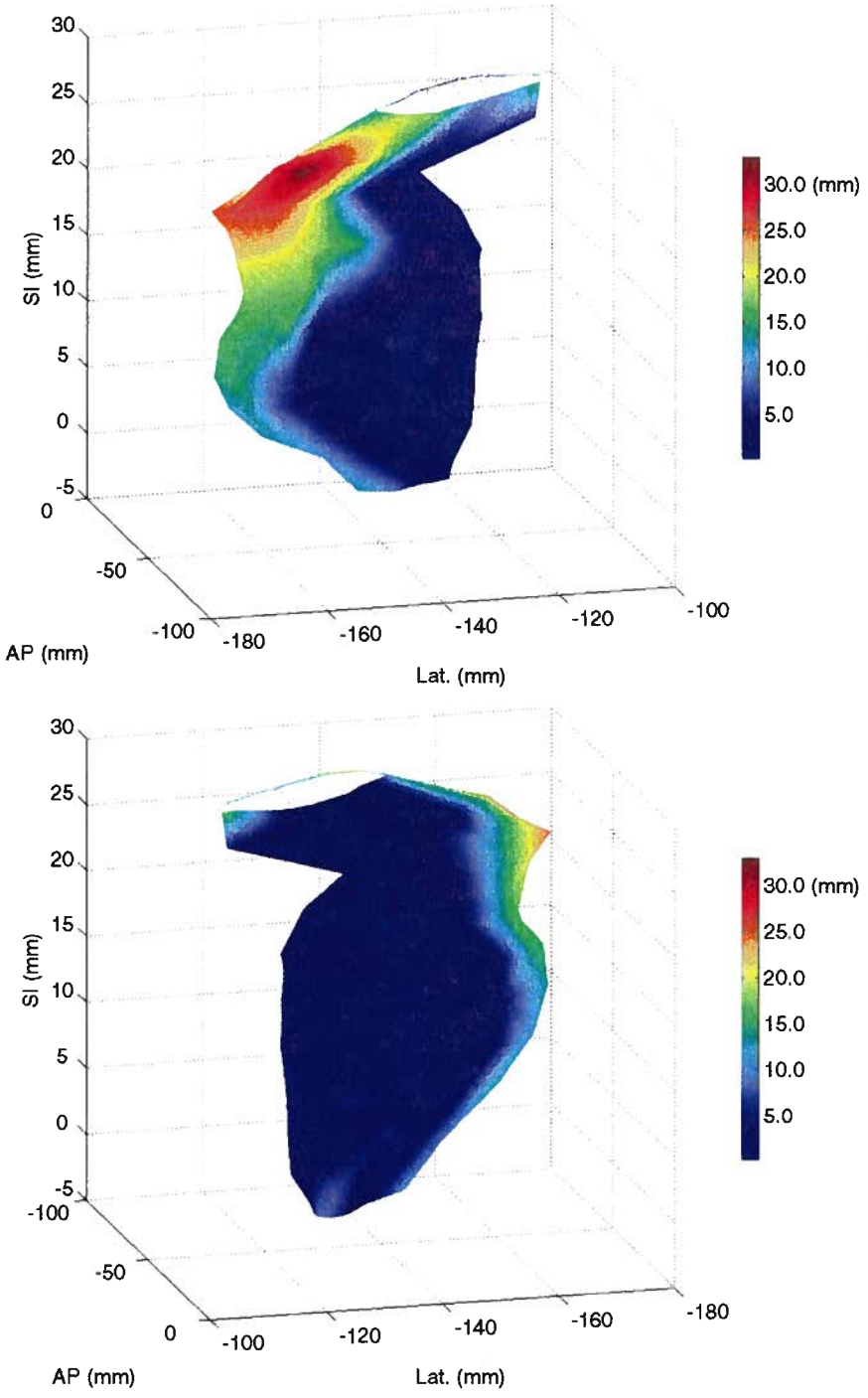

Figure A.4 Interobserver RSC SD map for Patient 4, Day 5 Treatment CT

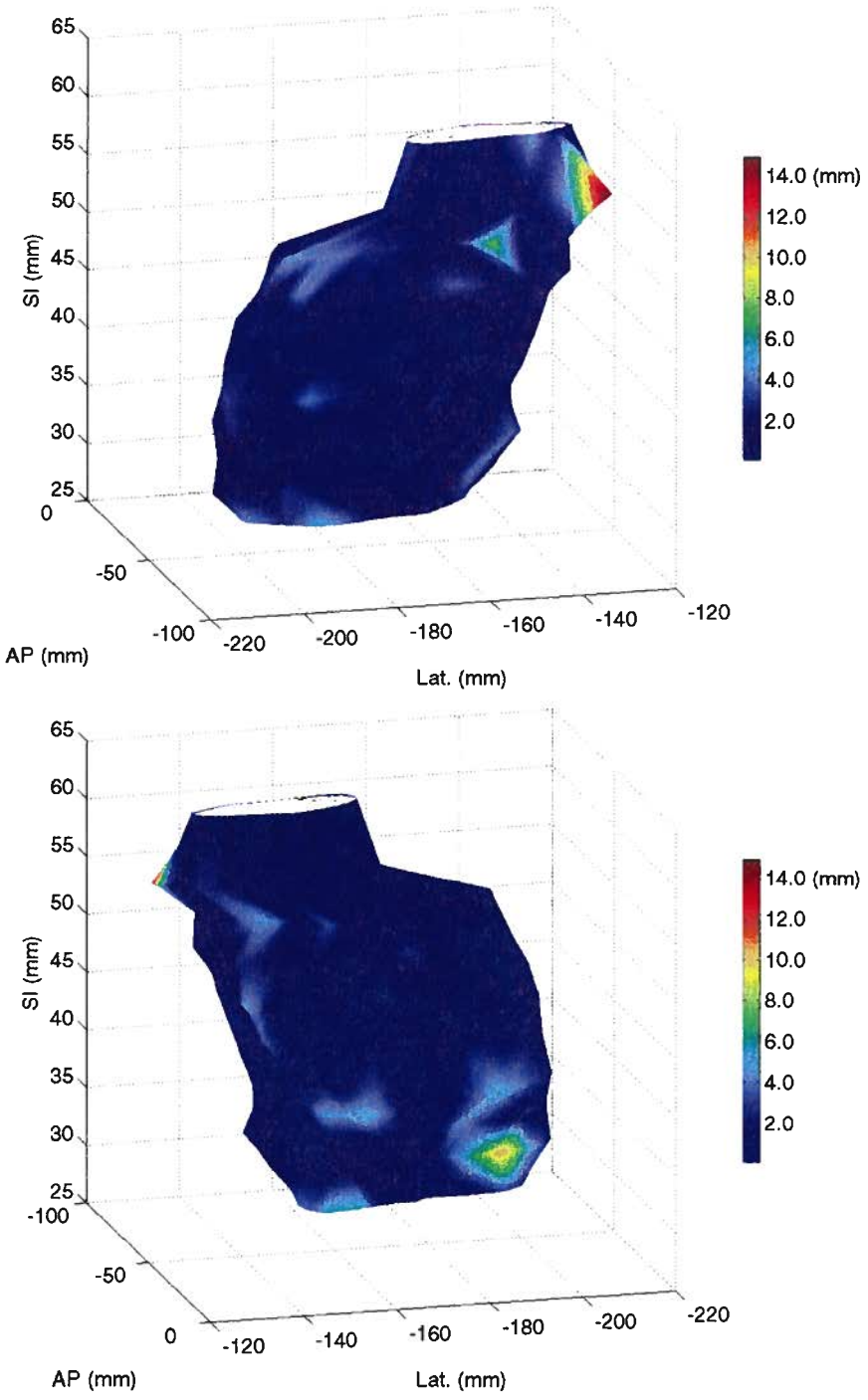

Figure A.5 Interobserver RSC SD map for Patient 5, Planning CT

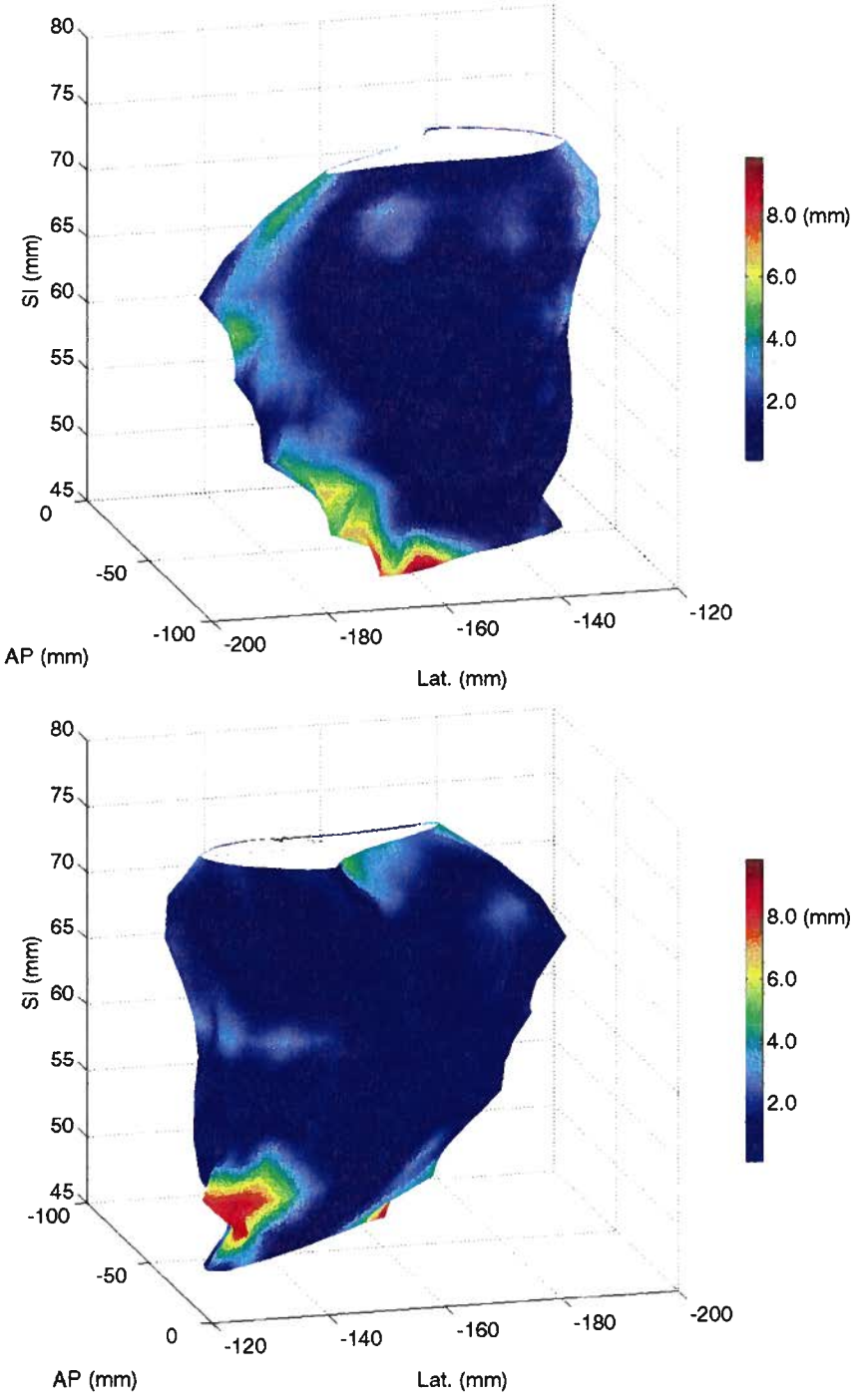

Figure A.6 Interobserver RSC SD map for Patient 6, Day 1 Treatment CT

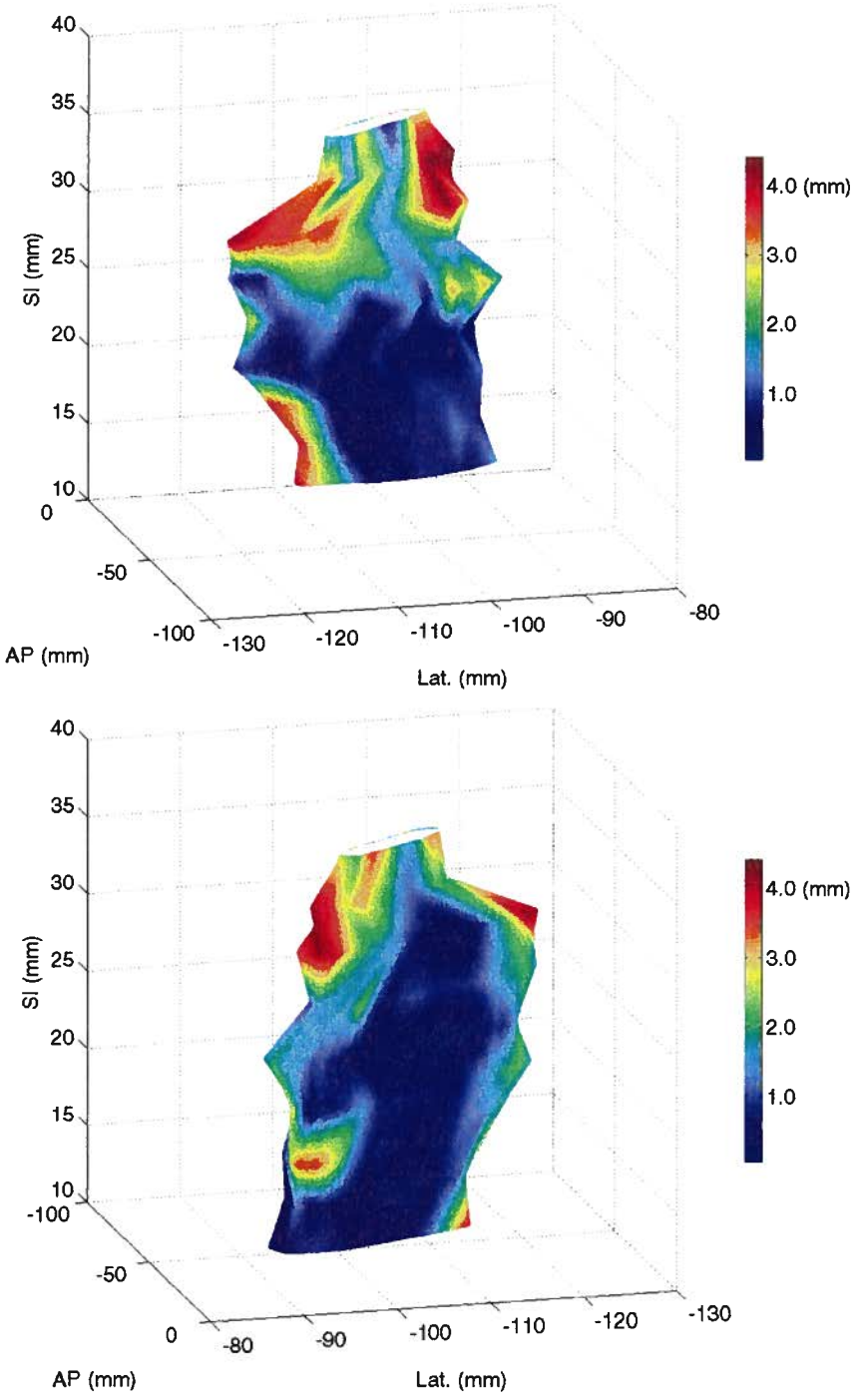

Figure A.7 Interobserver RSC SD map for Patient 7, Day 3 Treatment CT

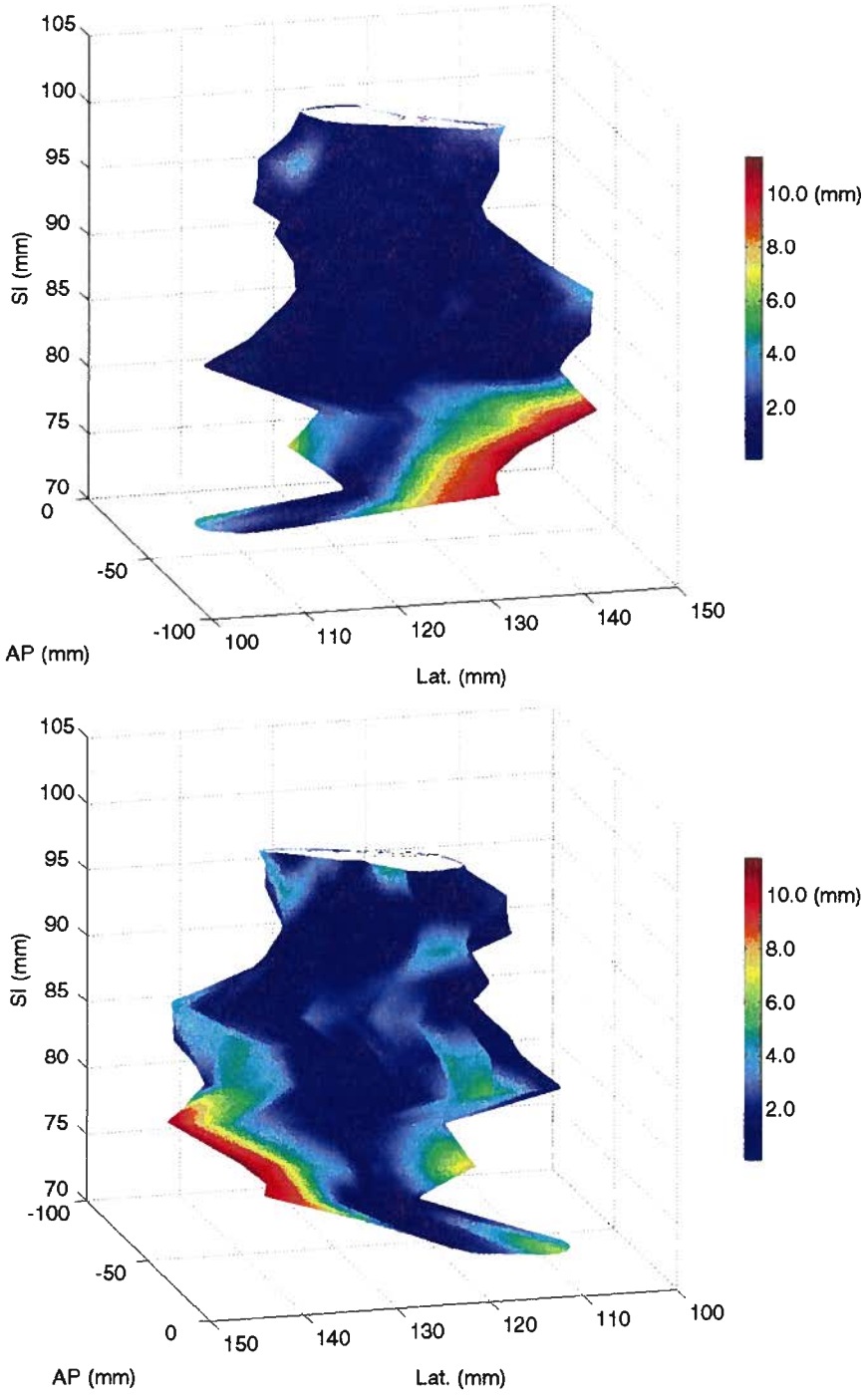

Figure A.8 Interobserver RSC SD map for Patient 8, Day 5 Treatment CT

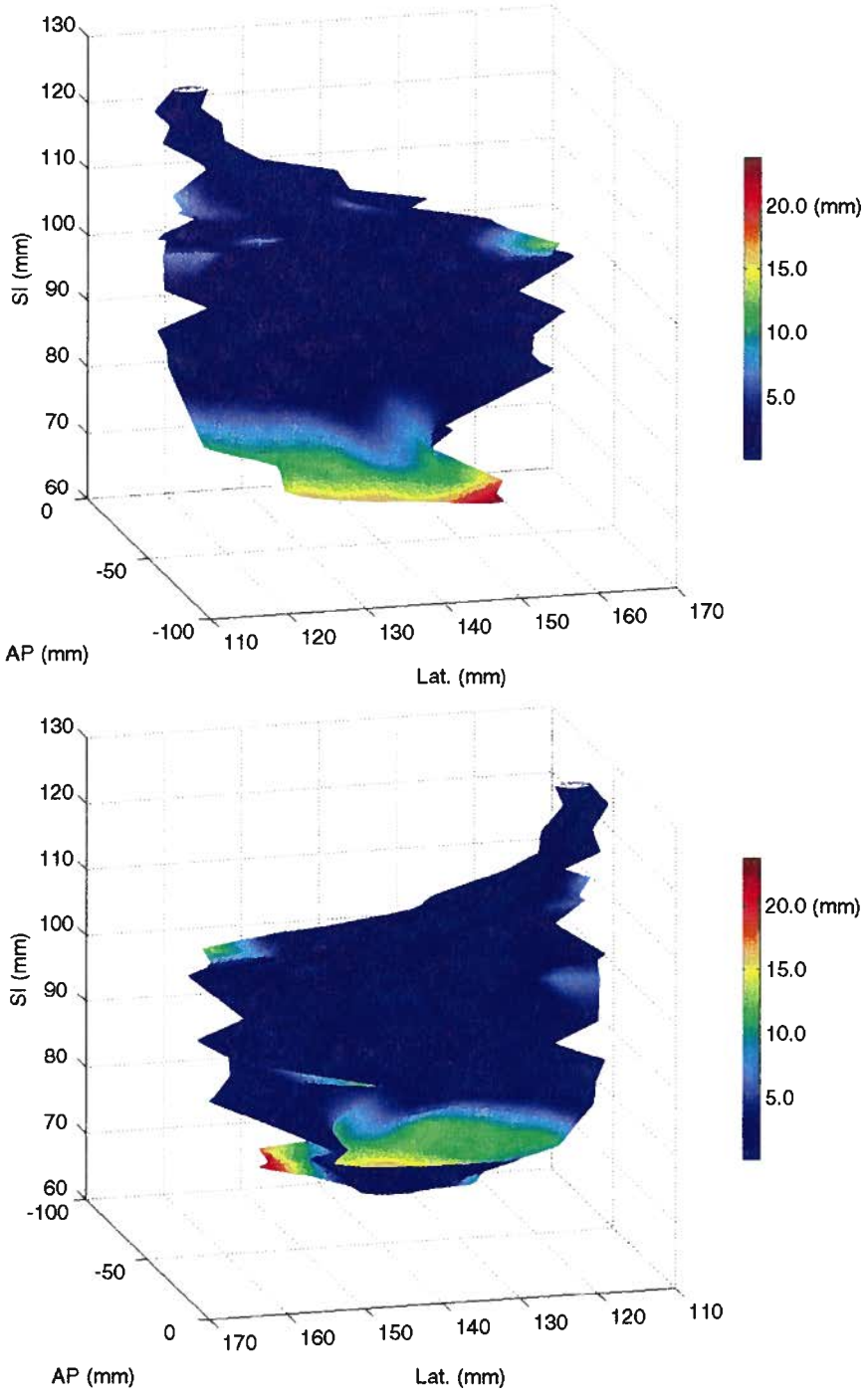

Figure A.9 Interobserver RSC SD map for Patient 9, Planning CT

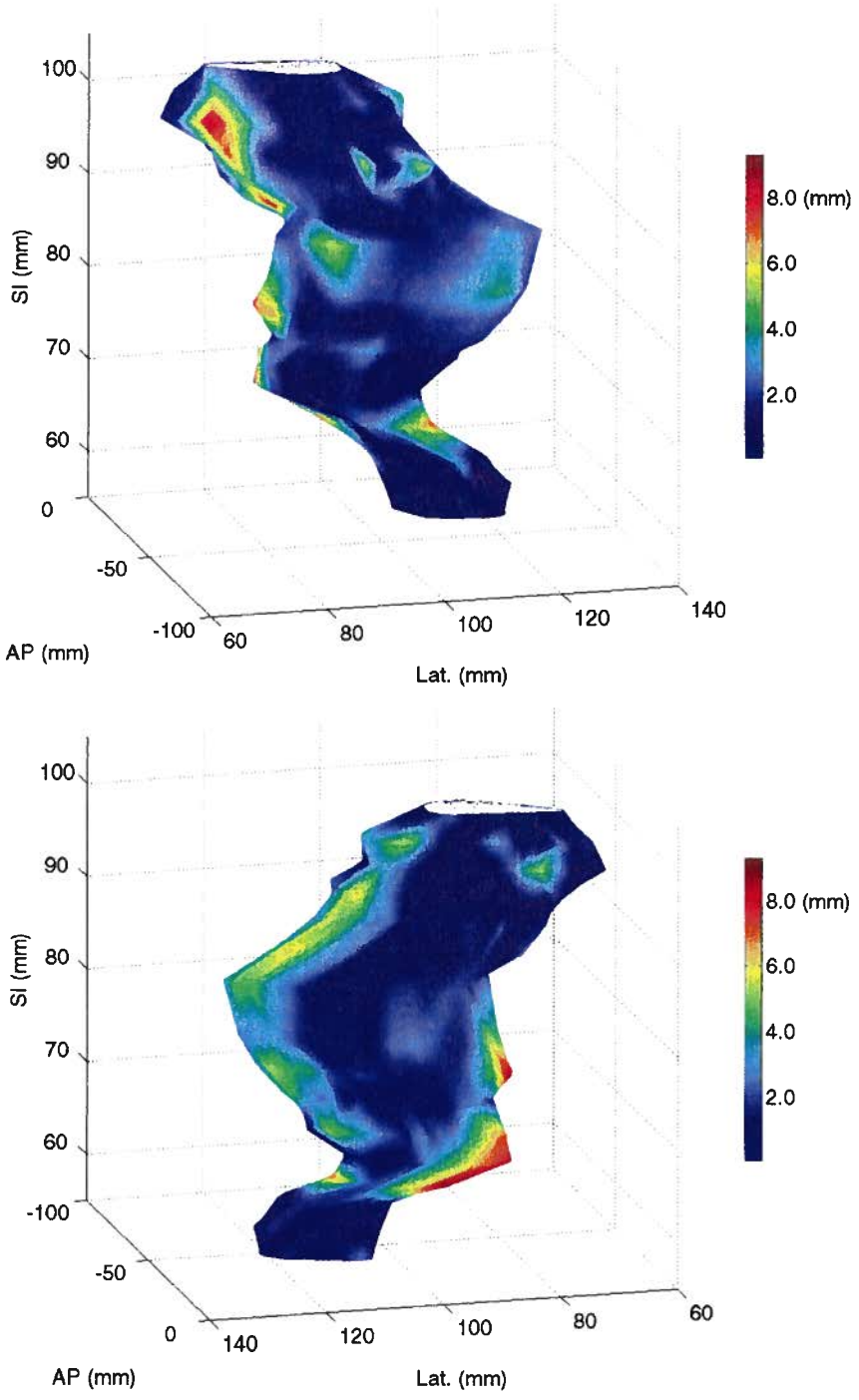

Figure A.10 Interobserver RSC SD map for Patient 10, Day 1 Treatment CT

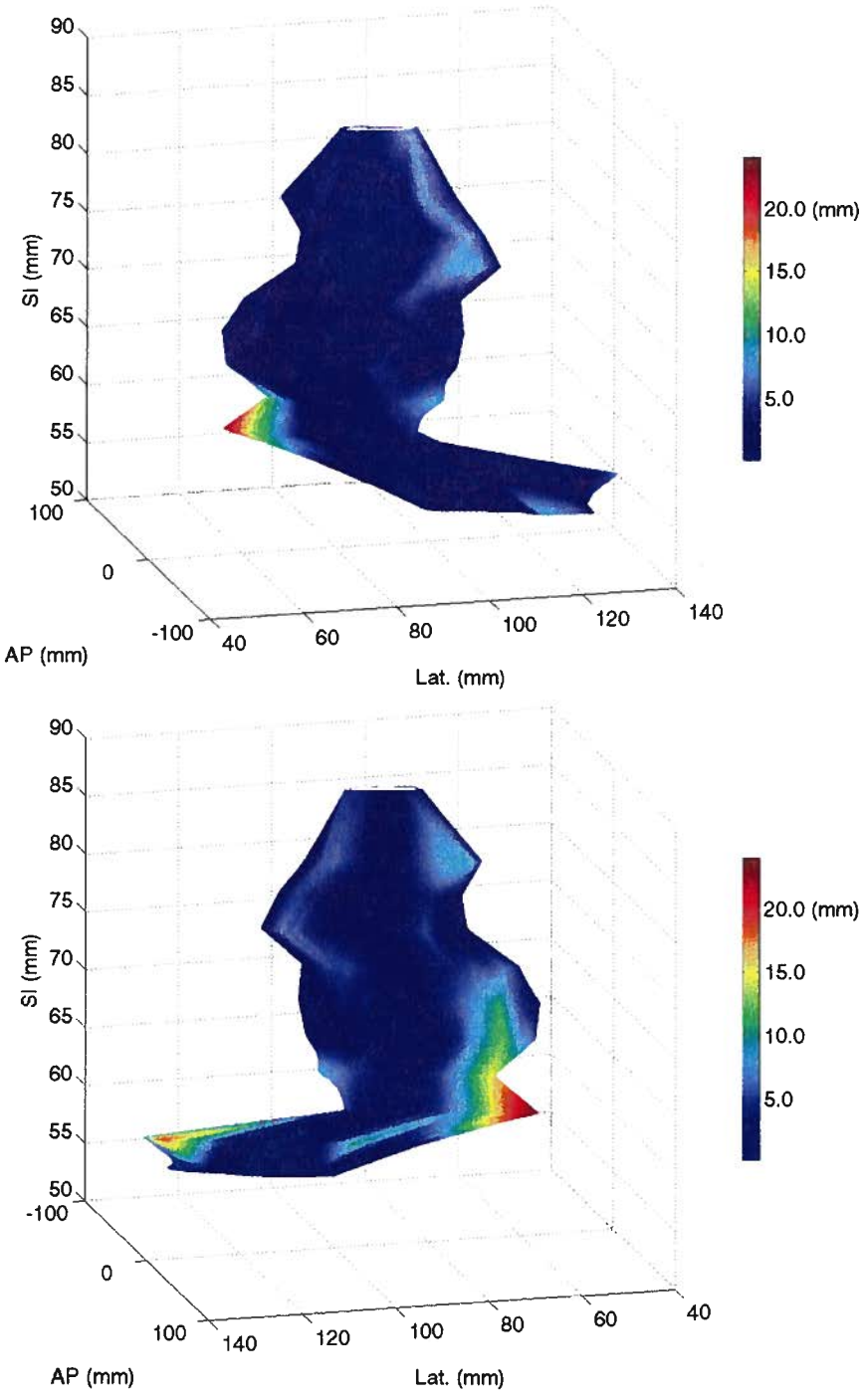

Figure A.11 Interobserver RSC SD map for Patient 11, Day 3 Treatment CT

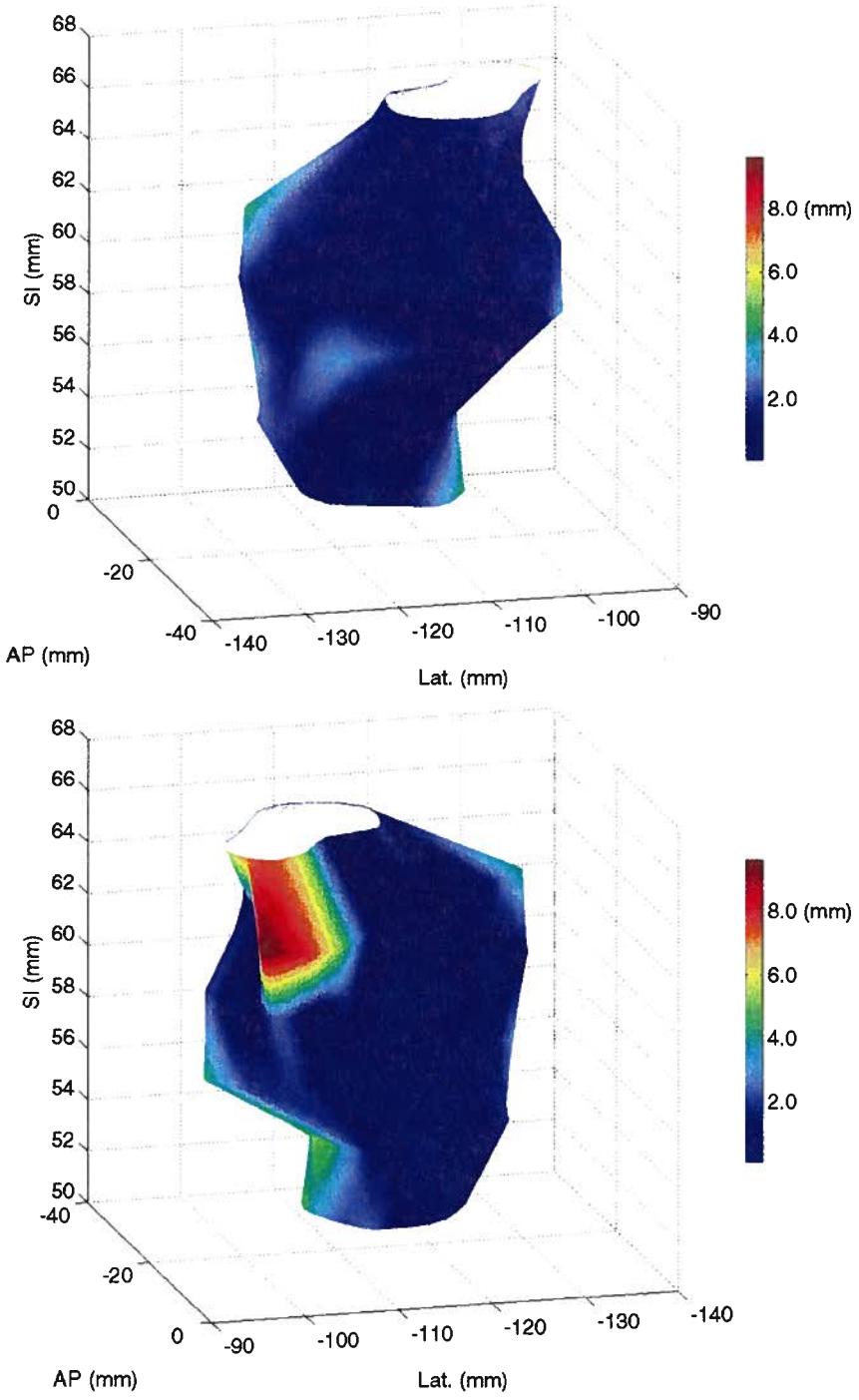

Figure A.12 Interobserver RSC SD map for Patient 12, Day 5 Treatment CT

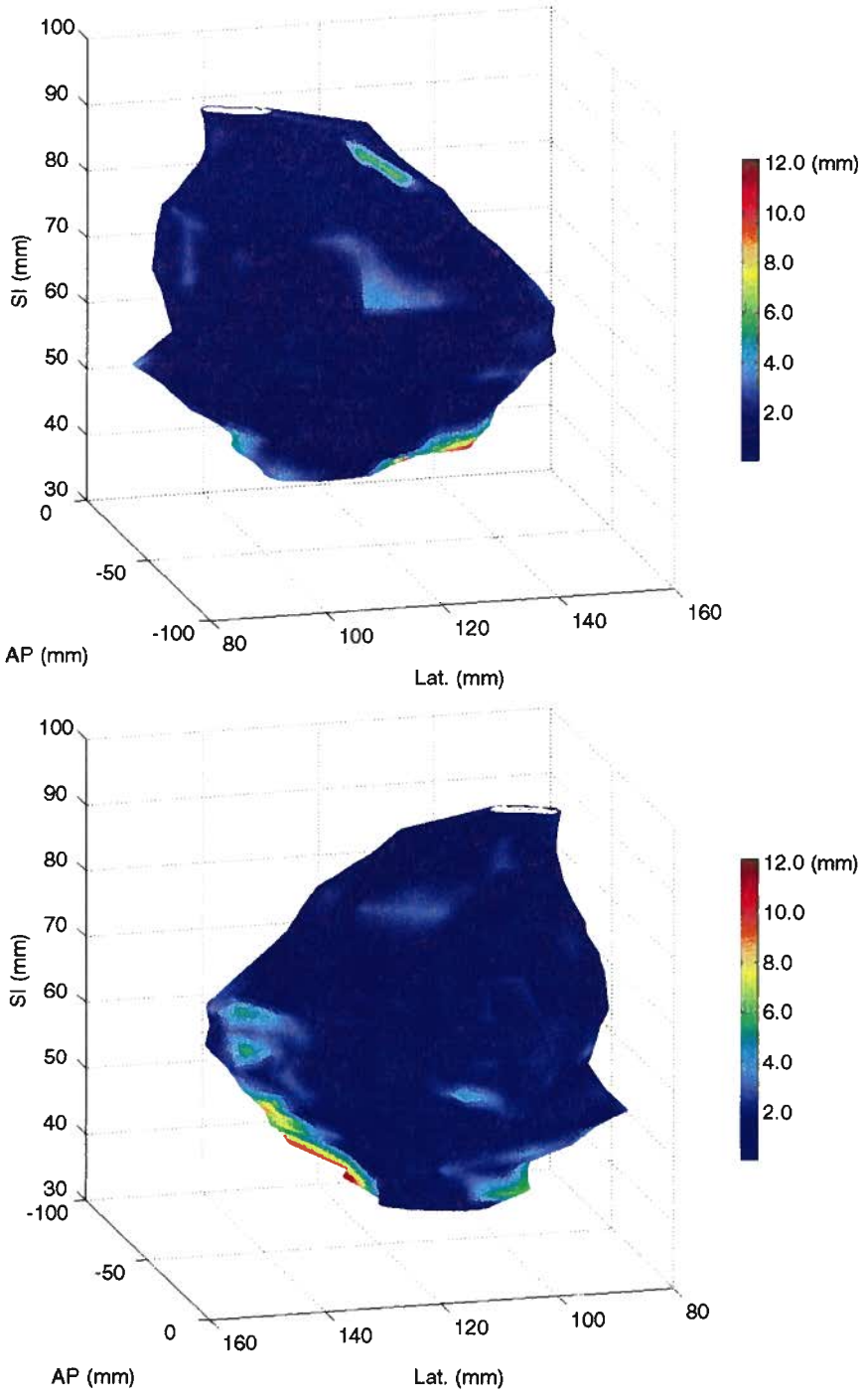

Figure A.13 Intraobserver RSC SD map for Patient 1, Oncologist 1, Planning CT

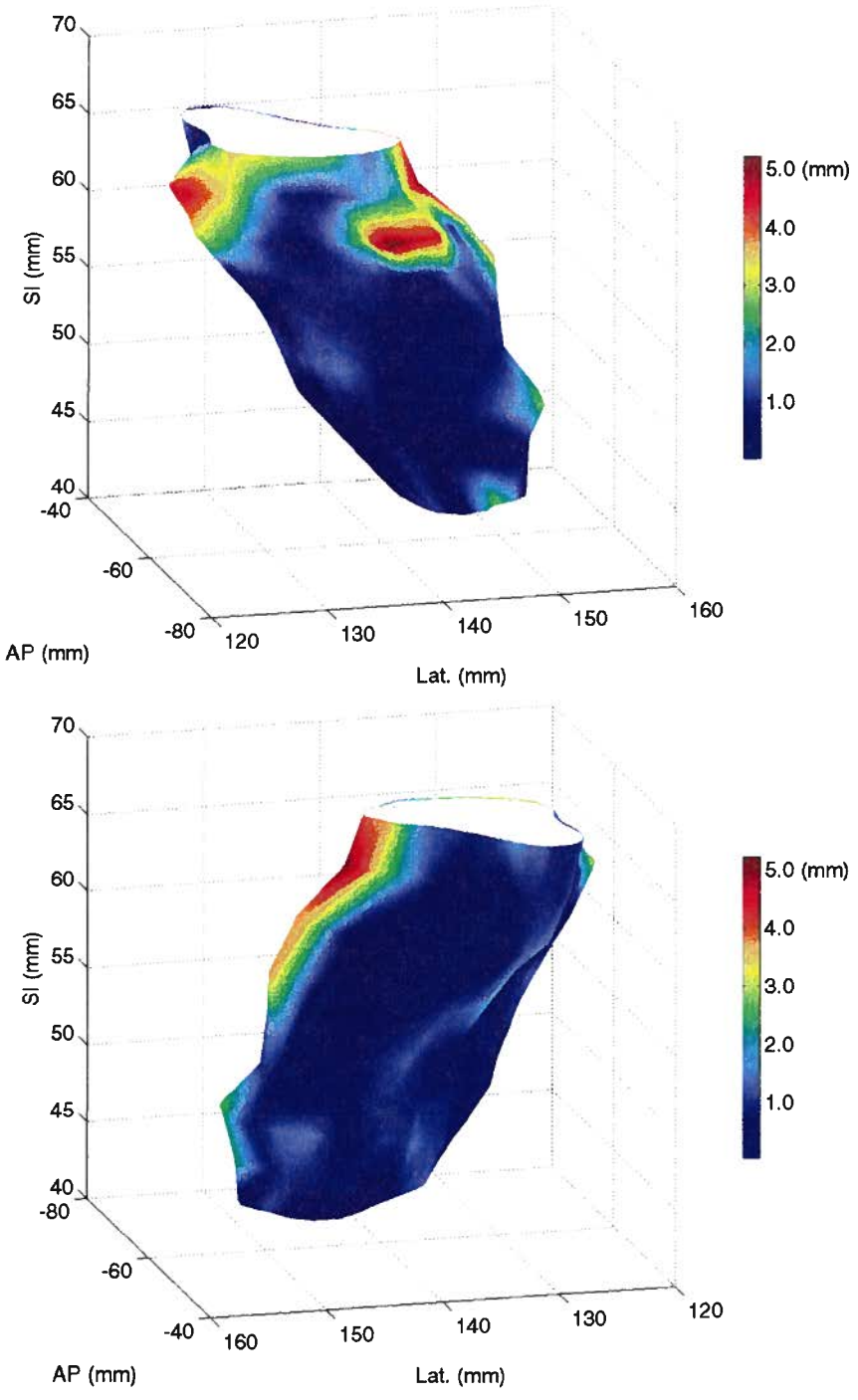

Figure A.14 Intraobserver RSC SD map for Patient 2, Oncologist 2, Planning CT

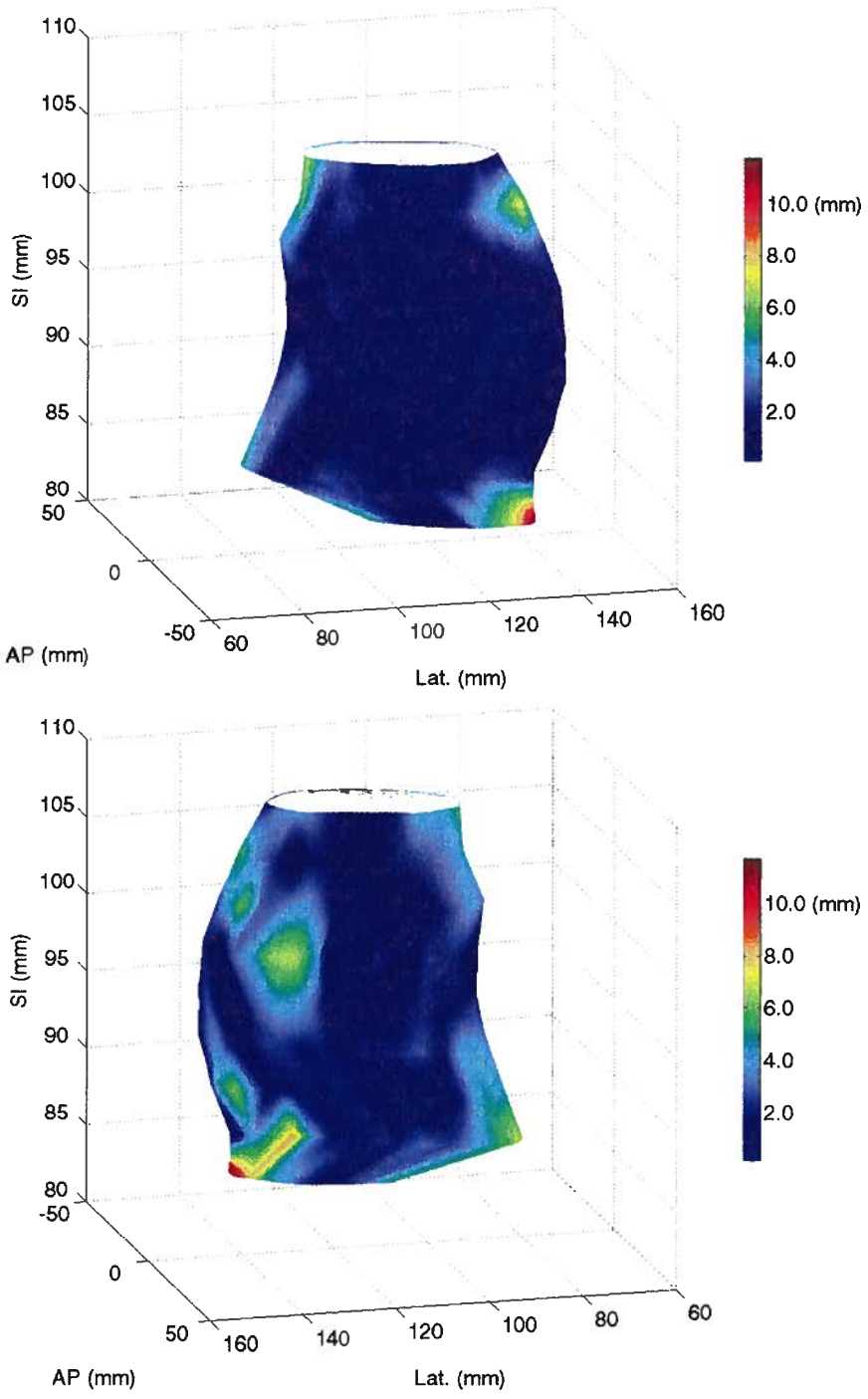

Figure A.15 Intraobserver RSC SD map for Patient 3, Oncologist 3, Planning CT

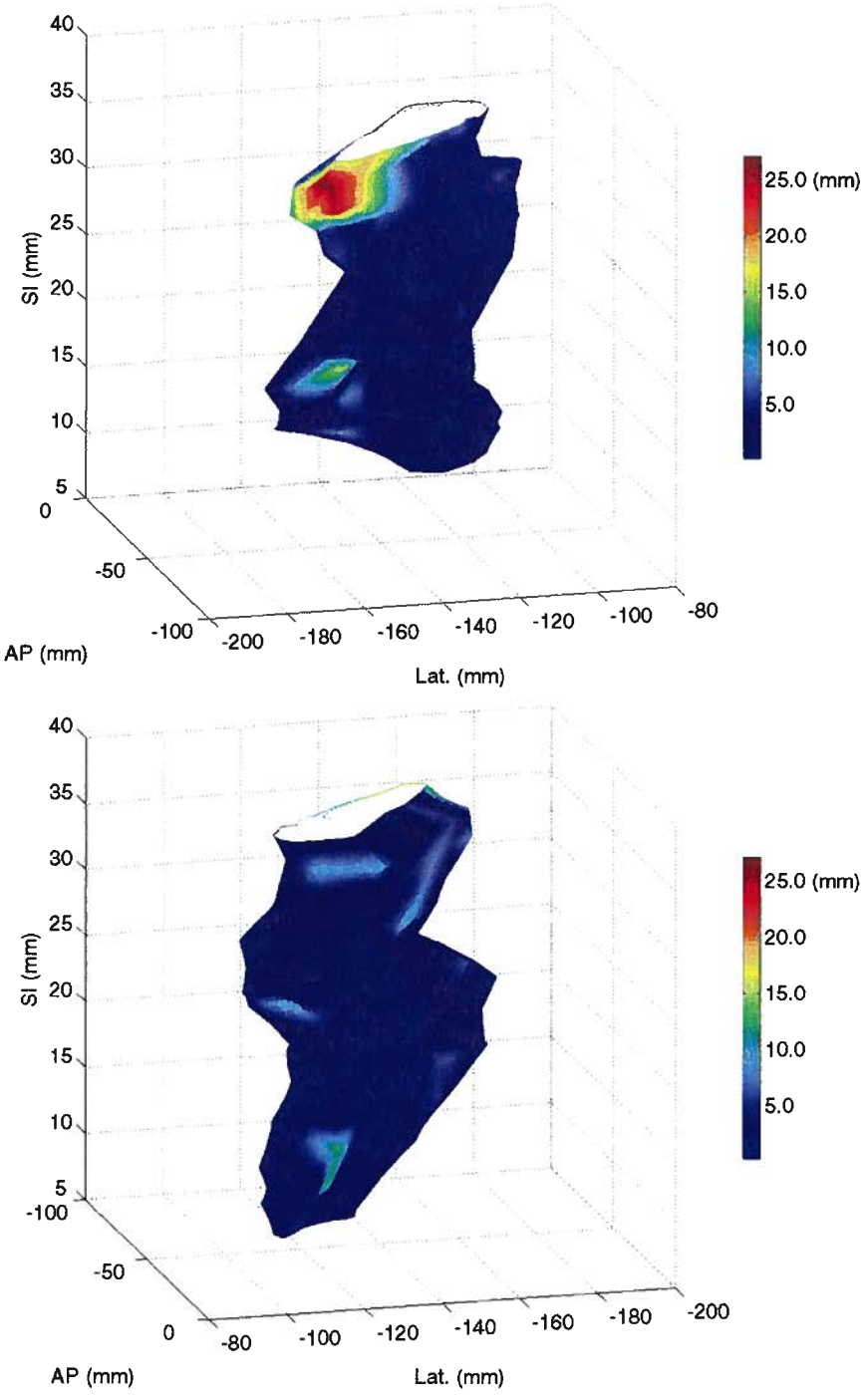

B. RSC SD Cumulative Histograms

Figure B.1 Interobserver RSC SD Cumulative Histograms for Patient 1

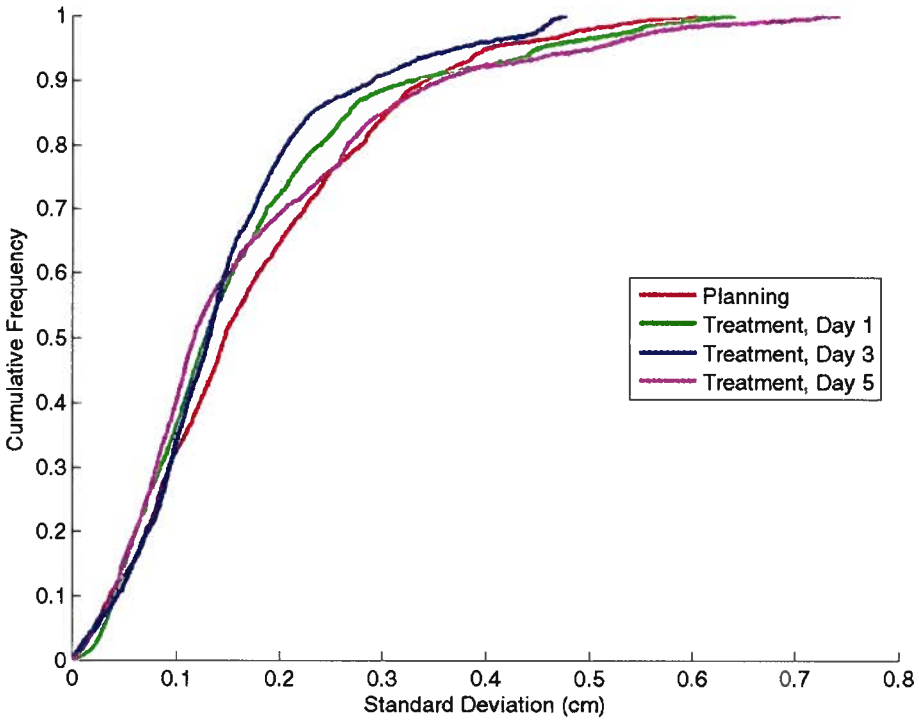

Figure B.2 Interobserver RSC SD Cumulative Histograms for Patient 2

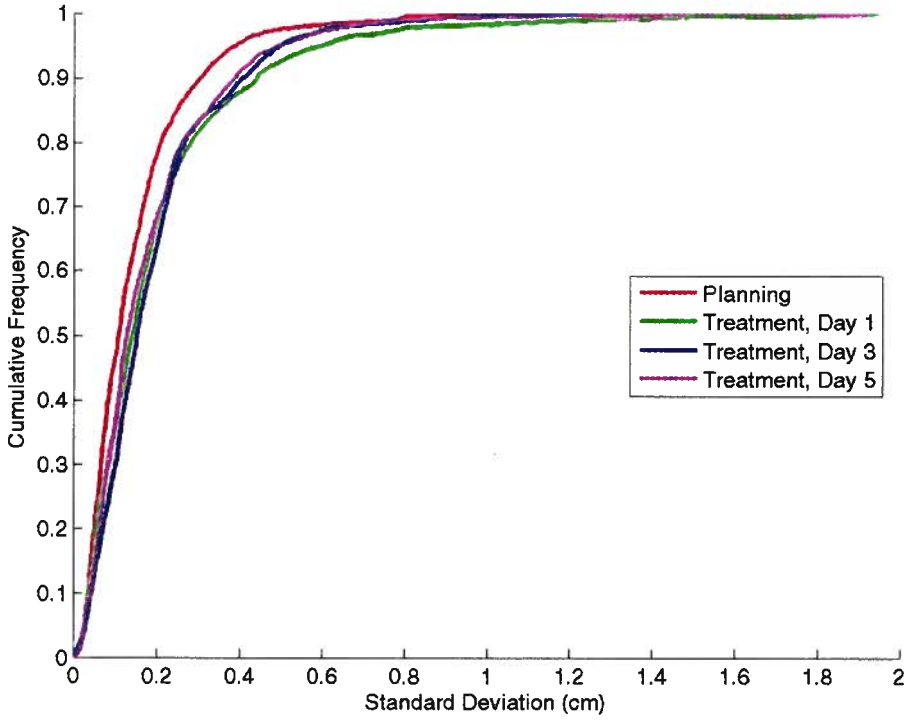

Figure B.3 Interobserver RSC SD Cumulative Histograms for Patient 3

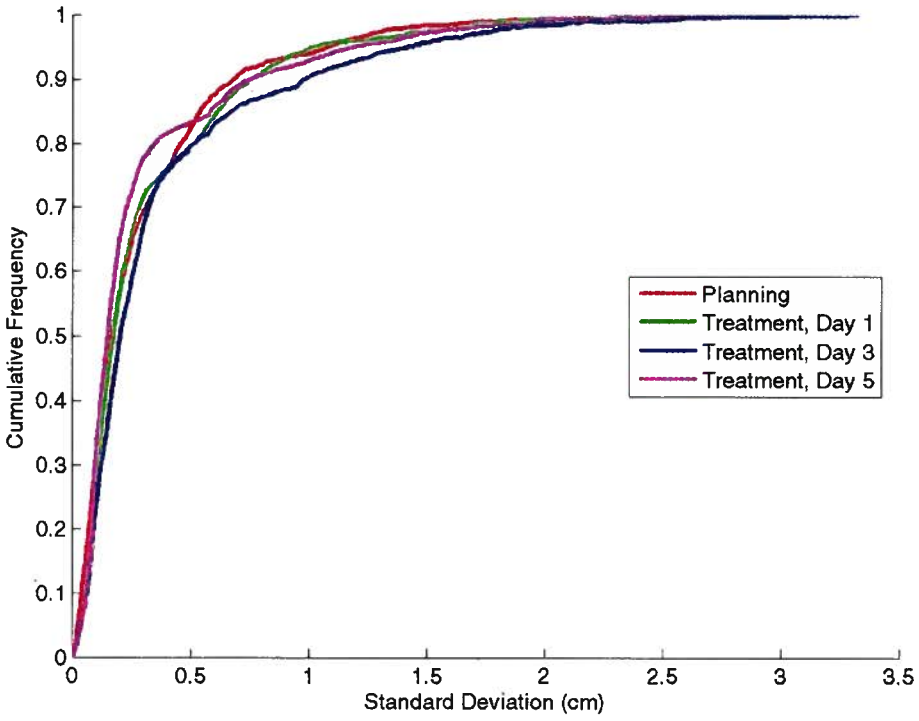

Figure B.4 Interobserver RSC SD Cumulative Histograms for Patient 4

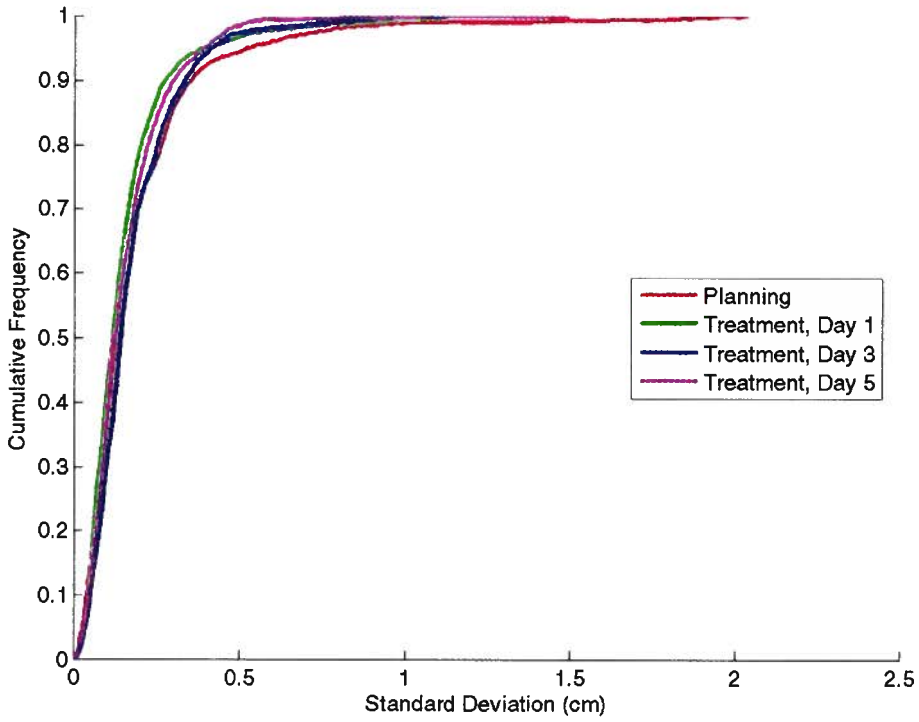

Figure B.5 Interobserver RSC SD Cumulative Histograms for Patient 5

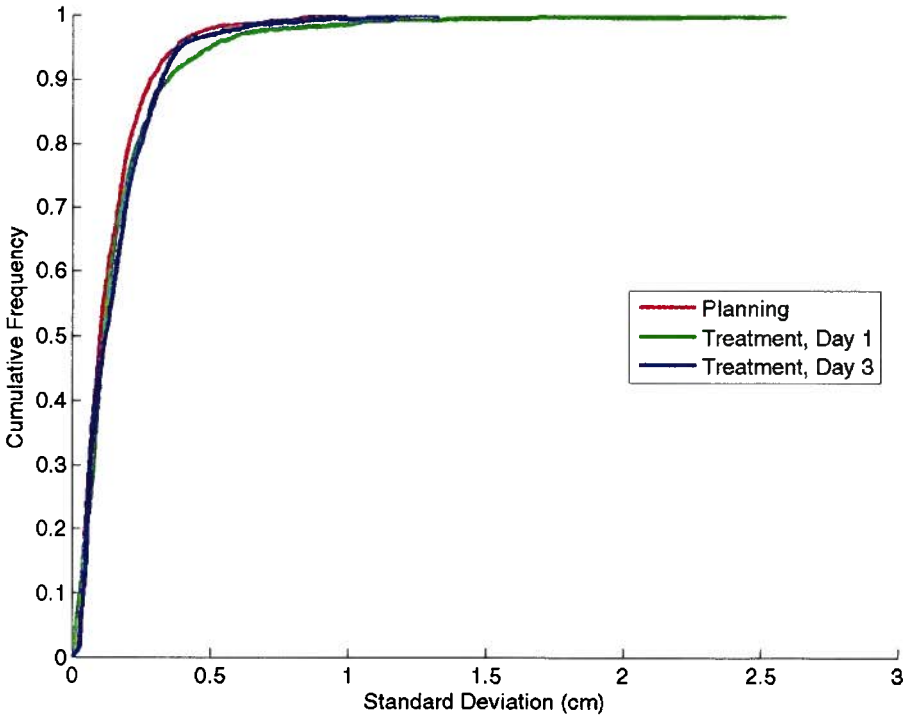

Figure B.6 Interobserver RSC SD Cumulative Histograms for Patient 6

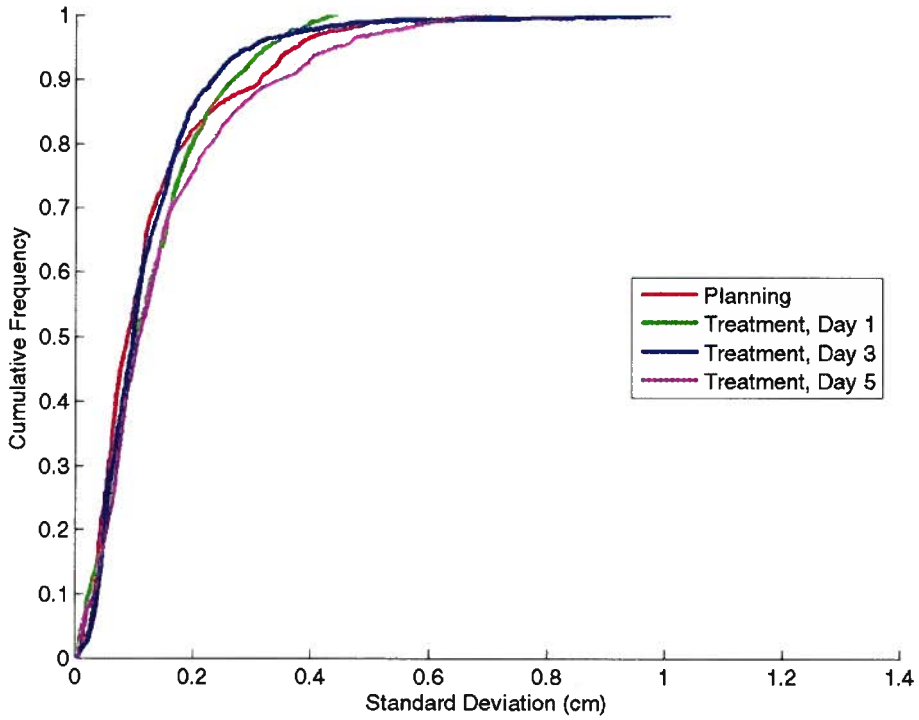

Figure B.7 Interobserver RSC SD Cumulative Histograms for Patient 7

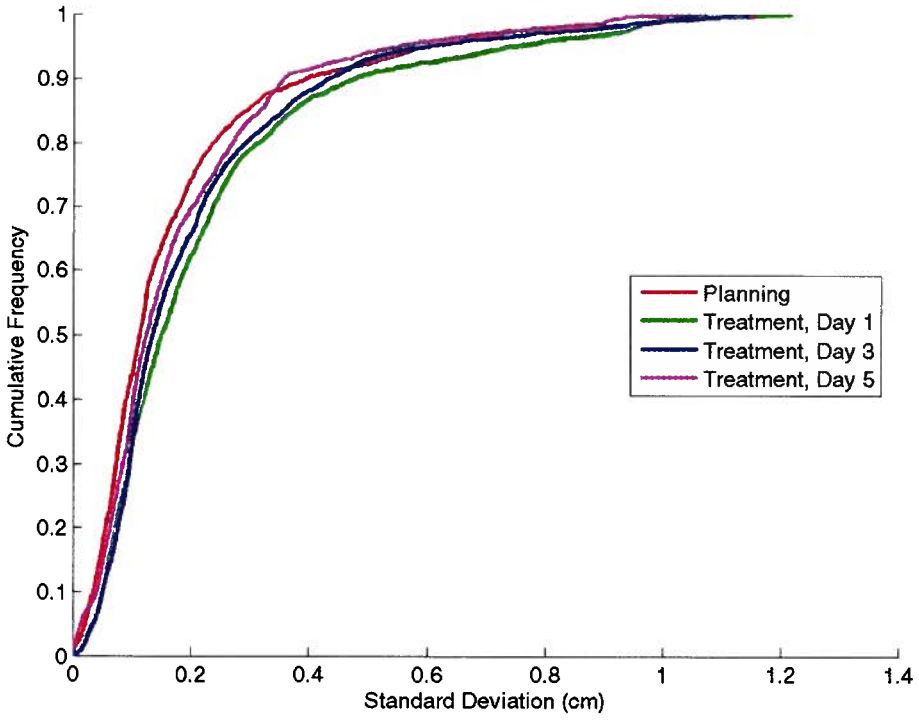

Figure B.8 Interobserver RSC SD Cumulative Histograms for Patient 8

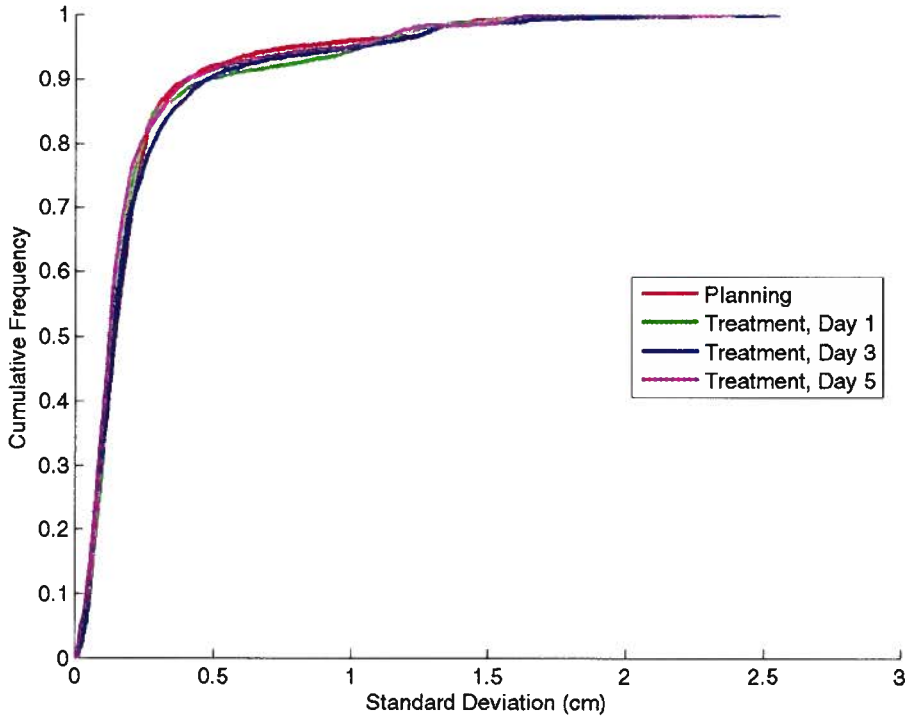

Figure B.9 Interobserver RSC SD Cumulative Histograms for Patient 9

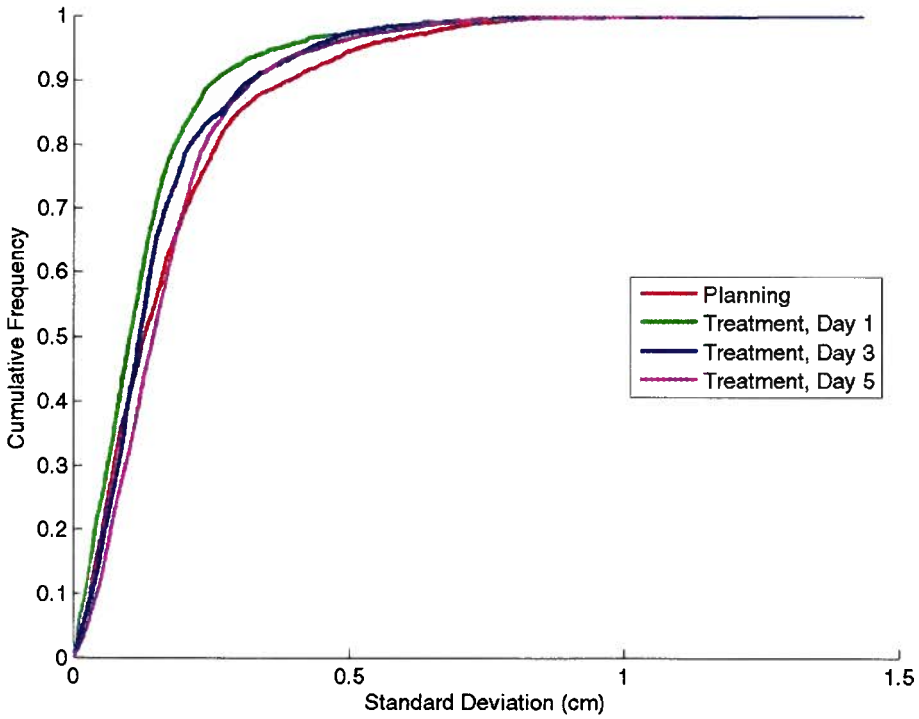

Figure B.10 Interobserver RSC SD Cumulative Histograms for Patient 10

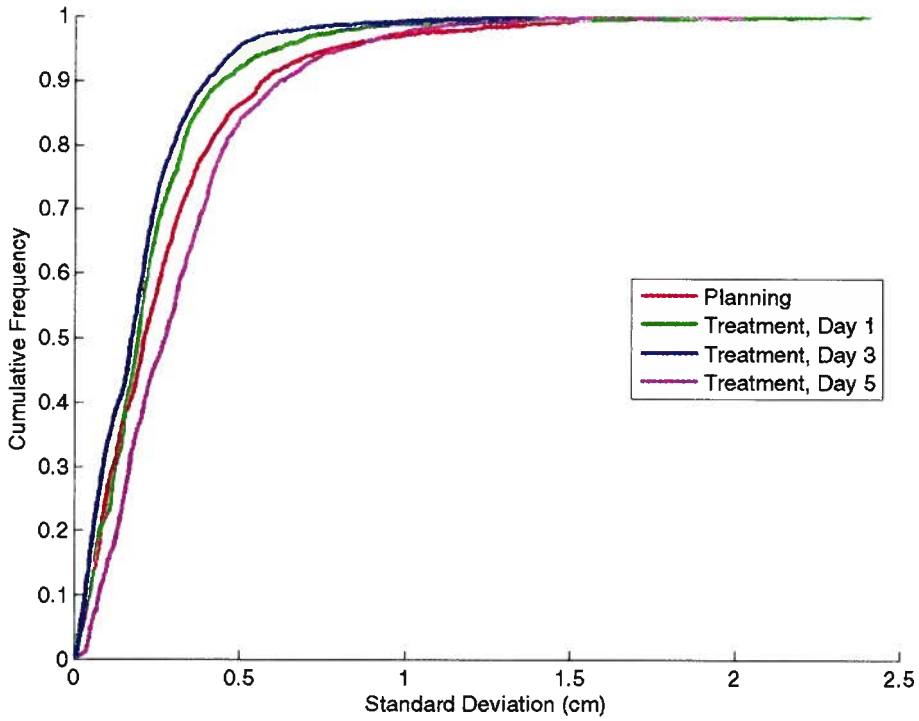

Figure B.11 Interobserver RSC SD Cumulative Histograms for Patient 11

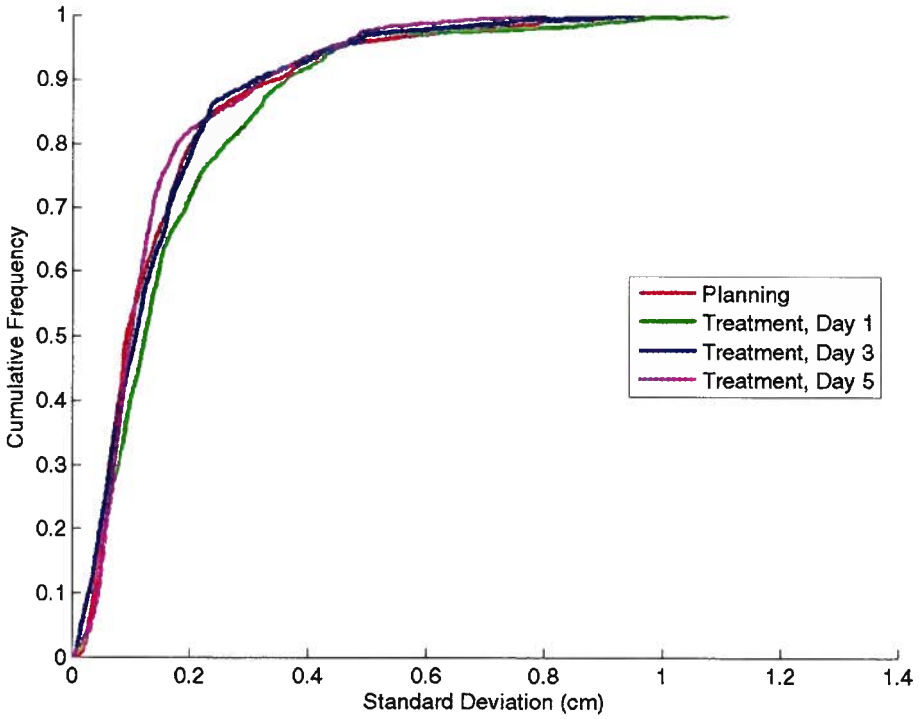

Figure B.12 Interobserver RSC SD Cumulative Histograms for Patient 12

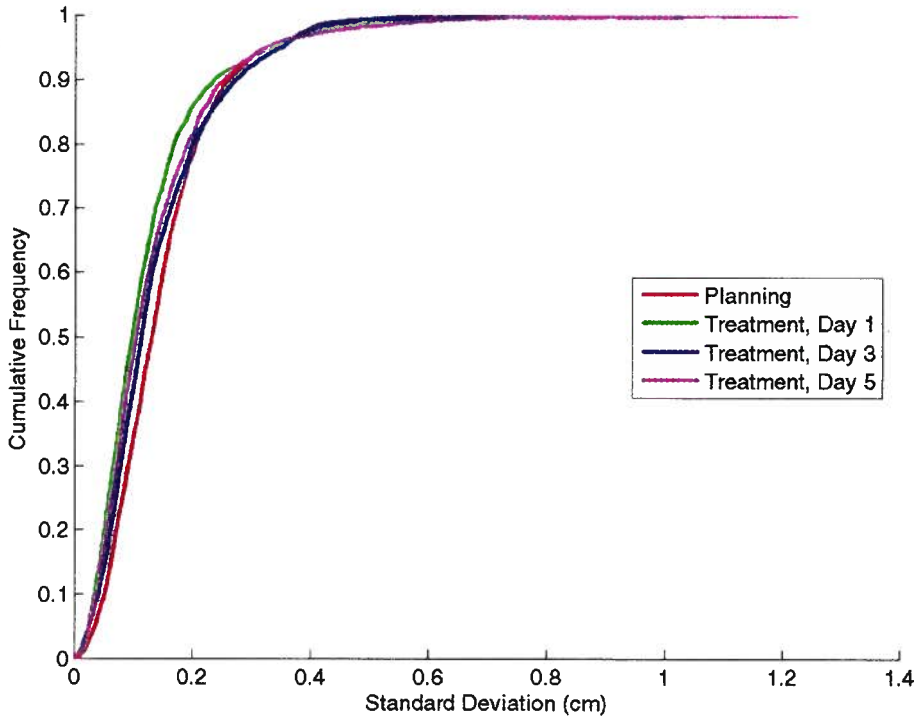

Figure B.13 Intraobserver RSC SD Cumulative Histograms (Patient 1, Oncologist 1)

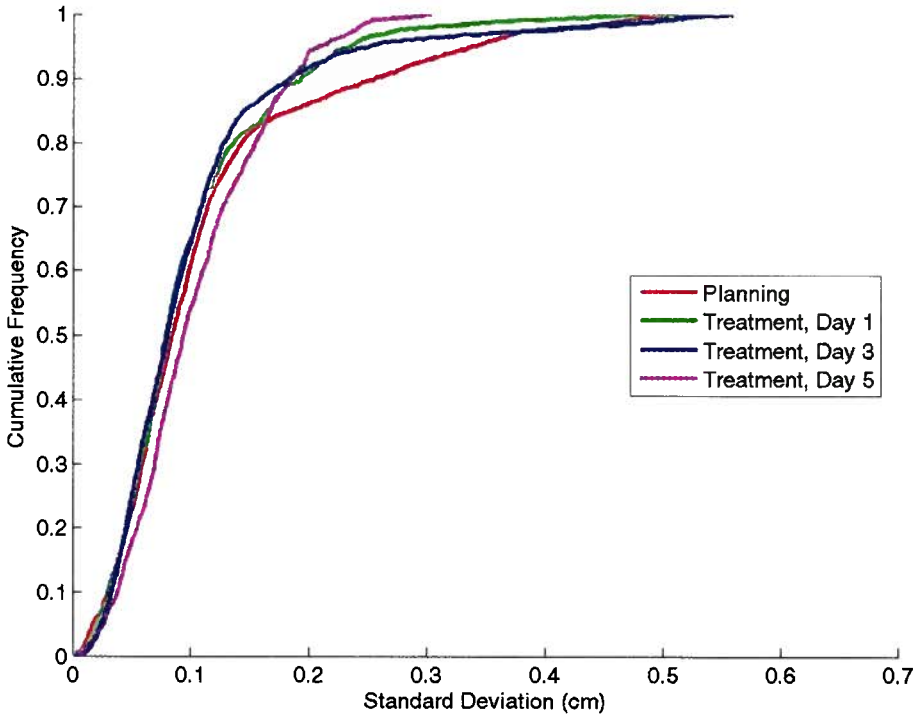

Figure B.14 Intraobserver RSC SD Cumulative Histograms (Patient 2, Oncologist 2)

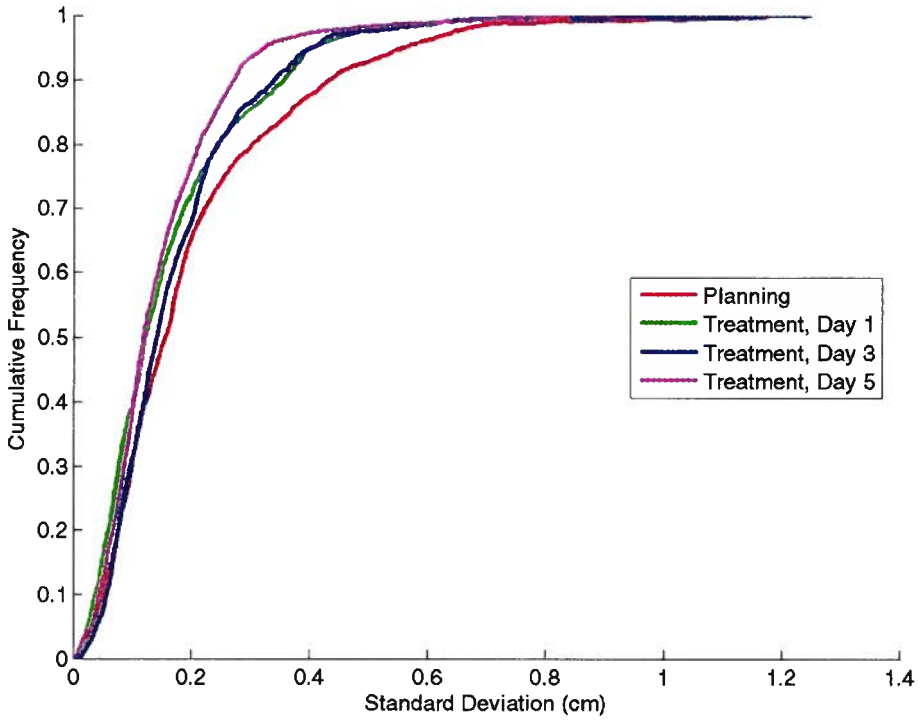

Figure B.15 Intraobserver RSC SD Cumulative Histograms (Patient 3, Oncologist 3)